The Insulin Signalling Pathway in Skeletal Muscle:

in Silico and in Vitro

The Insulin Signalling Pathway in Skeletal Muscle:
in Silico and in Vitro

PROEFSCHRIFT

ter verkrijging van de graad van doctor
aan de Technische Universiteit Eindhoven, op gezag van de
rector magnificus, prof.dr.ir. C.J. van Duijn, voor een
commissie aangewezen door het College voor
Promoties in het openbaar te verdedigen
op woensdag 29 april 2015 om 16.00 uur

door

Ceylan Çölmekçi Öncü

geboren te Karaman, Turkije

Dit proefschrift is goedgekeurd door de promotoren en de samenstelling van de promotiecommissie is als volgt:

voorzitter:	prof.dr. K. Nicolay
promotor:	prof.dr. P.A.J. Hilbers
copromotor:	dr.ir. N.A.W. van Riel
leden:	prof.dr. A.J. Wagenmakers (John Moores University)
	prof.fil.dr. J. Oscarsson (University of Gothenburg)
	dr.rer.nat. C. Ottmann
adviseur:	dr. G. Cedersund (Linköping University)
reserve:	dr. J.J. Prompers

Contents

Nomenclature

List of Symbols

Abbreviations

ADAPT	Analysis of Dynamic Adaptations in Parameter Trajectories
Akt	Protein Kinase B
GFP	Green Fluorescent Protein
GLUT4	Glucose Transporter Type 4
GSV	GLUT4 storage vesicle
IR	Insulin Receptor
IRS	Insulin Receptor Substrate
IRV	Insulin responding vesicle
KEGG	Kyoto Encyclopeida of Genes and Genomes
MPSA	Multi Parametric Sensitivity Analysis
PDK	Phosphoinositide-dependent kinase
PIP2	Phosphatidylinositol biphosphate
PIP3	Phosphatidylinositol trisphosphate
PI3K	Phosphoinositide 3-kinase
PKC	Protein Kinase C
PM	Plasma membrane

Chapter 1

Introduction

1.1   Type 2 diabetes and insulin resistance

Type 2 diabetes has become one of the main threats to human health in the 21st century, by affecting millions of people worldwide [120]. The pathogenesis of type 2 diabetes involves a combination of genetic and environmental factors, which cause insulin resistance in target tissues and impaired insulin secretion from the pancreatic beta-cells. Skeletal muscle is considered as one of the primary tissues in glucose homeostasis, because it accounts for 75 - 80 % of whole body insulin-stimulated glucose uptake [29]. Therefore, skeletal muscle insulin resistance is a major determinant of hyperglycemia and type 2 diabetes mellitus [70]. Skeletal muscle insulin resistance has been associated with the accumulation of total body fat. However, an even stronger association has been shown between intramyocellular fat storage and insulin resistance in animals [66, 91] and humans [79]. This suggests that aberrant storage of lipids or lipid intermediates in skeletal muscle contributes to the development of insulin resistance [106].

In vivo studies reveal that insulin resistance in skeletal muscle is one of the first measurable defects associated with type 2 diabetes [29]. The molecular basis

for the development of whole-body insulin resistance remains unclear, although decreased insulin-stimulated glucose transport activity has been observed in isolated skeletal muscle from lean and obese people with type 2 diabetes [123]. Because glucose transport is an early step in peripheral glucose utilization, a defect in glucose transport most likely plays a major role in the pathogenesis of peripheral insulin resistance [57]. Thus, an understanding of the mechanisms that control glucose transport into insulin-sensitive tissues is essential to develop strategies for reestablishing normal glucose homeostasis in people with type 2 diabetes. Insulin-stimulated glucose transport is achieved by translocation of the major insulin-responsive glucose transporter, GLUT4, from an intracellular vesicle storage site to the plasma membrane and transverse tubules. Reduced glucose transport activity in skeletal muscle from people with type 2 diabetes may be a consequence of impaired insulin signal transduction and/or alterations in the traffic and translocation of GLUT4 to the plasma membrane [68, 67].

A prevailing hypothesis is that the accumulation of lipids or lipid by-products (diacylglycerol, ceramides) in muscle and adipose tissues can cause inflammation and insulin resistance [21]. Defective GLUT4 translocation in muscle is a key feature of insulin resistance [62, 124], but to date, defects are assigned to alterations in insulin-derived signals and the possible contribution of proper intracellular sorting of GLUT4 has not been analyzed. Cellular studies have revealed that a cell permeable ceramide analog, C2-ceramide (C2-cer), inhibits Akt activation and GLUT4 translocation in response to insulin without affecting upstream insulin receptor substrate (IRS) or phosphoinositide 3-kinase (PI3K) activation [41, 102]. However, difficulty in defining the intracellular localization of the GLUT4-retaining, insulin-responding intracellular compartment (commonly termed as GLUT4-storage vesicles, abbreviated as GSV) has left untested the possibility that defective GLUT4 sorting may also contribute to C2-ceramide induced insulin resistance [32].

Activation of novel protein kinase C (nPKC), including PKC-θ, has been correlated with insulin resistance in a number of studies, especially in association with increased lipid availability [38, 6]. PKC-θ is a serine/threonine kinase and a member of the novel subfamily of PKC isoforms (δ, ϵ, θ, μ). PKC-θ consists of 707 amino acid residues (73 kDa protein) with highest similarity to PKCδ (67%). PKC-θ is expressed predominantly in skeletal muscle, T-cells, and platelets, with less expression in cardiac muscle, placenta, and liver. It is the main isoform present in skeletal muscle, a major target tissue for insulin [40].

A strong correlation between intramyocellular triacylglycerol concentrations and the severity of insulin resistance has been found and led to the assumption that lipid oversupply to skeletal muscle contributes to reduced insulin action. However, the molecular mechanism that links intramyocellular lipid content with the generation of muscle insulin resistance is still unclear. It appears unlikely that the neutral lipid metabolite triacylglycerol directly impairs insulin action. Hence it is believed that intermediates in fatty acid metabolism, such as fatty

acyl-CoA, ceramides or diacylglycerol (DAG) link fat deposition in the muscle to compromised insulin signalling. DAG is identified as a potential mediator of lipid-induced insulin resistance, as increased DAG levels are associated with protein kinase C activation and a reduction in both insulin-stimulated IRS-1 tyrosine phosphorylation and PI3 kinase activity. As DAG is an intermediate in the synthesis of triacylglycerol from fatty acids and glycerol, its level can be lowered by either improving the oxidation of cellular fatty acids or by accelerating the incorporation of fatty acids into triacylglycerol [106].

To explore any impairments in the insulin signalling cascade, it is of crucial importance to reveal the functioning and the dynamics of the pathway composed of signalling complexes that transfer the signal [78].

1.2 Signalling Pathways

Understanding cell signalling is pivotal because pathological alterations in cellular signalling are the main sources of not only diabetes but also diseases such as cancer, neurological diseases, cardiovascular diseases [45, 8, 125, 7, 73, 27, 28, 25]. Signalling pathways are essential elements for the maintenance of homeostasis in biological systems. They are responsible for transferring the signals initiated by the receptors and enabling cells to take action in response to environmental changes for maintaining equilibrium state. These signalling pathways can be seperated into two main groups depending on the way they are activated. Most of them are activated by external stimuli and are functional in transfering information from the cell surface to internal effector systems. On the other hand, some respond to signals arising from within the cell, usually in the form of metabolic messengers. For all of these signalling pathways, information is transmitted either through proteinprotein interactions or by diffusible elements, which are usually referred to as second messengers. Cells often employ a large number of these signalling pathways, and cross-talk between them is also an important feature. In this thesis, our attention is mainly focused on the properties of major intracellular signalling pathways which are operating in cells to regulate their cellular activity [9].

Spatial and temporal organisation of signalling pathways

The functions of cell signalling pathways and their efficiency are highly dependent on spatial and temporal organization of signalling pathways. The spatial organization of signalling components determines how signalling components transmit information to another. This spatial organization of signalling pathways depends on the molecular interactions that occur between signalling components. Signal transduction domains are utilized to construct signalling pathways. Usually, the components responsible for information transfer mechanisms are held in their locations by being attached to scaffolding proteins with which they together
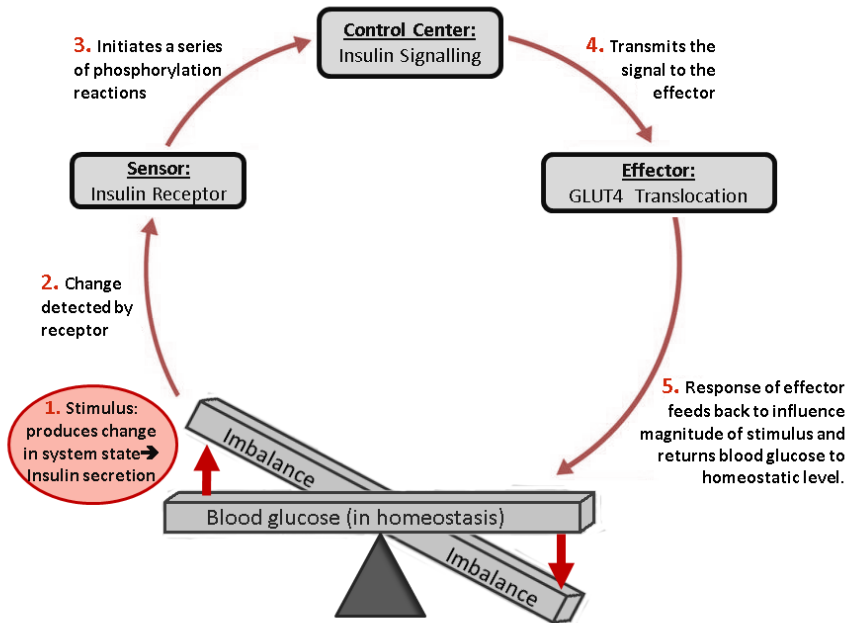
Figure 1.1: Homeostatic control of blood glucose.

form macromolecular signalling complexes. Sometimes these macromolecular complexes can be organized further by being localized in specific regions of the cell, as found in lipid rafts and caveolae or in the T-tubule regions of skeletal and cardiac cells [10].

Homeostasis, Feedback, Robustness

Maintenance of homeostasis in biological systems can be considered as a perfect application of control theory in nature. State variables in homeostasis such as blood glucose, body temperature, blood pressure are maintained in a physiological range by the use of homeostatic control (See the scheme in Fig. 1.1 for homeostatic control of blood glucose). When a signal is bound to its receptor, a specific intracellular signal transduction pathway is triggered, leading to both transcriptional and/or posttranscriptional changes in responsive cells. Ultimately these pathways regulate a variety of cellular outcomes, including both cell fate changes and morphogenetic responses. There are three basic problems that cells, and fields of cells, have to resolve when they receive such signals. The first one is to shut off or modulate the activation of the incoming signalling pathway, as

inappropriate cellular response(s) can result if the receiving cell sustains and amplifies its response to extra-cellular signals. The other two problems in regulation of incoming signals involve dimensional issues. In many instances, signals originate from a localized source and act over long distances. It is important not only to limit responses to a subset of the cells within the field, but also to generate distinct responses to different concentration thresholds of incoming signals. Negative feedback mechanisms are widely used to resolve these signalling issues.
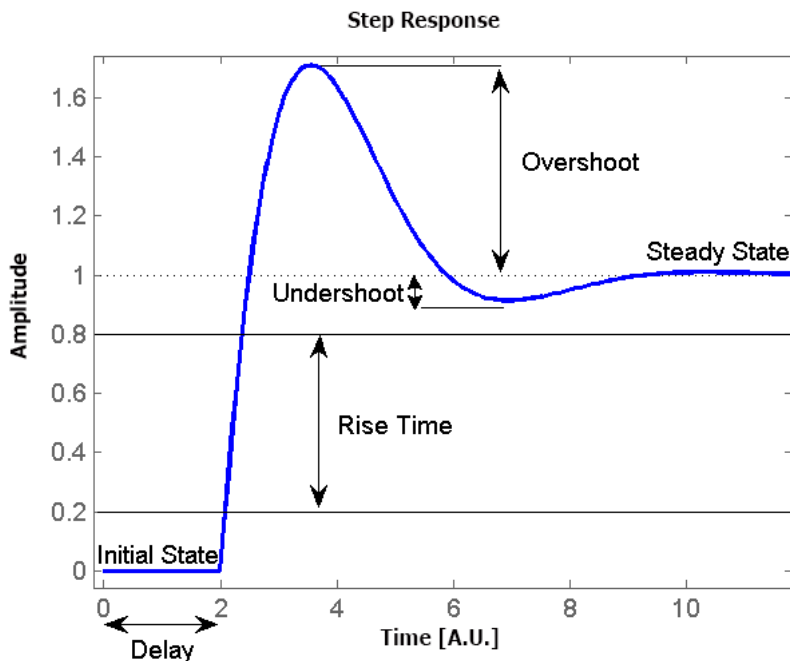
Figure 1.2: The dynamic characteristics of a signal.

Desirable signals must be robust enough to ensure that cells receive them at high enough levels to respond. Just as important is versatility. Not only there is a wide range of different cell types and tissue environments in which these signals must operate, but they must also function with different spatial and kinetic properties. These three main properties of intercellular signalling in development precision, robustness and versatility are stringent requirements and errors are serious [34]. Feedback can be defined as the ability of a system to adjust its output in response to monitoring itself. It is important to limit responses and to generate distinct responses to different concentration thresholds of incoming signals [81]. Feedback regulations help to improve the robustness of
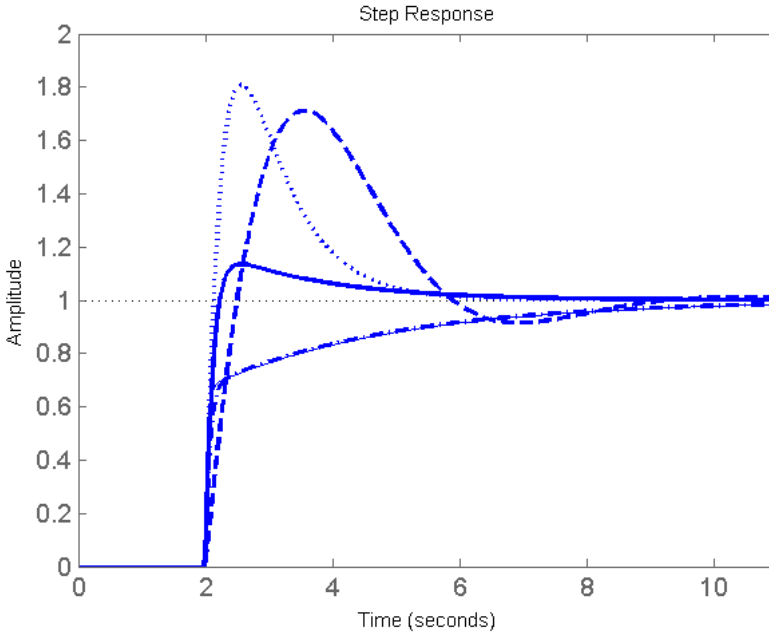
Figure 1.3: Variety in dynamic response profiles of signalling components.

biological systems against perturbations. Signalling pathways are also composed of the ON mechanisms that generate internal signals and the OFF mechanism that remove these signals as cells recover from stimulation.

1.3   Insulin Signalling Pathway

The insulin signalling pathway is a very complex network (See Fig. 1.4) that controls several processes and has a central role in several functions such as metabolism, growth, reproduction, and aging. Biological actions of insulin are initiated with the binding of insulin to its cell surface receptor. The transmission of information from the insulin receptor results in various effects in the cell such as increased glucose transport, mitogenesis, and regulation of enzymatic pathways (See Fig. 1.4). In the scope of this thesis, its role in metabolism, particularly its role in regulation of blood glucose is considered. We will focus on the insulin signal transmission from insulin receptors to the recruitment of GLUT4 proteins to the plasma membrane in skeletal muscle. In the subsequent chapters, the insulin signalling pathway that is referred to is the signalling cascade responsible for the insulin induced GLUT4 translocation.
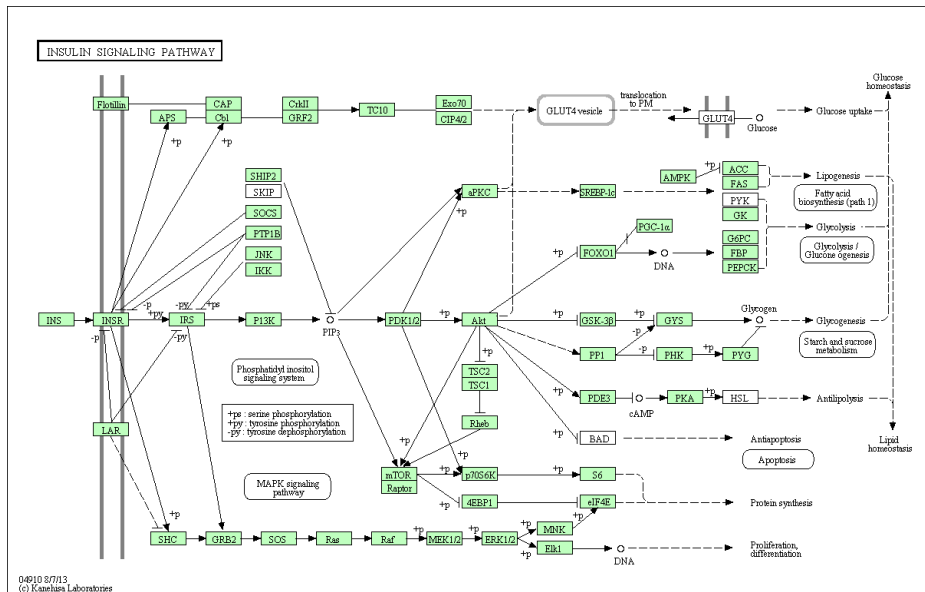
Figure 1.4: Insulin signalling pathway from KEGG database [53, 54].

Insulin signalling starts with binding of insulin to its receptor (IR) which in turn leads to tyrosine phosphorylation of IRS1. This adjoins activation of PI3-kinase (phosphoinositide 3-kinase) which converts PIP2 (phosphatidylinositol biphosphate) to PIP3 (phosphatidylinositol trisphosphate) in the plasma membrane and leads to phosphorylation of atypical protein kinase C (PKC) Phosphoinositide-dependent kinase-1 (PDK1), Phosphoinositide-dependent kinase-2 (PDK2) and Akt become associated with PIP3 and together induce the phosphorylation and activation of Akt [36]. The role of Ser473 phosphorylation in the COOH-terminal loop of Akt1/2 is controversial, but the emerging view is that Ser473 phosphorylation precedes and is required for Thr308 phosphorylation by PDK1. Dual phosphorylation of Akt is required for its full activation [104, 45]. Activated Akt then phosphorylates AS160 which is a Rab-GTPase-activating protein (GAP). This in return suppresses the target Rabs and mediates GLUT4 translocation to the PM.

GLUT4 is transported between intracellular depots and the PM by GLUT4 storage vesicles (GSVs), which traffick along a microtubular network underneath the PM. It was commonly accepted that in the absence of stimulation, GLUT4 is almost completely excluded from the plasma membrane. The addition of insulin causes GLUT4 to shift from its intracellular location to the plasma membrane [19]. However, more recent studies of GLUT4 translocation reported a new hypothesis [4, 74]. In the basal state, the GLUT4 vesicles which are trafficking

near the PM weakly, tether to the PM, and rarely fuse into it, slowly exchanging GLUT4 with the PM. Upon insulin stimulation, the vesicles tether to the PM tighter and more vesicles dock and fuse into the PM. Although insulin-facilitated interaction between GLUT4 vesicles and the PM can be experimentally observed, the underlying mechanisms still remain unclear. Bai *et al.* [4] indicate that the docking of GSVs to the PM might be the target of AS160, a substrate of Akt. The fusion step is also regulated by insulin and it is likely to involve a target of insulin action that is distinct from AS160. Substantial evidences also support a role for PKC-ξ, another downstream effector of PI3K, in GLUT4 translocation. However, it is not fully understood at which stage of translocation it plays a role [31].

1.4   Systems Biology Approach

Systems biology is a multidisciplinary approach that studies the interactions and regulations in a biological system, and how these interactions and regulations lead to the function and behavior of the system as a whole. Systems biology aims to create mathematical models that can represent the dynamical behaviour of signalling pathways and processes in order to gain a better understanding of their complex interactions and to develop quantitative descriptions of their dynamics. This model-based approach links fundamental chemical and physical principles, prior knowledge about signalling pathways, and experimental data of various types to develop tools for formalizing traditional molecular and cellular biology [1, 75, 26].

There are several modelling approaches that are widely used for the modelling of signalling pathways. The choice depends on the specific questions to be addressed. These mathemataical models can be in the form of discrete or continuous-time Ordinary Differential Equations (e.g. chemical reaction networks with mass action kinetics), Functional (Delay) Differential Equations (e.g. to describe maturation/growth in population dynamics), Stochastic Differential Equations (e.g. to model chemical reaction networks in which species are found in low copy numbers), Partial Differential Equations (e.g. to describe spatial dynamics), or even Hybrid models (which incorporate both discrete and continuous states) [2, 63]. In this thesis, we employ widely used continuous-time Ordinary Differential Equations since we focus on the overall behaviour of cell population assuming that the components of the insuling signalling pathway homogeneously distribute in the cell and stochastic effects can be ignored.

The challenges and aspects in dynamics of signaling pathways

Considerable efforts have been made so far in the field of systems biology for dynamical modeling and systems analysis of cellular signal transduction pathways.

Quantitative mechanism-based models could allow researchers to predict the comprehensive behavior of the specified system over time and to track its dynamics for each set of fixed system parameters [43, 11, 46, 3, 93, 22, 44]. However, all of the parameters including rate constants and initial components concentrations in the mathematical models must be experimentally measured or inferred to specify the model. Even for those models with experimentally estimated parameters, it is still uncertain whether the particular set of parameters closely approximates the corresponding biological system because some of the kinetic parameters are usually taken or estimated from measurements reported by different laboratories using different in vitro models and conditions. Given the inherent uncertainties in the structure and parameter values of the models, parameters can be assigned statistical distributions that reflect the degree of uncertainty and then simulation analysis can be performed by sampling from the distributions. It is therefore of vital importance not only to study the dynamical properties governed by the particular kinetic parameters but also to further investigate the effects of their perturbations on the overall system [121]. These mathematical models are used to reproduce experimental data and predict unobserved behaviors of the system. However, many sources of uncertainty including errors, inconsistency and noise of experimental data, absence of parameter information, incomplete representation of underlying process details, and poor understanding of the biological mechanisms impose a limit on model confidence. Furthermore, intrinsic variability or noise of the system such as the occurrence of stochastic events also affects the output of the model. Therefore, it is important not only to understand the dynamical properties of the model with particular parameter values, but also to further investigate the effect of their perturbations on the system. Sensitivity analysis is a powerful approach for investigating which parameters in a model have the strongest effect on overall behavior. In addition to identifying key parameters in a model, sensitivity analysis is valuable in pinpointing parameters, which should be in the focus of experimental perturbation [122]. Accuracy of results from mathematical and computer models of biological systems is often complicated by the presence of uncertainties in experimental data that are used to estimate parameter values. Current mathematical modeling approaches typically use either single-parameter or local sensitivity analyses. However, these methods do not accurately assess uncertainty and sensitivity in the system as, by default, they hold all other parameters fixed at baseline values. A multi-dimensional parameter space can be studied globally so all uncertainties can be identified. Further, uncertainty and sensitivity analysis techniques can help to identify and ultimately control uncertainties [75, 112, 113].

Applications in Pharmaceutical Industry System biology approach has also found a solid place in drug discovery research in pharmaceutical companies such as AstraZeneca, Glaxo Smith Klein, Pfizer, Roche. Because systems biology offer a novel way of approaching drug discovery by developing models that consider the global physiological environment of protein targets, predict the

effects of modifying them, and evaluate potential therapeutic compounds [83]. It is used in target identification and validation; biomarker identification and validation; clinical trial design and optimization.

By identifying key mechanisms that cause impairments in the signalling pathway via mathematical modelling, we can propose biomarkers to detect insulin resistance. Our predictive computational can be used as a virtual skeletal muscle to assist in the identification of biomarkers, evaluate and validate drug targets, predict human response and design clinical trials.

1.5   The outline of the thesis

The insulin signalling pathway plays an essential role in the maintenance of the glucose homeostasis. It has therefore been studied for decades for identifying the intermediates and their interactions. However, our understanding of the key mechanisms in insulin signalling and how the insulin signalling interfaces with the GLUT4 storage compartments is still limited. In this thesis, we utilize a systems biology approach that combines computational modeling techniques and experimental work to study the regulations in the insulin signalling pathway that describe the core dynamic behaviour of the insulin signalling pathway from insulin receptor to GLUT4 translocation.

Chapter 2 provides an introduction to the systems biology approach to study the insulin signalling pathway. Here we employ a hypothesis driven modeling approach to construct the first version of our predictive computational model for the insulin signalling pathway. The model consists of a set of ordinary differential equations and kinetic parameters. The parameterization of the model is based on the data gathered from literature. However, limited time course data on the signalling intermediates leads to the uncertainty of the model parameters, which in turn leads to the uncertainty in our model predictions. This result identifies the need for generating a high resolution time course data set for the development of a predictive model. To obtain high resolution experimental data, accurate quantification of raw data is as important as generating raw data. It is challenging especially for intracellular proteomics data due to wide range of protein concentrations.

Chapter 3 reports a discussion on the accuracy of the methods that are used to quantify the fluorophore-tagged proteins. In this chapter, we show that a pixel based method that is often used may result in misinterpretation of the dynamics of the proteins. To overcome the issue, we propose an intensity based method by which an automatic quantification of fluorophore-tagged proteins is provided. This method is used to quantify our new data in the following chapter.

In Chapter 4, we present the results of our study of the dynamics of the insulin signalling pathway in vitro. We perturb rat skeletal muscle cells with various insulin inputs and quantify the frequently sampled response of several intermediates in the pathway. Immunocytochemistry assays for phosphorylation

of (p-) IRS-1, Akt-S473, Akt-T308, AS160, and GLUT4 proteins are combined with high-throughput fluorescence microscopy in order to trace and quantify the temporal profile of the proteins in the pathway. We show that the measured intermediates of the insulin signalling pathway have consistent dynamic behaviour regardless of the inter-experimental heterogeneity.

In Chapter 5, the data generated is used to develop the second generation of the model by using a hypothesis driven approach. Profile likelihood and Multi Parameter Sensitivity Analysis (MPSA) show that the model parameters are identifiable. The simulations of the model show that not only the measured intermediates, but also unmeasured intermediates are highly correlated with each other. The model is then used to test the hypotheses on lipid induced insulin resistance.

Chapter 6, concludes the thesis with the main contributions and provides an outlook at the model of the insulin signalling pathway. As an outlook, we analyse the insuling signalling pathway from a broader perspective. The Analysis of Dynamic Adaptations in Parameter Trajectories (ADAPT) is used to inquire if any further topology change is required in our model and to identify the points of crosstalks of the insulin signalling pathway with other pathways.

Chapter 2

Systems biology approach to study the dynamics of the insulin signalling pathway

Abstract

Insulin signalling pathway plays an essential role in the maintenance of the glucose homeostasis. It has therefore been studied for decades for identifying the intermediates and their interactions. However, our understanding of the key mechanisms in insulin signalling and how the insulin signalling interfaces with the GLUT4 storage compartments are still limited. In this chapter, we use a data-hypothesis driven modelling approach to study the missing regulations in the insulin signalling pathway that describe the core dynamic behaviour of the insulin signalling pathway from insulin receptor to GLUT4 translocation.

2.1   Introduction

Insulin which is an essential hormone of glucose homeostasis initiates the phosphorylation of the intermediates by binding to its receptor. With the phosphorylation of the insulin receptor, the signal is transmitted through the phosphorylation / activation of the intermediate proteins. That in turn, promotes the translocation of the insulin-responsive glucose transporter GLUT4 from intracellular compartments into the plasma membrane (PM). understanding insulin-stimulated GLUT4 translocation at the cellular level, involves two separate fields of inquiry: (a) insulin signalling and (b) GLUT4 membrane trafficking [116]. However, the underlying mechanisms that link insulin signalling to GLUT4 translocation are not fully understood yet.
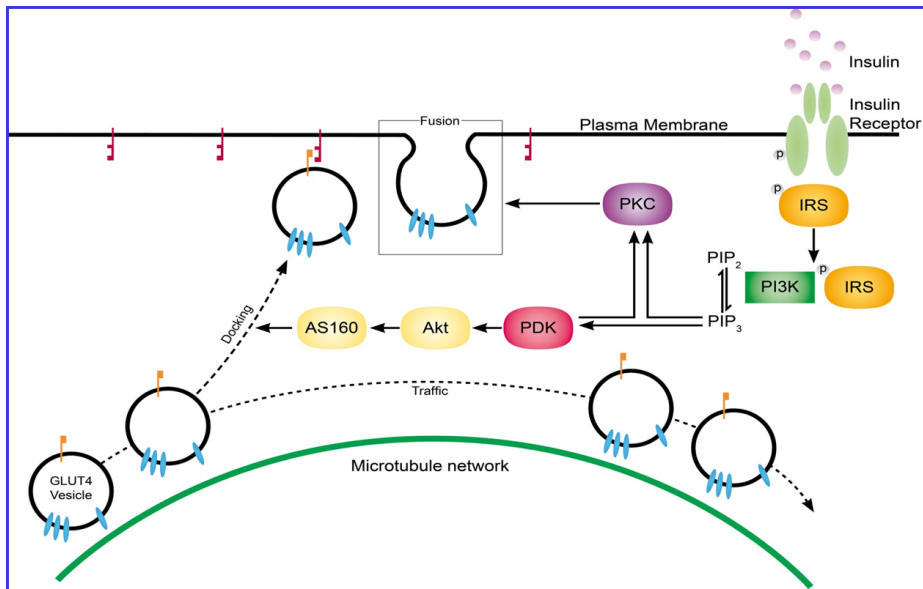
Figure 2.1: The overview of the insulin signalling pathway.

Insulin Signalling. It is widely accepted that GLUT4 redistribution is initiated when insulin binds to its specific receptor (IR) at the PM, and therewith, promotes tyrosine kinase activity of IR. Phosphorylation sites on the receptor act as binding sites for IR substrates (IRS), such as IRS-1, the best characterized substrate. Phosphoinositide 3-kinases (PI3Ks) bind to IRS proteins, and traffick to the PM where they can convert PIP2 into PIP3. This leads to to the phosphorylation and activation of downstream kinases, namely Akt and PKC-ξ, which then continue the signal transduction and pass on the insulin signal to the GLUT4 carrying vesicles to be translocated to the PM. Numerous experiments

on insulin-stimulated GLUT4 translocation have been performed. However, time course data describing the dynamics of the insulin signalling is limited. Understanding the dynamic behaviour of the insulin signalling is essential for the physiological function of the insulin signalling. To develop an ODE based computational model as part of the systems biology approach one needs such data to parameterize the model. Therefore, a few mathematical modeling studies on insulin signalling pathway have been carried out. Sedaghat *et al.* [95] proposed a large-scale detailed model for insulin signalling in which they included both the cycling of IR and the effects of feedback from downstream intermediates. In their work the model parameters (rate constants and initial component concentrations) were taken from the previous models without validation. Although this forward simulation approach produced some expected qualitative behaviors, its model predictions might not be sufficiently reliable because the parameter values might be chosen unrealistic, taking into account that most of those values are unknown, especially in vivo. The effects of these uncertainties on the predictions were not analyzed. Moreover, the model was constructed by combining previously existing models without validation. Cedersund *et al.* [20] adopted a different type of modeling approach by fitting model parameters according to experimental data and tested possible mechanisms for the early steps of insulin signalling; IR and IRS phosphorylation. Cedersund model successfully described the rapid transient overshoot of IR and IRS upon insulin stimulation and thus paves the way for further investigation.

GLUT4 Trafficking. GLUT4 is transported between intracellular depots and the PM by specialized vesicular compartments, also called GLUT4 storage vesicles (GSVs), which traffick along a microtubular network underneath the PM. It was commonly accepted that in the absence of stimulation, GLUT4 is almost completely excluded from the plasma membrane. The addition of insulin causes GLUT4 to shift from its intracellular location to the plasma membrane [19]. However, more recent studies of GLUT4 translocation reported a new hypothesis [4, 74]. In the basal state, the GLUT4 vesicles which are trafficking near the PM weakly, tether to the PM, and rarely fuse into it, slowly exchanging GLUT4 with the PM. Upon insulin stimulation, the vesicles tether to the PM tighter and more vesicles dock and fuse into the PM. Although insulin-facilitated interaction between GLUT4 vesicles and the PM can be experimentally observed, the underlying mechanisms still remain unclear. Bai *et al.* [4] indicate that the docking of GSVs to the PM might be the target of AS160, a substrate of Akt. The fusion step is also regulated by insulin and it is likely to involve a target of insulin action that is distinct from AS160. Substantial evidences also support a role for PKC-ξ, another downstream effector of PI3K, in GLUT4 translocation [31]. In this case, we hypothesize that PKC might be the regulator of the fusion step.

To investigate the regulatory interactions between insulin signalling and GLUT4 trafficking, a computational modeling approach is used in this chapter.

With this, we aim to gain a system-level understanding of the dynamics of the insulin signalling pathway by analyzing biological data with computational techniques. Two mathematical models have been developed (a mechanistically detailed model and a simplified model), covering both insulin signalling and GLUT4 trafficking, with AS160 and PKC-ξ as the convergence points. The experimental data used in this chapter were extracted from literature through text mining. Both models consist of ordinary differential equations (ODEs) and their parameters (i.e. the reaction rate constants)- and initial component concentrations were estimated by fitting the model to experimental time course data of observables. The developed models with these calibrated parameters were used for the analysis of the system dynamics, yielding useful predictions of unknown interactions. In order to obtain reliable quantitative information from the model, it is crucial to determine if the parameters were estimated accurately based on the data provided.Therefore, profile likelihood analysis is carried out to examine the identifiability of the parameters (i.e. How well model parameters are determined by the amount and quality of the provided experimental data) and determine their confidence intervals. Multi-parametric sensitivity analysis (MPSA) is then employed for identifying the network components and rate constants that are most critical to GLUT4 translocation. As robustness is an essential property of biological systems [60], both models were examined in terms of their ability to cope with environmental changes (parameter perturbations).

2.2 Model Development

2.2.1 ODE-model

The mathematical models used in this chapter are built up of first order nonlinear ordinary differential equations based on the study of Liu *et al.* [72]. The reaction rates are given by mass action kinetics. Suppose that the protein B activates the protein A by phosphorylating A into A^P:

$$A + B \underset{k_{-1}}{\overset{k_1}{\rightleftharpoons}} A^P \tag{2.1}$$
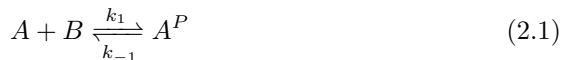
Based on the mass action kinetics of the phosphorylation reactions, the change of concentration for A and A^P in time can be described in the following ODEs:

$$\dot{x}_A = -k_1 x_A x_B + k_{-1} x_{A^P}, \tag{2.2}$$

$$\dot{x}_{A^p} = k_1 x_A x_B - k_{-1} x_{A^P}, \tag{2.3}$$

where x_A, x_B, and x_{A^P} are concentrations of A, B, and A^P respectively and k_1 and k_{-1} refer to the rate constant of the phosphorylation and the dephosphorylation respectively. Therefore, a mathematical model for a system with N components can be expressed as:

$$\dot{\vec{x}}(t) = f(\vec{x}(t), \vec{u}, \vec{\theta})$$
$$\vec{y}(t) = g(\vec{x}(t), \vec{u}, \vec{\theta}) \tag{2.4}$$
$$\vec{x}(0) = \vec{x}(t_0)$$

where $\dot{\vec{x}}$ is a vector of first derivatives of states $\vec{x}$. The initial concentration of $\vec{x}$ are given by $\vec{x}(0)$. The set of differential equations with the state variables of the system together with input function u and the kinetic parameters, θ, describe the dynamics and provide the future state and the output of the system given by $\vec{y}$.
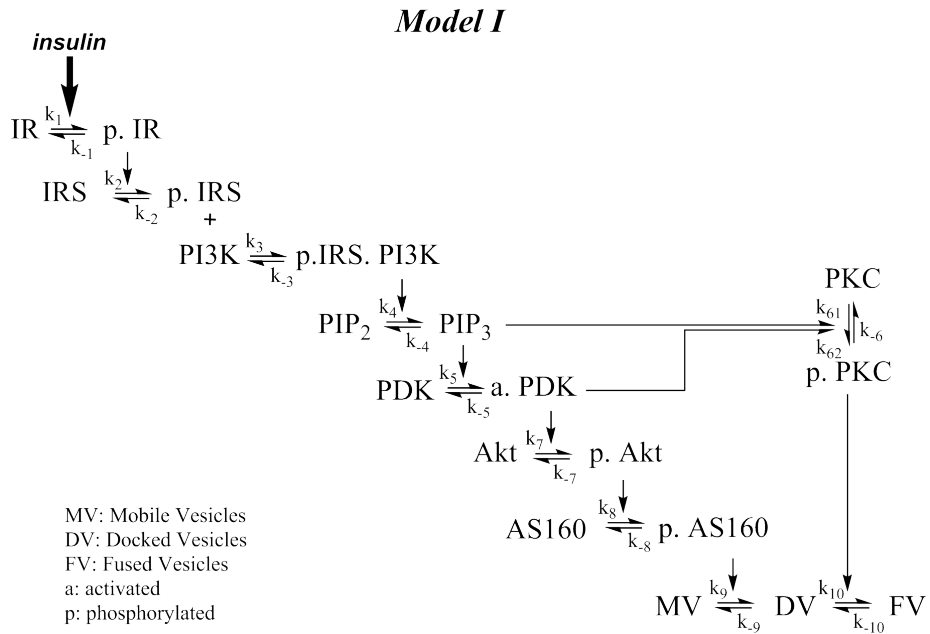
Model I

Figure 2.2: The scheme of *Model I*.

Based on the insulin signalling scheme proposed by Kyoto Encyclopeida of Genes and Genomes (KEGG) and GLUT4 trafficking scheme proposed by Lizunov *et al.* [74], an initial model, *Model I* is constructed, shown in Fig. 2.2. GLUT4 proteins traffick along microtubule as the cargo of GSVs. Insulin binds to IR and triggers the signalling cascade. Through a series of phosphorylation events, the signal is passed on to two PI3K-dependent mediators, AS160 and PKC-ξ, which link the insulin signalling to GLUT4 trafficking by regulating GSVs docking and fusion to the PM, respectively. The model is translated into a set of nonlinear ordinary differential equations (2.5-2.24) which are derived from the mass balance equations for each intermediate of the signalling cascade. Mass

action kinetics is used to refer the rate of phosphorylation/activation reactions.
Each reaction is assumed to be reversible. The model consists of 19 state variables
x and 23 kinetic parameters p, and 1 input u.

$$x_1 = u_1, \tag{2.5}$$

$$\dot{x}_2 = -k_1 x_1 x_2 + k_{-1} x_3, \tag{2.6}$$

$$\dot{x}_3 = k_1 x_1 x_2 - k_{-1} x_3, \tag{2.7}$$

$$\dot{x}_4 = -k_2 x_3 x_4 + k_{-2} x_5, \tag{2.8}$$

$$\dot{x}_5 = k_2 x_3 x_4 - k_{-2} x_5 - k_3 x_5 x_6 + k_{-3} x_7, \tag{2.9}$$

$$\dot{x}_6 = -k_3 x_5 x_6 + k_{-3} x_7, \tag{2.10}$$

$$\dot{x}_7 = k_3 x_5 x_6 - k_{-3} x_7, \tag{2.11}$$

$$\dot{x}_8 = -k_4 x_7 x_8 + k_{-4} x_9, \tag{2.12}$$

$$\dot{x}_9 = k_4 x_7 x_8 - k_{-4} x_9, \tag{2.13}$$

$$\dot{x}_{10} = -k_5 x_9 x_{10} + k_{-5} x_{11}, \tag{2.14}$$

$$\dot{x}_{11} = k_5 x_9 x_{10} - k_{-5} x_{11}, \tag{2.15}$$

$$\dot{x}_{12} = -k_{61} x_{11} x_{12} - k_{62} x_9 x_{12} + k_{-6} x_{13}, \tag{2.16}$$

$$\dot{x}_{13} = k_{61} x_{11} x_{12} + k_{62} x_9 x_{12} - k_{-6} x_{13}, \tag{2.17}$$

$$\dot{x}_{14} = -k_7 x_{11} x_{14} + k_{-7} x_{15}, \tag{2.18}$$

$$\dot{x}_{15} = k_7 x_{11} x_{14} - k_{-7} x_{15}, \tag{2.19}$$

$$\dot{x}_{16} = -k_8 x_{15} x_{16} + k_{-8} x_{17}, \tag{2.20}$$

$$\dot{x}_{17} = k_8 x_{15} x_{16} - k_{-8} x_{17}, \tag{2.21}$$

$$\dot{x}_{18} = -k_9 x_{17} x_{18} + k_{-9} x_{19}, \tag{2.22}$$

$$\dot{x}_{19} = k_9 x_{17} x_{18} - k_{-9} x_{19} - k_{10} x_{19} x_{13} + k_{-10} x_{20}, \tag{2.23}$$

$$\dot{x}_{20} = k_{10} x_{19} x_{13} - k_{-10} x_{20}, \tag{2.24}$$

where x stands for concentration of each element in the signalling pathway.

x_1	= insulin input		x_{11}	= activated PDK
x_2	= unphosphorylated IR		x_{12}	= unactivated PKC
x_3	= phosphorylated IR		x_{13}	= activated PKC
x_4	= unphosphorylated IRS-1		x_{14}	= unphosphorylated Akt
x_5	= phosphorylated IRS-1		x_{15}	= phosphorylated Akt
x_6	= unactivated PI3K		x_{16}	= unphosphorylated AS160
x_7	= IRS-1/PI3K complex		x_{17}	= phosphorylated AS160
x_8	= PI(3,4)P2		x_{18}	= mobile GLUT4 vesicles (MV)
x_9	= PI(3,4,5)P3		x_{19}	= docked GLUT4 vesicles (DV)
x_{10}	= unactivated PDK		x_{20}	= fused GLUT4 vesicles (FV)

2.2.2 Data obtained from the literature

A data- and hypothesis-driven modeling approach has been used for the studies presented in this chapter, which requires a comprehensive set of quantitative data. In order to have a quantitative mathematical model for signalling pathways, the kinetic parameters of the model need to be parameterised. However, in practice most of the quantitative information such as kinetic rate constants for interactions and enzymatic reactions are lacking. Accurate parameterisation of the model can be achieved through parameter estimation based on time course data of the intermediates of signalling cascades. The values of the parameters are estimated by fitting the model predictions to the time course of the intermediates. Thus, quantitative time course data has crucial role in developing the mathematical models.

To gather the required experimental data from the literature, a comprehensive text mining is conducted in collaboration with AstraZeneca. QUOSA Information Manager (Quosa) is used to extract specified full-text documents from PubMed database. Queries are classified per signalling intermediate, species, tissue, and sampling frequency. The purpose of this study is to collect frequently sampled, dynamic data from the same species and the same tissue, in particular, skeletal muscle is of interest among the other insulin-sensitive tissues. Although insulin signalling pathway has been studied for decades, most of the data available in the literature constitutes of the dose response data, steady state analysis and mostly (semi-)qualitative data. The quantitative time course data for the intermediates of the insulin signalling pathway is limited for the same species and tissue. Therefore, a composite data set from different studies, tissues [20, 67, 97, 98], which was obtained by Westernblotting, has been gathered to be used in the parameterisation of the generated models. To minimize the variety in the experimental conditions that may cause to uncertainty in the model predictions, the heterologous data needs to be normalised.

2.2.3 Parameter Estimation

Model parameters are estimated by fitting the model to the experimental data by using a weighted least square estimation algorithm. To this end, a cost function to be minimized is defined as follows:

$$\chi^2(\theta) = \sum_{i=1}^{n} \sum_{j=1}^{d_i} \left(\frac{y_i(t_j) - y_i(t_j|\theta)}{\sigma_{ij}} \right)^2, \tag{2.25}$$

where $y_i(t_j)$ denotes the data-point for the ith observable state, measured at time point t_j, $y_i(t_j|\theta)$ stands for the ith observable state predicted by the parameters θ at t_j, and σ_{ij} represents the standard deviation of the jth data-point of the ith observable state. The standard deviations (σ_{ij}) of the experimental data-points are used as the weighting criteria for the error between the corresponding data

point and the estimated observable state. A higher standard deviation of a data-point results in a lower weighting coefficient for the corresponding error (between the estimated state and the actual data-point).

To minimize the cost function in Eqn. 2.25, *lsqnonlin* routine in Matlab optimisation toolbox is utilised. A parameterised model is then used to estimate the dynamic profiles of the states which are not measured in the experiments, therefore it is important to check if the optimisation routine can find a unique solution for the model parameters. For this purpose, 500 uniformly distributed initial parameters (values between 0 and 1) are used in the optimisation routine. The lower bound for the parameters is set to 0 while there is no upper bound set. The estimated values which yield the 30 (taken arbitrarily) lowest cost function are referred to as the best estimated parameter sets in this chapter and the one with the lowest cost function is taken as the reference parameter set θ_{ref}.

The initial conditions are defined such that, at the beginning of the simulation, the unphosphorylated state variables are assumed to contain the total concentration of the intermediate (*e.g.* IR, MV) and hence, the concentration of the phosphorylated/activated state is 0. Most of the experimental data is obtained by western blotting, and therefore, is expressed in arbitrary units relative to a basal level. The steady state values of the system response to an insulin stimulation with an amplitude of 1 (arbitrarily chosen) are taken as the basal level of the state variables. To mimic the actual insulin stimulation, a step input with an amplitude of 10 is used. The normalisation of the experimental data allows for the arbitrary choice of the amplitude of the insulin input. Moreover, our main focus in this study lies on dynamic profiling of states in signalling pathways and not their actual values. Due to the lack of absolute concentrations of signalling intermediates, we limit our study to semi-quantitative modelling.

2.2.4   Introduction of feedback

Model parameters are estimated by fitting the model response to insulin stimulation to the experimental data. However, the model with estimated parameters cannot reproduce the overshoot behaviour of IR and IRS phosphorylation upon insulin stimulation which is characterized by a rapid initial transient response higher than the quasi-steady state level (experimentally observed by Cedersund *et al.* and Kublaoui *et al.* [20]). This is an expected outcome of *Model I* because no feedback regulation is incorporated yet. This result proves the need to augment the model with a regulatory feedback which is an important element of signalling pathways. Recent evidences suggest that some downstream intermediates may participate in positive and negative feedbacks in insulin signalling pathway [87, 88]. Cedersund *et al.* also indicated some downstream intermediates play a role in regulating IR phosphorylation by modeling a negative feedback from downstream intermediate, to explain the overshoot behaviour of IR and IRS upon insulin stimulation. However, the source of the feedback is not fully known.

To identify which intermediate most likely participates in this regulation, several negative feedback scenarios from downstream intermediates (PKC-ξ, Akt, AS160) have been introduced into *Model I*. The models are named as *Model IIa*, *Model IIb*, and *Model IIc* (shown in Fig. 2.3) for the feedback scenarios from PKC-ξ, Akt, and AS160 respectively. Michaelis Menten mechanism is adopted to model the negative feedback. The ODEs for p-IR and p-IR are modified as:

$$\frac{dx_2}{dt} = -k_1 x_1 x_2 + x_3 \left(k_{\text{-}1} + \frac{k_{fmax} x_i}{x_i + k_{fM}} \right), \qquad (2.26)$$

$$\frac{dx_3}{dt} = k_1 x_1 x_2 - x_3 \left(k_{\text{-}1} + \frac{k_{fmax} x_i}{x_i + k_{fM}} \right), \qquad (2.27)$$

where k_{fmax} and k_{fM} are parameters for feedback effect from x_i, describing the maximal activation and x_i concentration corresponding to half activation, respectively. For each scenario, the complete model is fitted to the experimental data by optimising parameter sets.

2.3 Model Analyses

2.3.1 Identifiability

The developed model is used for description of the dynamic behaviour of the signalling network, such as time courses of species concentrations that have not been experimentally observed. Since the models are parametric, to make sure that the model predictions are reliable, the model parameters should be well determined. In many cases, not all the biological reactions are experimentally observable. Insufficiency of experimental data could result in non-identifiability of parameters. Therefore, it is important to evaluate which parameter(s) of the model are identifiable. An approach exploiting profile likelihood to detect identifiability has been applied in this chapter [86].

The idea of the approach is to explore the parameter space for each parameter in the direction of the least increase in the cost function χ^2 (see Eqn.2.25). It can be calculated for each parameter individually:

$$\chi^2_{PL}(\theta_i) = min_{i \neq j} \left[\chi^2(\theta) \right], \qquad (2.28)$$

by re-optimisation of χ^2 with respect to all parameters $\theta_{i \neq j}$, for a range of values of parameter θ_i, therefore keeping χ^2 as small as possible alongside θ_i.

Confidence intervals of estimated parameters can be derived using a threshold in the likelihood [86]. An approximate likelihood-based confidence region for the parameter is the set of all values of θ such that:

$$\left\{ \chi^2_{PL}(\theta_i) - \chi^2_{PL}(\hat{\theta}_i) < threshold \right\} \qquad (2.29)$$
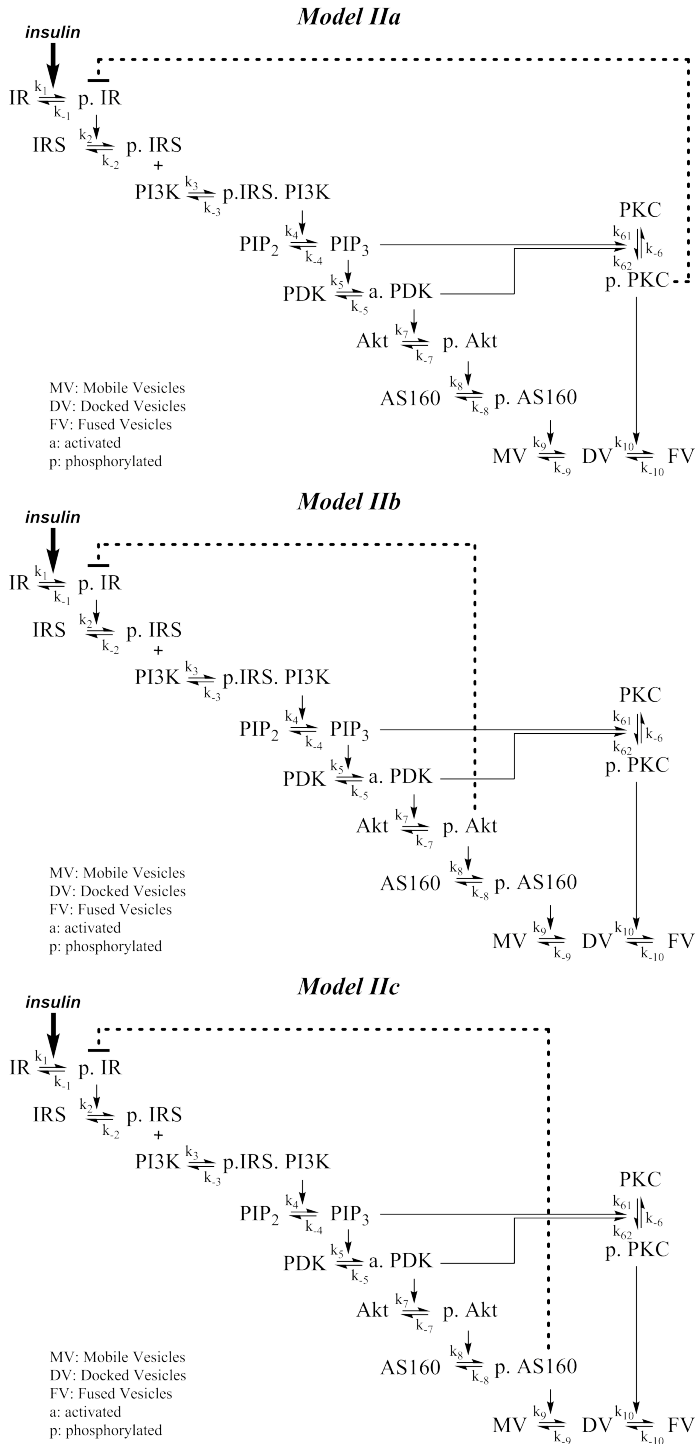
Figure 2.3: The schemes of *Model IIa, Model IIb, Model IIc.*

2.3.2 Multi Parametric Sensitivity Analysis

The model parameters are likely associated with a high degree of uncertainty as the experimental data used for parameter estimation are limited and heterologous. It is therefore important not only to study the dynamical properties governed by the particular kinetic parameters, but also to further investigate the effects of their perturbations on the overall system by performing MPSA. Sensitivity analysis also assists in the identification of the critical steps in the system [109].

Latin Hypercube Sampling (LHS) method has been used to sample the parameter values in the ranges 10% to 1000% of θ_{ref}. LHS is an efficient method to sample random parameter vectors while guaranteeing that individual parameter ranges are evenly covered. The model is simulated for each chosen set of parameter values and the corresponding objective function is calculated. The objective function is defined as the sum of squared errors between the observed and perturbed system output values. That is

$$f_{obj}(k) = \sum_{i}^{n} \left(x_{obs}(i) - x_{cal}(i, k)\right)^2 \tag{2.30}$$

where f_{obj} is the objective function that describes how much the system output deviates from the observed data by varying the parameters, $x_{obs}(i)$ denotes an observed system output value at the ith sampling time (this is to be substituted by the simulation result from the reference parameter values), $x_{cal}(i, k)$ denotes the perturbed system output value at the ith sampling time for the parameter variation set k, and n is the number of sampling time points [121].

The mean of the sensitivity values for all parameter sets is then defined as the threshold to determine the acceptable and unacceptable parameter sets. The parameter set that leads to a sensitivity value greater than the threshold is classified as an acceptable case while that less than the threshold is classified as an unacceptable one. For each selected parameter, the cumulative frequency is computed for both acceptable and unacceptable cases. We evaluate the sensitivity by a direct measure of the separation of the two cumulative frequency distributions. We use the following Kolmogorov-Smirnov (K-S) statistic:

$$K\text{-}S = max(|S_a(x) - S_u(x)|) \tag{2.31}$$

where S_a and S_u are the cumulative frequency functions corresponding to acceptable cases and unacceptable cases, respectively, and x is the given parameter. The statistic K-S is determined as the maximum vertical distance between the cumulative frequency distribution curves for n acceptable and m unacceptable cases. A larger value of K-S indicates that the system is sensitive to variation in the given parameter. Five dummy parameters are incorporated in the sensitivity analysis which have no influence on the model. The sensitivity algorithm assigns the dummy parameters small but non-zero sensitivity values. Parameters with

sensitivity less than or equal to the maximum sensitivity of the five dummy parameter should be considered not significantly different from zero.

Implementation To solve the systems of ODEs, Matlab ODE solver - ode15s has been chosen, which is able to handle stiff problems effectively. Although there is no precise definition of the stiffness, a differential equation can be said to be stiff when certain numerical methods for solving the equation are numerically unstable. Stiffness generally manifests when there are well-separated 'fast' and 'slow' time scales present. A given trajectory of such a system will generally exhibit rapid change for a short duration (corresponding to the fast time scales) called the 'transient', and then evolve slowly (corresponding to the slow time scales) [85]. For the function ode15s, error tolerances have to be defined. They are specified as relative and absolute tolerance. Relative error tolerance of 10^{-5} has been used in this chapter. As for absolute error tolerance, Matlab default value of 10^{-6} has been taken. To speed up the simulation, mex files generated by CVode Wrapper package for Matlab has been utilized [110].

2.3.3 Robustness Analysis

Robustness is considered as an important phenomena of biological systems for the maintenance of homeostasis [59]. For a single signal transduction pathway, relative rate constants in different cellular contexts may vary due to variations in individual cells. To investigate the ability of the system to maintain its behaviour against random perturbations, a robustness analysis method proposed by Zi *et al.* [122] has been applied. LHS was again used to sample parameter values. For each set of parameters, the system output of interests (in this chapter, the system output for robustness analysis was defined as steady state level of a certain component, such as GLUT4 content in the PM after insulin stimulation) was computed against the total parameter variation (TPV), which is defined as:

$$TPV = \sum_{i=1}^{N_p} \left| log_{10} \left(\frac{\theta_i}{\theta_{ref,i}} \right) \right|, \qquad (2.32)$$

where N_p is the number of the parameters and θ_i, $\theta_{ref,i}$ represent perturbed parameter value and reference parameter value respectively. A robustness metric, defined in Eqn. 2.33, is introduced to quantify the change of system output:

$$R_{TPV} = \frac{-\sum_{j=1}^{N_s} \left| log_{10} \left(\frac{y_j}{y_{ref,j}} \right) \right|}{N_s}, \qquad (2.33)$$

where y_j and $y_{ref,j}$; stand for the corresponding system output of the model with varied parameters and reference parameters ref , respectively. N_s is the total number of simulations. The closer R_{TPV} is to zero, the more robust the model is against the parameter variation.

Table 2.1: Summary of the changes of the GLUT4 vesicle docking and fusion rates upon insulin stimulation in *Model II*. Results are obtained from simulations with respective to 10 best estimated parameter sets.

	Docking rate fold increase	*Fusion rate fold increase*
Experimental data	2	8
Model IIa	5.09 ± 0.01	2.06 ± 0.09
Model IIb	4.94 ± 0.13	6.97 ± 0.61
Model IIc	2.29 ± 0.17	7.82 ± 0.05

2.4 Results

Feedback Three negative feedback scenarios from downstream intermediates (PKC-ξ, Akt, AS160) have been introduced into *Model I* to mimic the overshoot behavior of IR and IRS phosphorylation (See Fig.2.3). Each model (*Model IIa*, *Model IIb*, *Model IIc*) is fitted to the experimental data by optimising parameter sets as described earlier. According to the steady state analysis, each model is able to reproduce the overshoot of IR and IRS phosphorylation, and the simulated time courses are in close agreement with experimental observed time courses. Thus, new experimental data about GLUT4 vesicles change from Bai *et al.* has been taken as additional criterion. For each model, simulations with respect to 10 best estimated parameter sets have been performed to compute the increased fold of GLUT4 vesicle docking and fusion rate after insulin stimulation (see Table 2.1). Only *Model IIc* - the scenario with negative feedback from AS160 to IR phosphorylation - predicted the experimental results well. Thus, AS160 has been suggested as the source of the negative feedback in insulin signalling pathway. *Model IIc* - the scenario with negative feedback from AS160 to IR phosphorylation has been selected as the best model and was used in further analyses in the name of *Model II* in this chapter.

Time-Course Analysis. The simulation results regarding to the best parameter sets for *Model II* are shown in Fig. 2.4. The simulated time courses are in close agreement with the experimental data, which can be concluded from the analysis of the residuals. Upon insulin stimulation, both IR and IRS display a rapid initial transient response that is higher than the quasi-steady state level attained after about 5 minutes. This result is in accordance with the simulation result presented in the work of Cedersund *et al.*. Furthermore, the activity of Akt is also stimulated rapidly within the first 5 minutes and the level of stimulation remains elevated until it reaches the steady state. AS160, as the substrate of Akt, also exhibits the same behaviour. The MVs, in response to the insulin, deplete over time because more MVs tether and dock to the PM (see Fig. 2.5

). Despite of the increased docking rate (the rate that the MVs turn into DVs, which is denoted as $k_9 x_{17}$, (Eqn. 2.22),the number of DVs decreases as their fusion with the PM is facilitated by insulin. Meanwhile, the number of GLUT4 in the PM reaches and stabilizes at a value of 2.5-3 times over the basal level after 10 minutes.
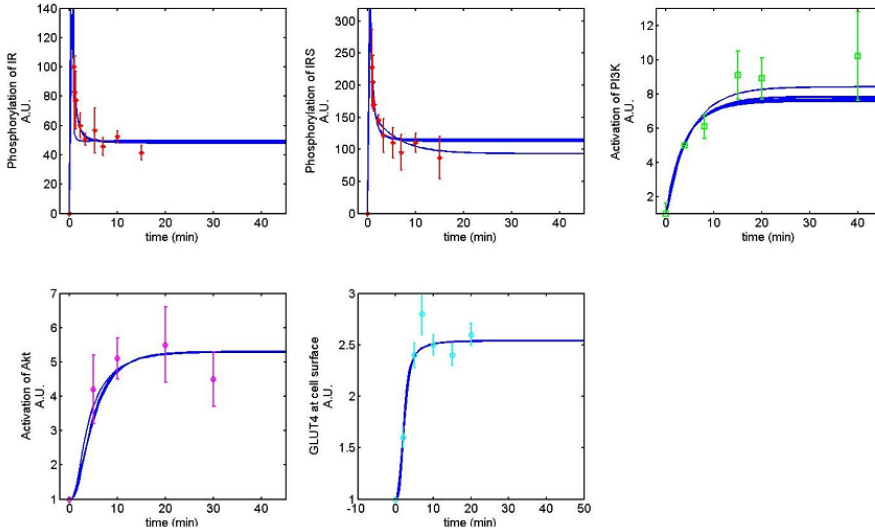
Figure 2.4: The simulations of the *Model II* (shown in blue lines). The experimental data from different sources are shown in different colours.

Independent data have been used to validate *Model II*. Bai *et al.* [4] have developed an approach to dissect and analyze the docking and fusion steps of GSVs, by which increases (≈8-fold) in the fusion rate and (≈2-fold) in the docking rate have been demonstrated. Earlier work by Koumanov *et al.* also reported an 8-fold increase of fusion activity stimulated by insulin [64]. The model well predict the increase the docking and fusion rates as (2.29 ± 0.17-fold) and (7.82 ± 0.05-fold).

Uncertainty and Identifiability Analysis Once the model describes the data, it is important to assess the certainty level of the model predictions. It is possible via quantifying the degree of confidence in the existing experimental data and parameter estimates [75, 111].The confidence interval of an estimate of a parameter is determined by setting a threshold for the increase of the profile likelihood. A parameter is considered identifiable if the confidence interval is finite, and vice versa. For non-identifiable parameters, Raue *et al.* [86] discussed two phenomena accounting for it: a) structural non-identifiability which is
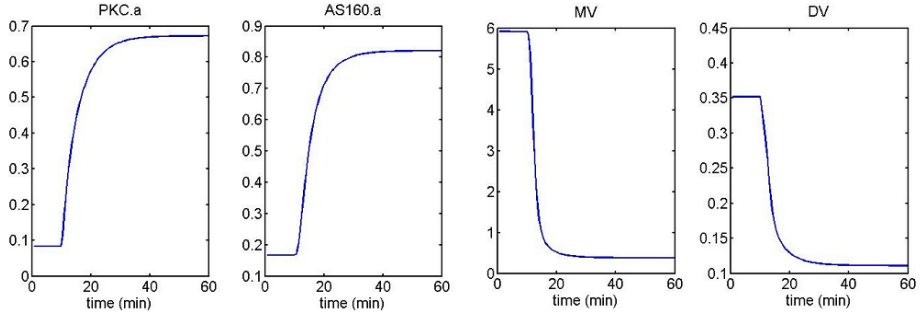
Figure 2.5: Model II Time courses of the variables that are not measured: PKC phosphorylation, AS160 activation, MVs and DVs.

related to a redundant parameterization in the model structure; b) practical non-identifiability which arises due to insufficient amount and quality of experimental data used for calibration.
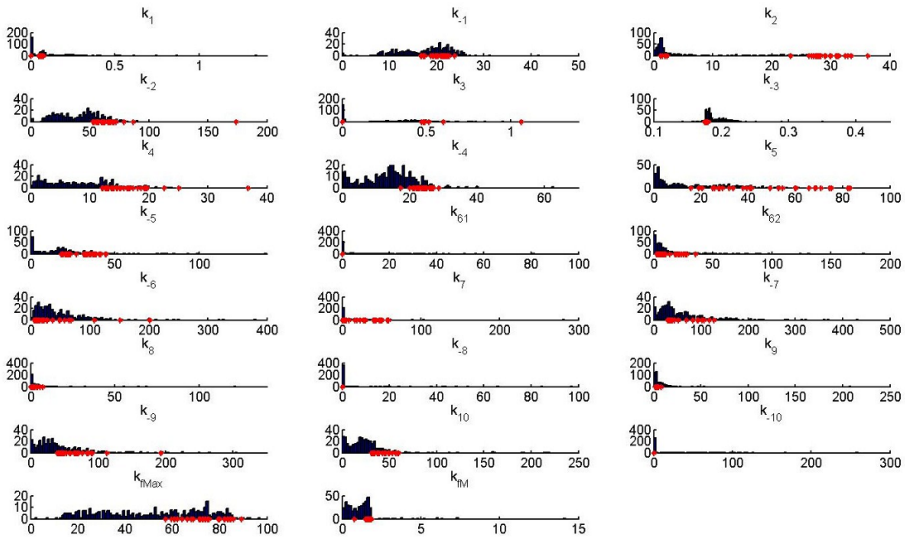
Figure 2.6: Distributions of each individual parameter of *Model II* after optimisation of the initial parameter distribution (500 runs). The red dots indicate the parameter values that yield the 30 lowest cost functions.

In this chapter, the profile likelihood of each parameter in *Model II^R* is exploited, as shown in Fig. 2.9. The result reveals that parameter k_1, k_2, k_3, k_{-3},

Table 2.2: Likelihood-based confidence intervals of *Model II^R*. θ_{ref} denotes the values of the reference parameters.

Parameter	θ_i	σ^-	σ^+
k_1	6.39e-005	$-\infty$	$+\infty$
k_{-1}	2.91	$-\infty$	12.39
k_2	0.79	$-\infty$	$+\infty$
k_{-2}	0.16	0.11	0.26
k_3	18.89	$-\infty$	$+\infty$
k_{-3}	8.91	$-\infty$	$+\infty$
k_4	38.25	10.19	$+\infty$
k_{-4}	1.69	0.28	$+\infty$
k_5	0.01	$-\infty$	$+\infty$
k_{-5}	0.56	0.25	3.75
k_6	13.95	$-\infty$	$+\infty$
k_{-6}	39.09	$-\infty$	$+\infty$
k_7	66.81	$-\infty$	$+\infty$
k_{-7}	0.53	0.18	2.51
k_{fmax}	6.64	3.90	24.76
k_{fM}	0.06	0.01	$+\infty$

k_5, k_6, k_{-6}, k_7 have relatively low profile likelihood along both increasing and decreasing directions, indicating their structural non-identifiability. However, parameter k_1, k_4, k_{-4}, k_{fM}, are practically non-identifiable, since they have a low profile likelihood for either increasing or decreasing directions, which indicates that either the amount or the quality of experimental data does not provide enough information to restrict the corresponding reaction rates.

Model reduction: *Model II* is based on a detailed insulin signal transduction scheme, where most identified intermediates are included. However, the large number of ODEs and the fact that data is measured with finite accuracy and only a subset of the state variables is accessible experimentally resulted in non-identifiability of many parameters. That in turn, increases the uncertainty of the model predictions. Therefore a reduced model *Model II^R* (shown in Fig. 2.7) has been developed covering the reactions/interactions of most interests. *Model II^R* was translated into ODEs with reduced number, 13, of state variables and 16 parameters. The model parameters are estimated by fitting model to the experimental data, as described before.

k_{-2}, k_{-5}, k_{-7}, k_{fmax} are identifiable and their likelihood-based confidence intervals are as listed in Table 2.

Multiple Parametric Sensitivity Analysis The parameters are associated with a high degree of uncertainty (See Fig. 2.6), and therefore, it is essential to examine the uncertainty of the model behaviour which generate from variations
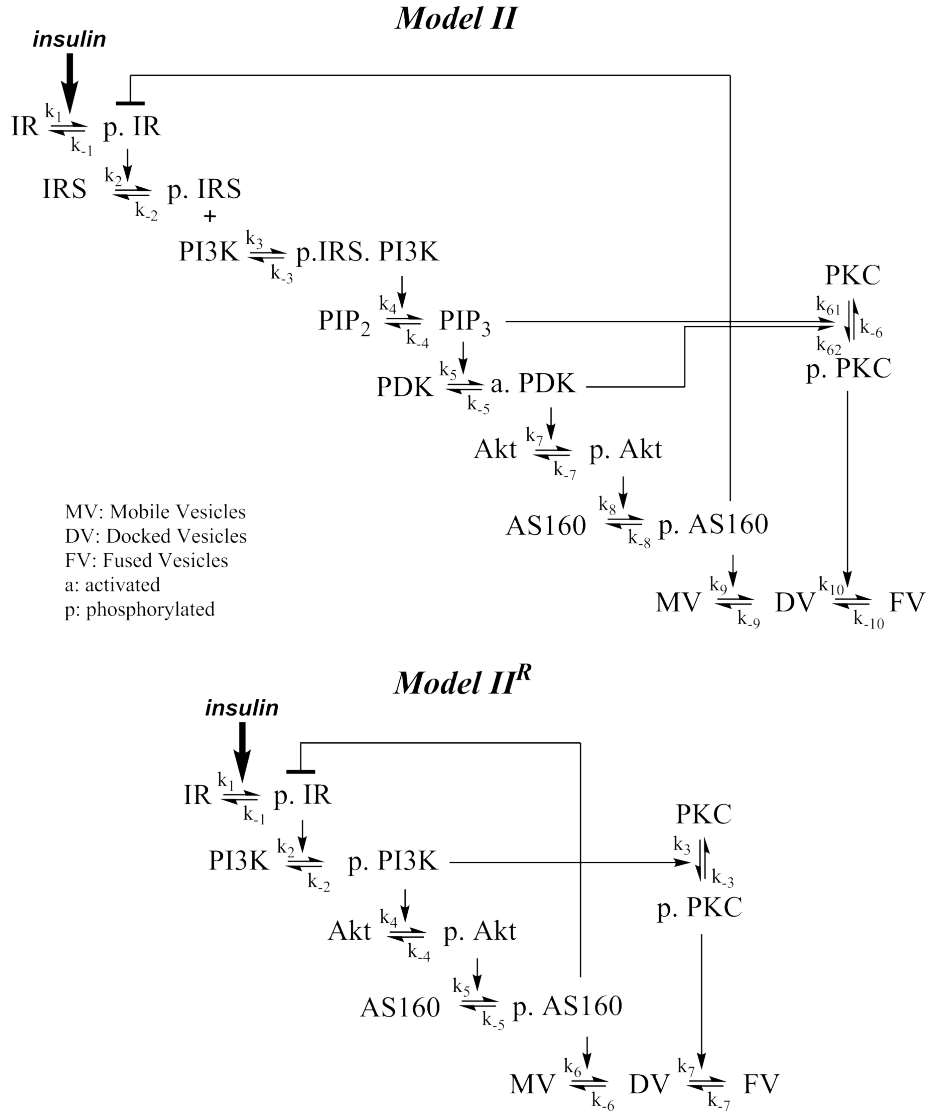
Figure 2.7: The schemes of *Model II* and *Model II^R* (*Model II Reduced* for the insulin signalling pathway.
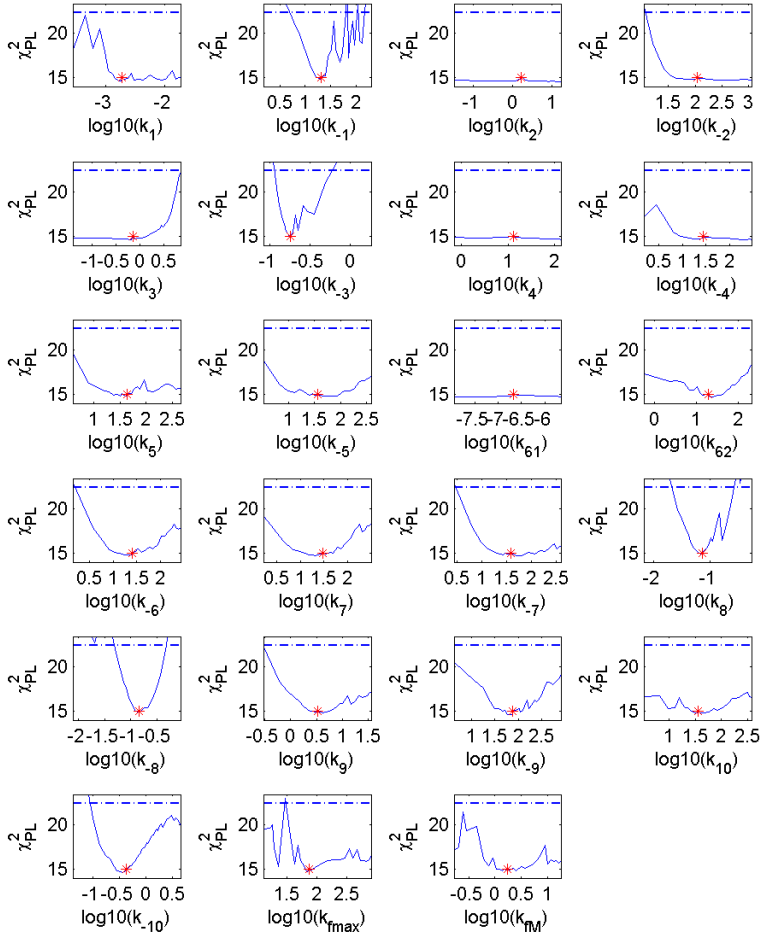
Figure 2.8: Profile likelihood of parameters for *Model II.* Red stars represent the calibrated parameter values θ_{ref}. The dashed line represents the threshold utilized to asses likelihood-based confidence regions for a confidence level σ.

in parameters by performing MPSA. As sensitivity analysis assesses how variations in model outputs can be apportioned, both qualitatively and quantitatively,
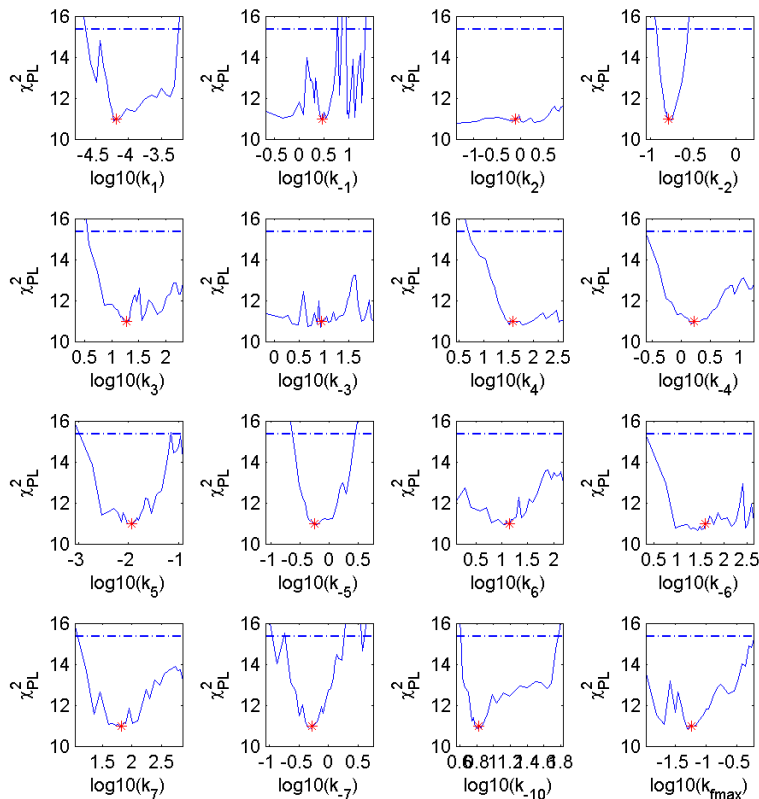
Figure 2.9: Profile likelihood of parameters for *Model II^R*. Red stars represent the calibrated parameter values θ_{ref}. The dashed line represents the threshold utilized to asses likelihood-based confidence regions for a confidence level σ.

to different input sources, it can also be used for identifying the critical steps in the system [75, 109]. For identifying the critical process in the insulin action, the sensitivity value is quantified by the summation of the weighted least square errors between the experimental time-course of GLUT4 in the PM upon insulin stimulation and the corresponding simulation results.

For the sensitivity analysis, 10000 uniformly distributed parameter sets were sampled by LHS. There is no aprior exact rule for determining the appropriate sample size. In order to determine if the sample size is sufficient, the method

adopted in this chapter systematically increases the sample size and checks if the sensitivity algorithm can consistently capture and rank a similar set of most important effects. If this holds between two consecutive experiments, it is concluded that there is no evident advantage in increasing the sample size. The corresponding MPSA results are shown in Fig. 2.10. Due to the fact that the dummy parameters should have no influence on the system, the maximum value of dummy parameter results has been taken as the threshold for determination of the sensitive parameters. Parameters that fall below this threshold are then considered as not the limiting step in the signalling process, because they only have minor effect on the system. On the contrary, high sensitivity of parameters suggests that these corresponding reactions have a critical role in the system response.

a)

b)

Figure 2.10: MPSA results for *Model II* based on **a)** GLUT4 translocation and **b)** the model fitness. The horizontal dotted line indicates the maximum sensitivity of the dummy parameters. Note that the parameters represent different reactions/interactions in the model.

In *Model II*, k_{62}, k_{-6}, k_9, k_{-9}, k_{10} and k_{-10} display high sensitivity with respect to their variations. This indicates that the corresponding reactions, namely PKC-ξ activation, GLUT4 vesicle docking and fusion have critical roles in the GLUT4 translocation. This result is consistent with the MPSA results for *Model II^R*, in which k_3, k_{-3}, k_6, k_{-6}, k_7, k_{-7} have relatively higher sensitivity values than the other parameters. When the sensitivity value is quantified as the summation of the weighted least square error between the complete experimental data and the simulation results (see Eqn. 2.25), the MPSA instead reveals the uncertainty in the model output that is caused by uncertainty in parameter input

variations and offers a way to assess the identifiability of parameters. If the
system output is highly sensitive to the variation of a parameter, this parameter
can be considered as being identifiable. It is obvious from the MPSA results that
more than half of the parameters in *Model II* display no significant impact on
the system output, herewith indicating non-identifiability of them, whereas most
of the parameters in both *Model II* and *Model II^R* exhibit a high influence on
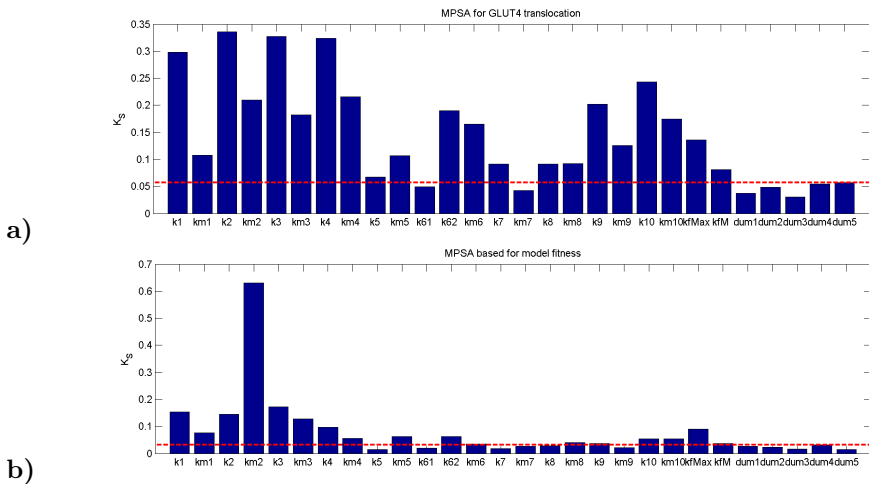the system output (see Fig.
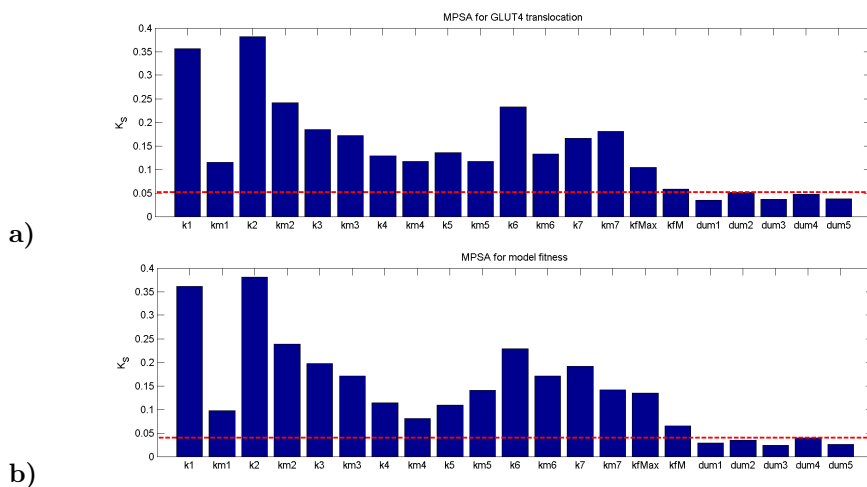
Figure 2.11: MPSA results for *Model II^R* based on **a)** GLUT4 transloca-
tion and **b)** the model fitness. The horizontal dotted line
indicates the maximum sensitivity of the dummy param-
eters. Note that the parameters represent different reac-
tions/interactions in the model.

Robustness Analysis The robustness of the system against parameter
variations has been tested, for which the results are shown in Fig. 2.12. The
system output is defined as steady state concentration of PKC-ξ, Akt, AS160,
DVs, and FVs respectively. The quantitative robustness metric for each system
output has then been computed and system output versus total parameter
variation is plotted. According to the definition, the smaller the robustness
metric value is, the more robust the system can be considered. In general, we
can conclude that *Model II^R* is more robust than *Model II*. This is in accordance
with the fact that *Model II^R* is more identifiable.

2.5   Discussion

The insulin signalling pathway has been of great interest to researchers in the past decades. Both experimental work and modeling were carried out to gain a better understanding of the underlying mechanisms. In this chapter, we established an ODE-based quantitative model (*Model II*) of insulin signalling pathway which is based on the experimental data. This model covers both a lately proposed GLUT4 trafficking scheme as well as the insulin signalling pathway. This approach differs from the previous pioneering work by Sedaghat *et al.*, where parameters and components concentrations in the model were taken directly from existing literature. Although they were able to reproduce some experimental data, the Sedaghat model was not comprehensively validated. The model validation was performed only on a small portion of the state variables and was merely of qualitative nature. Therefore, most assumptions and restrictions that used in the Sedaghat model remained unvalidated. Due to the lack of validation and questionable origin of component values, the Sedaghat model has not been widely used by other researchers. The model developed in this chapter does not include insulin receptor recycling (including receptor synthesis, degradation, exocytosis and endocytosis) which was applied by Sedaghat *et al.*, as our main interest lies on the downstream part, the potential 'metabolic effects' of insulin on GLUT4 translocation. The published experimental data sets used for parameter estimation cover the time courses of five molecules, among which the time courses of IR and IRS phosphorylation exhibit an 'overshoot' behaviour, in accordance with the study by Kublaoui *et al.*. Thus the model is built not only to mimic the insulin stimulation on the GLUT4 translocation but also to reproduce the overshoot of IR and IRS phosphorylation at the initial steps of the insulin signalling pathway. The insulin regulation on GLUT4 recruitment is believed to be accomplished via downstream intermediates, namely Akt and PKC-ξ.

However, the comprehensive understanding about the two proteins' role in the insulin signalling pathway is still lacking. Recent studies have suggested that GLUT4 vesicles' docking and fusion into the PM might be the main targets of the insulin action and that AS160 regulates the docking of GLUT4 vesicles. It was also pointed out, based on the experimental observations, that the increase of fusion rate is main regulatory step of insulin stimulation. Thus we propose a possible link between PKC-ξ and GLUT4 fusion step. The role of PKC-ξ was validated by comparing the simulation result (increase fold of both docking and fusion rates) to independent experimental data (other than the ones used for parameter estimation). The potential interaction between insulin signalling and GLUT4 trafficking was then addressed.

Two models have been built in this chapter to explore the potential interactions between insulin signal transduction and GLUT4 translocation: one with a detailed signalling cascade (*Model II*) and one with only important intermediates

of most interest (*Model II^R*). Despite the structural difference, both models were able to reproduce experimentally observed time course of IR, IRS phosphorylation, PI3K, Akt activation and GLUT4 content in the PM, as well as the change of GLUT4 vesicles' fusion rate upon insulin stimulation. During identifiability analysis, however, two models showed different properties. Although insufficient experimental data used for calibration introduced uncertainty of parameters, a few parameters of *Model II^R* are identifiable, with finite profile-likelihood-based confidence intervals. Some parameters are practical non-identifiable, suggesting further improvement of experimental data could improve their accuracy. As for *Model II*, most parameters have relatively at profile likelihood curves, denoting the structural non-identifiability, which is caused by redundant parameterization and can be improved by reduction of the model. Plus, *Model II^R* is more robust than *Model II*, considering the change of the interested system output against total parameter variations. Therefore, *Model II^R* is preferred in this chapter.

Insulin regulation of GLUT4 translocation is considered to be a multi-step process [4, 49, 116], yet identifying and biochemically characterizing the key regulatory step is challenging. To investigate which step(s) could be the main regulation target of insulin, the MPSA has been used to test the system output sensitivity against parameter variation for both models. As the convergence point of insulin signalling and GLUT4 trafficking was indicated to lie in downstream steps, the MPSA mainly focused on the parameters associated with downstream signalling cascade. Assuming each GLUT4 vesicle contains the same amount of GLUT4 proteins, the time course of vesicles fused into the PM is interpreted as the time course of the GLUT4 content in the PM, considering all the experimental data are relative values. The MPSA results indicate that, for both models, PKC-ξ activation, GLUT4 vesicles' docking and fusion into the PM are the critical steps in the system. As insulin is hypothesized in both models to regulate the fusion step via PKC-ξ, the main targets of insulin action were concluded to be the vesicle docking and fusion events. This is in accordance with recent studies on GLUT4 translocation: biochemically, the fusion of GLUT4 vesicles with the muscle or fat cell membrane is mediated by the SNAP-associated receptor (SNARE) proteins VAMP2, syntaxin4 and SNAP23 [61]. The t-SNAREs syntaxin4 and SNAP23 in the plasma membrane form a ternary complex with the v-SNARE VAMP2, which is contained in the GLUT4 vesicles. It is hypothesized that in the basal state, association of Synip with syntaxin4 functions to reduce the plasma membrane docking/fusion of GLUT4 vesicles. A signal from the activated IR then induces the dissociation of Synip from syntaxin4, freeing additional plasma membrane docking sites for VAMP2 and permitting GLUT4 vesicle fusion [19, 52, 76]. Also the MPSA results suggest the relevance of further investigation on the potential effector(s) on the GLUT4 vesicles docking and fusion steps.

Activation of cell-surface receptors and their downstream targets leads to spatial relocation of multiple proteins within the cell. The insulin signalling pathway involves not only protein-protein interactions and phosphorylation

events, but also the translocation of signalling proteins to specific cellular location (*e.g.* Akt phosphorylation in the insulin signalling pathway is spatial confined to the PM [77]). However, both models in this chapter do not include the spatial dynamics of the system. As the regulation of signalling within the cellular space has the effect on a number of physiological processes [58], future models should evaluate the importance of relocation of signalling proteins in the insulin signalling pathway and integrate experimental data on spatio-temporal dynamics of signalling from different cellular compartments.

In sum, we have developed mathematical models to gain reliable metabolic insights in insulin stimulated GLUT4 translocation and proposed the potential interactions between insulin signal transduction and GLUT4 trafficking: insulin signalling intermediates AS160 and PKC-ξ pass on the signal and regulate the GLUT4 vesicle docking and fusion to the PM, respectively. Moreover, AS160 has been suggested as the source of the negative feedback to insulin receptor. However, to further support this suggestion, experiments with AS160 protein as target should be performed to quantify its effects on regulation of IR phosphorylation and the whole insulin signalling process. Both GLUT4 vesicle docking and fusion have been suggested as the critical process of the system. Thus, quantitative experimental study on vesicle docking and fusion events, as well as PKC-ξ regulation effect on fusion-associated proteins are suggested.

The need of own data set

The parameters of the developed model are estimated based on the composite data set which combines heterogenous studies. These studies were conducted for different cell types under different experimental conditions. Most of the parameters in *Model II* have been observed to be non-identifiable which might be caused by combining different sources due to the fact that the kinetic parameters of interactions of proteins in signalling cascade are highly dependent on cell type. Each study provides data for only a limited number of intermediates and data could only be sampled for limited time points due to practical restrictions in Western blotting method. Therefore, understanding of intermediate steps in signalling through GLUT4 translocation is still limited and the system level information on the short term dynamics of the intermediates of the insulin signalling pathway is lacking. The nonidentifiability of most of the model parameters in *Model II* indicates the uncertainty of the model predictions. The underlying reason of identifiability problems of the developed model is the mismatch between the available and the data required to uniquely identify the model structure. A possible approach for decreasing the non-identifiability (which arises from the limited data in the interactions) to some extent, is to reduce *Model II* into *Model II^R*, which results in comprimising the obtainable information on the intermediates on IRS, PIP2, PIP3, and PDK. A more favorable solution for overcoming this limitation is to generate a high resolution temporal data set for a broader subset of intermediates from the same cell type in order to develop an

identifiable model that can provide predictions with higher certainty. In Chapter 4, such data from skeletal muscle cells is generated by a combined platform of high-throughput techniques in immunocytochemistry and fluorescence imaging. In the following chapter, the methodology with respect to the quantification of the data is presented.

2.6   Appendix

Both *Model II* and *Model II^R* well predict the increase of fusion rates (see Table 2.1). However, the simulated docking rate increase from *Model II* is closer to the experimental observation than that from *Model II^R* as seen in Table 2.3.

Table 2.3: Summary of the changes of the GLUT4 vesicle docking and fusion rates upon insulin stimulation

	Docking rate fold increase	*Fusion rate fold increase*
Experimental data	2	8
Model II	2.3	7.8
Model II^R	4.9	8.0
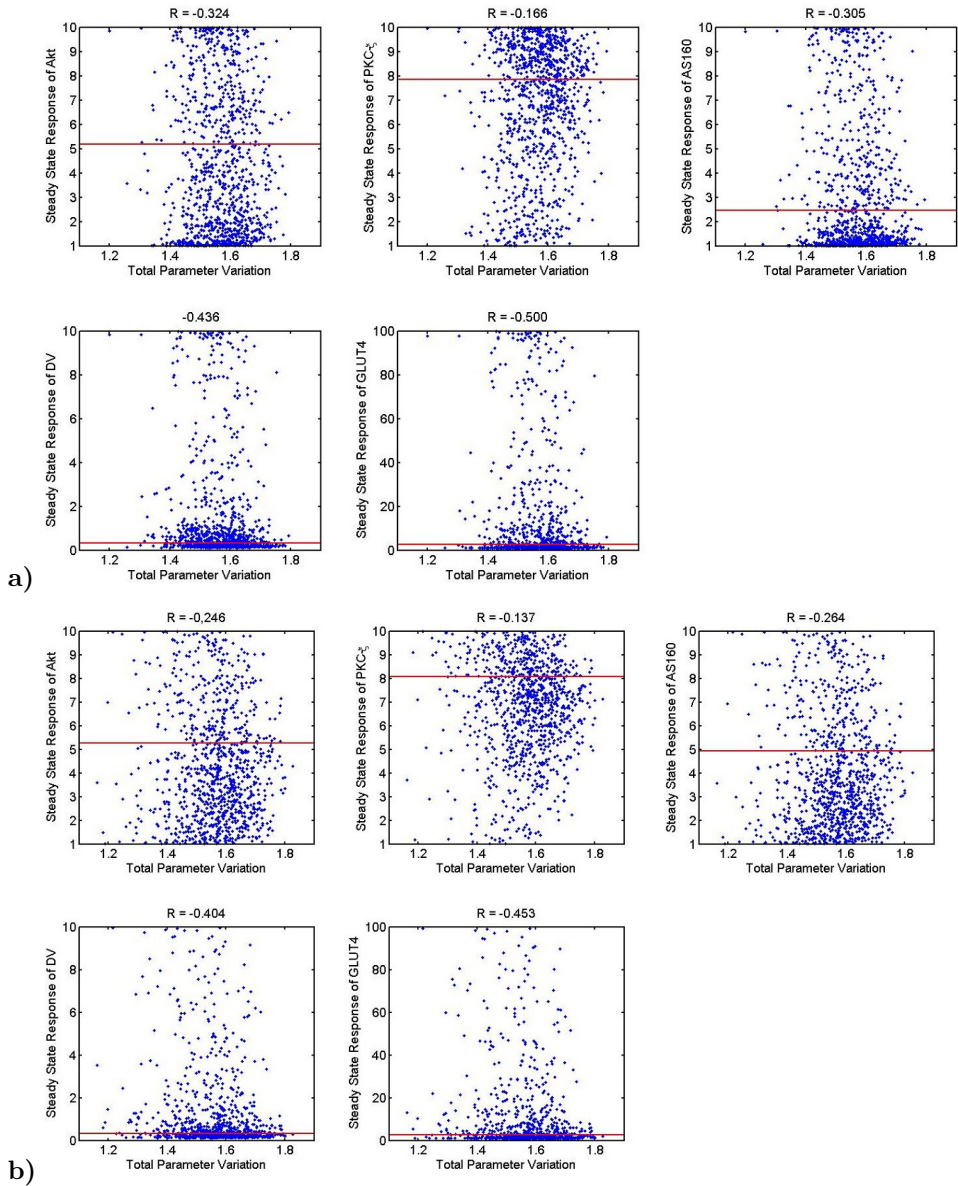
Figure 2.12: Robustness analysis of the steady state response of **a)** *Model II* and **b)** *Model II^R* respectively, against simultaneous variations of the parameter values. The red lines correspond to the reference steady state response. The blue points correspond to the steady state response under perturbed parameter values. The corresponding robustness metric are also shown.
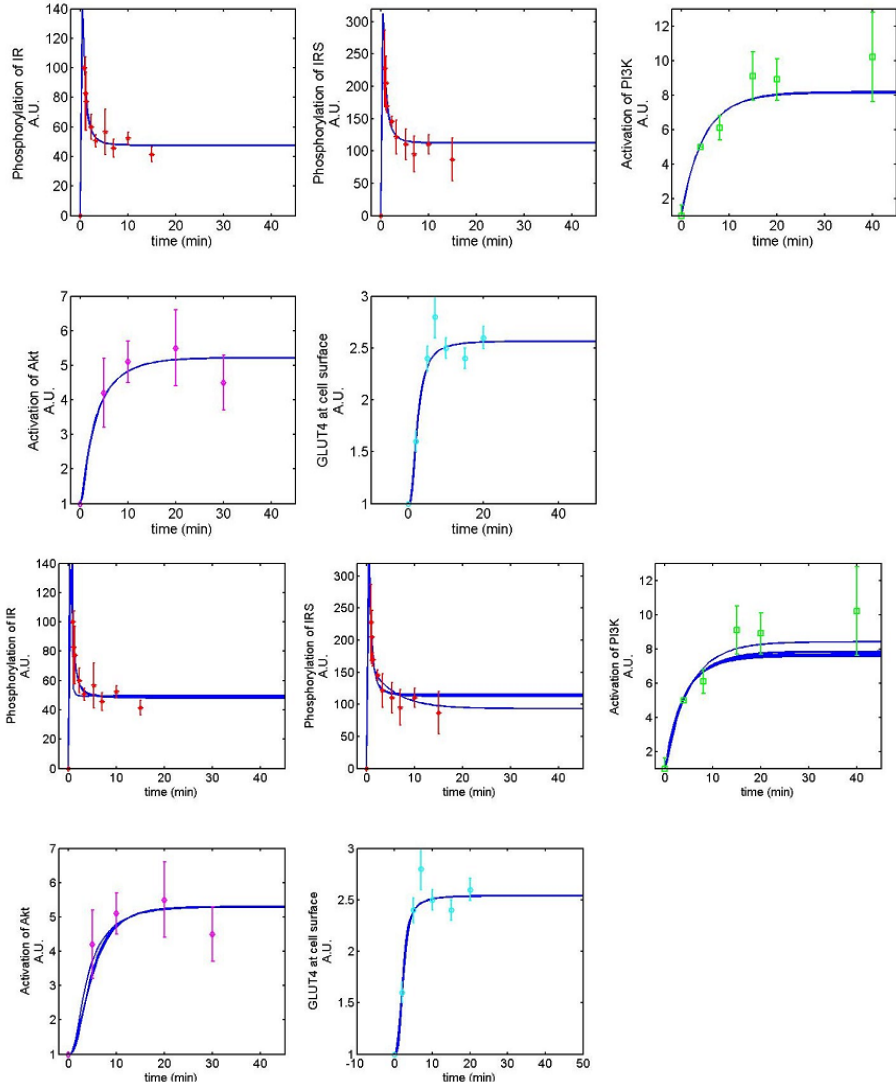
Figure 2.13: Simulation results of *ModelIIa* (feedback from PKC)(top)
and *ModelIIb* (feedback from Akt)(bottom): time courses
for IR, IRS-1 phosphorylation, PI3K, Akt activation and
GLUT4 content in the PM upon insulin stimulation. Both
the experimental data and simulation results with respect
to 30 best parameter sets are shown. Data from different
researches are labeled with different colors and expressed in
arbitrary unit
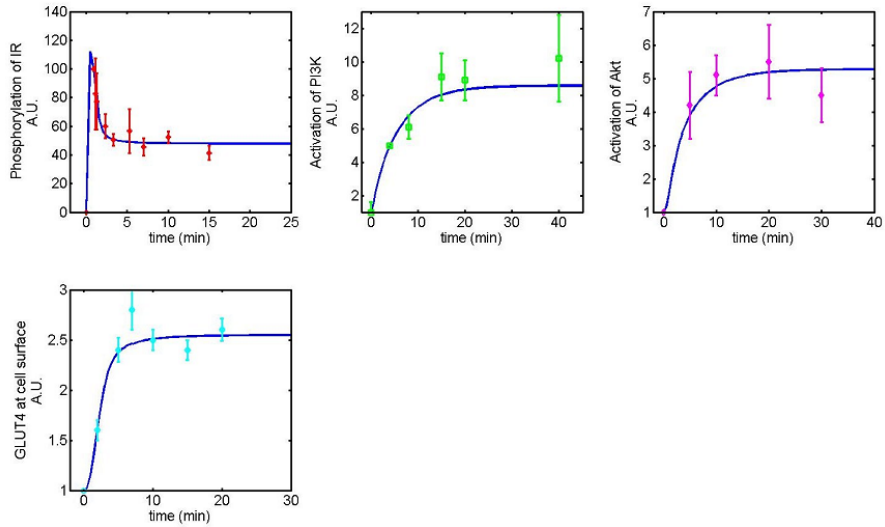
Figure 2.14: The simulations of the *Model II^R*.
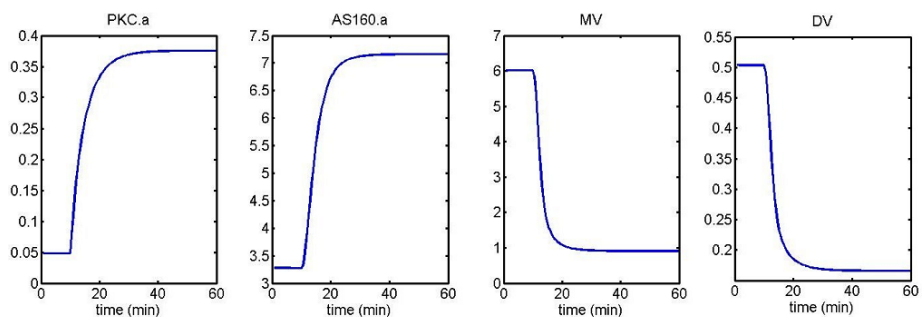
Figure 2.15: Model II^R simulation results: Time courses of the variables that are not measured: PKC phosphorylation, AS160 activation, MVs and DVs.

Chapter 3

Fluorescence image quantification for systems approaches of signalling pathway dynamics

Abstract

To generate reproducible data, quantification of the raw data (fluorescent images) is as important as generating the data. The methodology used to quantify the raw images may lead to inconsistencies in data presented in Chapter 4. In this chapter, we study the accuracy of the thresholding method to detect the accurate dynamic profile of the proteins in insulin signalling pathway. We show that the thresholding method can result in misinterpretation of the dynamics of the proteins. To overcome the misinterpretation of the data, we propose a method which provides an automatic quantification of the fluorescent data.

3.1   Introduction

The availability of new fluorescent labeling reagents, such as Alexa probes, makes it possible to choose an optimal fluorophore within a defined wavelength range. The expression of fluorescent chimeric proteins (Green Fluorescent Protein (GFP) and variants) [71] has become a widely used methodology to study the behaviour of proteins in living cells. In parallel, high resolution, multi-mode and automated fluorescence microscopes have been developed with improved, better performances for analyzing protein dynamics and interactions. Fluorescence image analysis allows us to measure concentrations of fluorescent probes in cells with microscope spatial resolution. It can be used for quantification of in situ hybridization signals, immunofluorescence labeling, fluorescence staining, Green Fluorescent Protein (GFP) expression and for microarray reading [33]. With quantitative and objective data, it is possible to better detect changes, i.e. in fluorescence intensity or in the extent of labeling, and to classify specimen and interpret the results in relationships with experimental, functional, biochemical or clinical data [100].

Fluorescent microscope imaging technologies have seen rapid developments in recent years. High-throughput 2D fluorescent imaging platforms are now in wide use and are being applied on a proteome wide scale. Multiple fluorophore imaging of cells is being used to give detailed localization and subcellular structure information. However, quantication and calibration of images in fluorescence microscopy is notoriously difficult [5]. In parallel with the developments in imaging technologies, significant research has gone into developing new methodologies for quantifying and extracting knowledge from the imaging data [42]. High-throughput screening of large numbers of images requires higher throughputs for image acquisition and image analysis. Furthermore quantitative descriptions of subcellular localization patterns and cell characteristics are needed. High-throughput systematic and quantitative analysis of protein phosphorylation patterns would enable to visualize the signals going through the signalling pathways.

The quantification of the acquired data is also essential in building mathematical models of signalling pathways which can provide insight in the kinetics of signalling. The data is used in identification, parameterization, and development of mathematical models. The protein-protein interaction networks can be quantitatively constructed in the light of accurately quantified, reproducible data. Therefore, accurate quantification of fluorescent data is as important as generating the data set. In this chapter, we discuss the drawbacks of the widely used thresholding method for the quantification of fluorescent data which is generated to detect the phosphorylation of the proteins within the insulin signalling pathway from a systems biology perspective. To overcome these drawbacks, we propose an image analysis framework that combines an automated thresholding method with an intensity based method optimized for the quantification of the
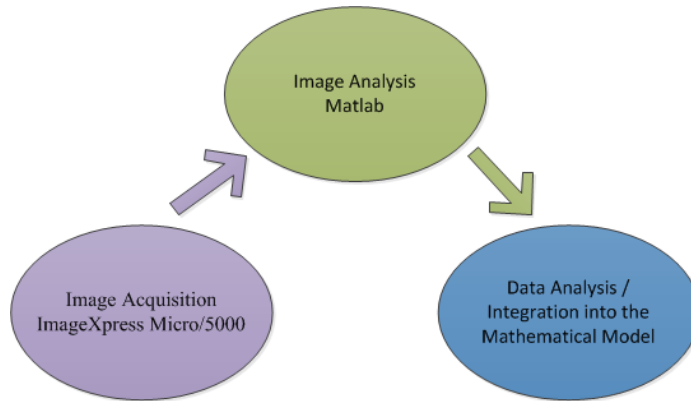
Figure 3.1: Schematic diagram of fluorescent image processing.

phosphorylated proteins in skeletal muscle cell lines.

3.2 Fluorescent Image Quantification

The fluorescent raw images used in this chapter are acquired by fluorescence imaging (See Chapter 4) following the immunocytochemistry assays on insulin stimulated skeletal muscle cell lines. Multiplexing is used in immunocytochemistry assays to detect the nuclei, the differentiated muscle cells, and the target phosphorylated protein. In this case, Alexa-488(green) fluorescence was used to detect the targeted protein, Hoechst (blue) was used to detect nuclei in the cells and Cy5 labeled Tubulin antibody (red) was utilized for differentiated muscle cells. In quantification of the target phosphorylated proteins (e.g. green fluorescence), tubulin (red) staining has an important role in detecting the objects/masks that refer to the differentiated muscle cells.

There are mainly two methods to quantify the fluorescence images depending on the focus of the study, namely, 1) Pixel based (e.g. thresholding) and 2) Intensity based methods. For the pixel based quantification method, the commonly used algorithm is as follows:

3.2.1 Pixel based quantification in selected regions

In pixel-based image analysis algorithms, objects of interest are extracted through a series of filters, including intensity thresholds, proximity, gradients, and edges. The upper and lower thresholds for the intensity are calculated based on window setting and intensity distribution in the neighborhood of a seed point. Both the window settings and the seed point are provided by the user.

The current algorithm used in quantification of the fluorescent images is as follows:

- Segmentation of the image in pixels,

- Selection of the low and high threshold for tubulin staining to determine the differentiated tubes in the wells as dark and bright tubes,

- Selection of the mask regions using tubulin staining which refer to differentiated tubes in the wells,

- Determinination of the threshold for dark and bright markers in target staining,

- Counting the number of pixels within the mask which have target protein signal higher than the target protein threshold.

In this method it is really crucial how the threshold is selected since the quantification and hence the dynamics of the phosphorylation are highly dependent on the thresholds for determination of the mask and the detection of the target protein within these masks, as can be seen in Fig. 3.2, 3.3, 3.4. In order to provide reproducible data set, the selection of the thresholds need to be automized.

Table 3.1: Peak time of the phosphorylation of Akt-T upon 100 nM insulin for various thresholds

Thresholds	*Thresholds for target*					
for tubulin	8500	9000	9500	10000	10500	11000
	Peak Time[min]					
9000	25	25	25	3	3	3
9500	25	25	25	3	3	3
10000	25	25	25	3	3	3
10500	25	25	25	3	3	3
11000	25	25	25	3	3	3
11500	25	25	3	3	3	2
12000	25	25	3	3	3	2
12500	25	3	3	3	2	2
13000	25	5	3	2	2	2

Two separate threshold values are selected for the quantification of multiplexed fluorescent data. First is selected to determine the masks which are the differentiated tubes in cells. Second is used to detect the target phosphorylated proteins within these masks (e.g. differentiated tubes). Here we show that the manual selection of these thresholds may result in inaccuracies. It can be seen in
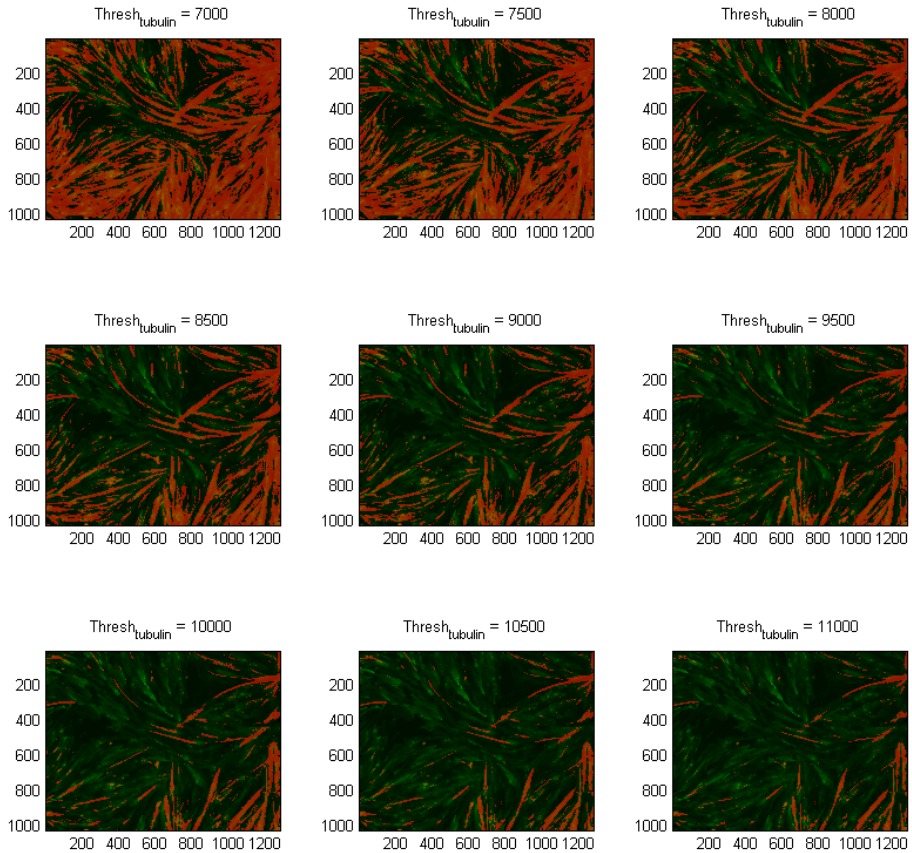
Figure 3.2: Influence of thresholding on tubulin staining. The intensity threshold for mask determination is changed from 9000 to 13000. Masks are shown in red and target protein signal is shown in green in each figure. Axes represent the coordinates of the images.
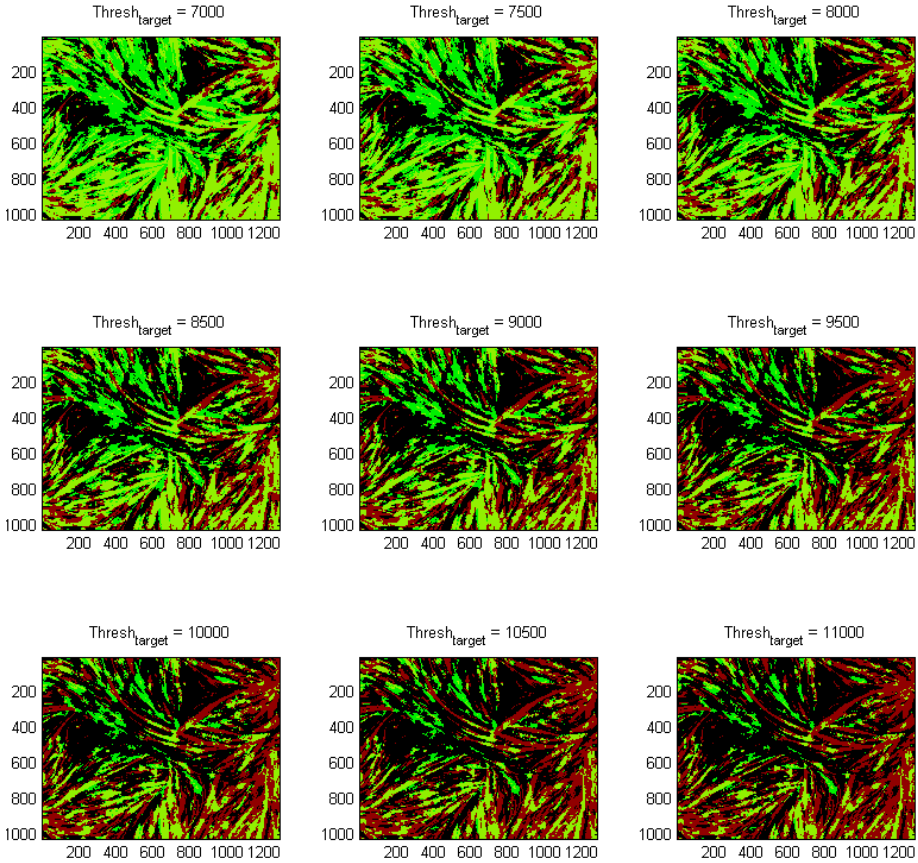
Figure 3.3: Influence of thresholding on target staining. The intensity
threshold for target marker is changed from 7000 to 11000.
Masks are shown in red and target protein signal is shown in
green (outside of masks) and yellow (inside of masks) in each
figure. Axes represent the coordinates of the images.
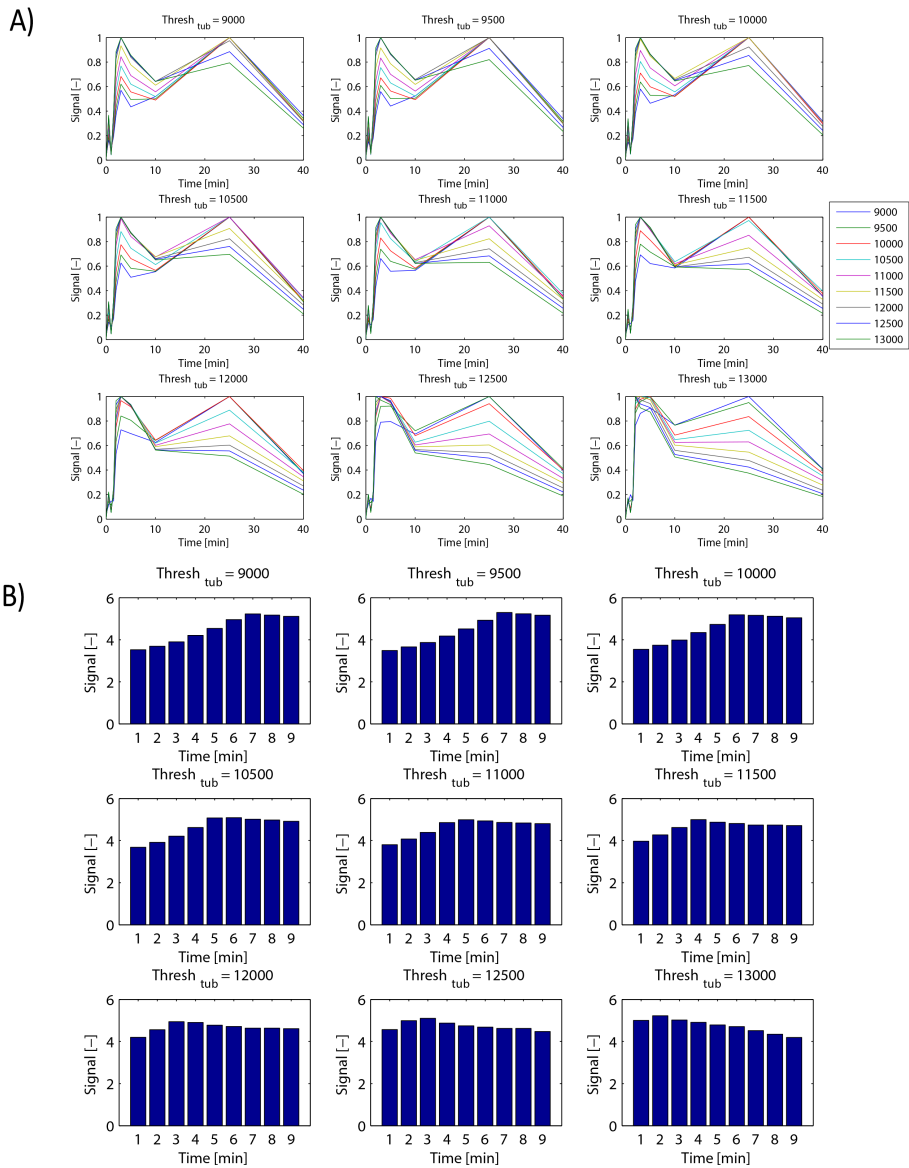
Figure 3.4: A) Each figure represents quantification of p-AktT using different tubulin thresholds for mask determination (Tubulin threshold range = 9000-13000). The signal is normalised with respect to the maximum value. The curves in different colors represent different marker thresholds (Marker threshold range= 7000-11000). B) Area under the curves given in A).

Fig. 3.4 and Table 3.1 that varying the thresholds for target staining can result in different kinetic parameters such as peak times and the area under curve in the phoshorylation of the proteins. These parameters are then used in the identification of the dynamics of the signalling pathway. The uncertainty arising from manual selection can therefore lead to misinterpretation of the dynamics of the protein activation. Moreover, data/information loss can occur due to heavy filtering of thresholding in tubulin staining that is used in object/mask detection. Furthermore, inaccurate thresholding can also lead to quantization error and misinterpretation of the data. Hence, there is need for an advanced method for the quantification of the data.

3.2.2   Intensity based quantification in selected regions

Due to the aforementioned drawbacks of the thresholding method, we developed an alternative automated quantification method which is robust to the selection of thresholds in determining the mask and the target proteins within the masks. The algorithm of the proposed method is as follows:

- Use tubulin staining for mask determination.

- Select an optimum threshold for mask determination.

- Check the intensity of the target staining in the mask.

- Grow the mask region via flood filling algorithm.

  1. Choose the seed objects in tubulin staining.
  2. Determine the neighboring pixels by using convolution theorem.
  3. Check the target intensities in the neighboring pixels and add them to the region if they are above the mean of the intensity of the target protein.
  4. Repeat step 2 for each of the newly added pixels; stop if no more pixels can be added.

- Sum the target intensities within the grown masks.

- Calculate the volume and the area of the masks.

- Normalise the sum of the target intensities in all the masks (objects) with respect to the total volume of the masks and area of the masks in each image.

The intensity threshold for tubulin staining to determine the seed objects is calculated once per one plate of cells. The same threshold is used in determining the seed objects in all the wells from the same plate. The neighboring pixels are determined by using the convolution theorem. The area of the seed objects are
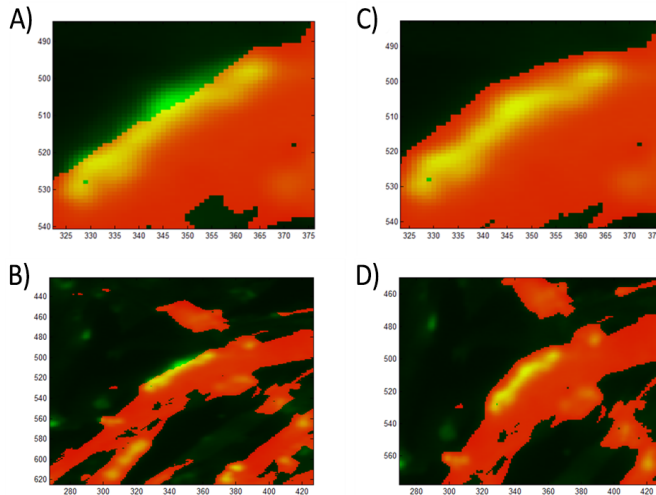
Figure 3.5: A) and B) Seed masks; C) and D) New masks updated by region growing algorithm. Masks are shown in red and target protein signal is shown in green in each figure. Axes represent the coordinates of the images.

extended by adding the neighboring pixel if the target intensity in that specific pixel is higher than a certain threshold. The threshold for target staining is calculated for each target staining individually and kept constant for the time course of each protein phosphorylation. In each addition of the neighboring pixel to the seed objects the seed objects are updated. The region growing routine is repeated until there is no change between the area of the new objects and the seed objects. The area of the objects is calculated by summing the pixels whereas the volume is calculated by summing the tubulin intensities within the object area. The normalised data for each object are summed through the whole site. Then target intensities within the objects (tubes) are summed and normalised with respect to the total area of the objects and to the volume of the objects within each image.

It can be seen in Fig. 3.5 that region growing algorithm allows us to catch the signal near by the edge of the mask and prevents data losses. After obtaining the tubes (final grown masks), the sum of target intensities in the tubes are normalised with respect to the area and the volume of the all tubes separately.

3.3   Evaluation of the methods in the view of systems aproaches

The raw data (fluorescent images) acquired in ImageXpress 5000 was used in comparing the quantification methods.
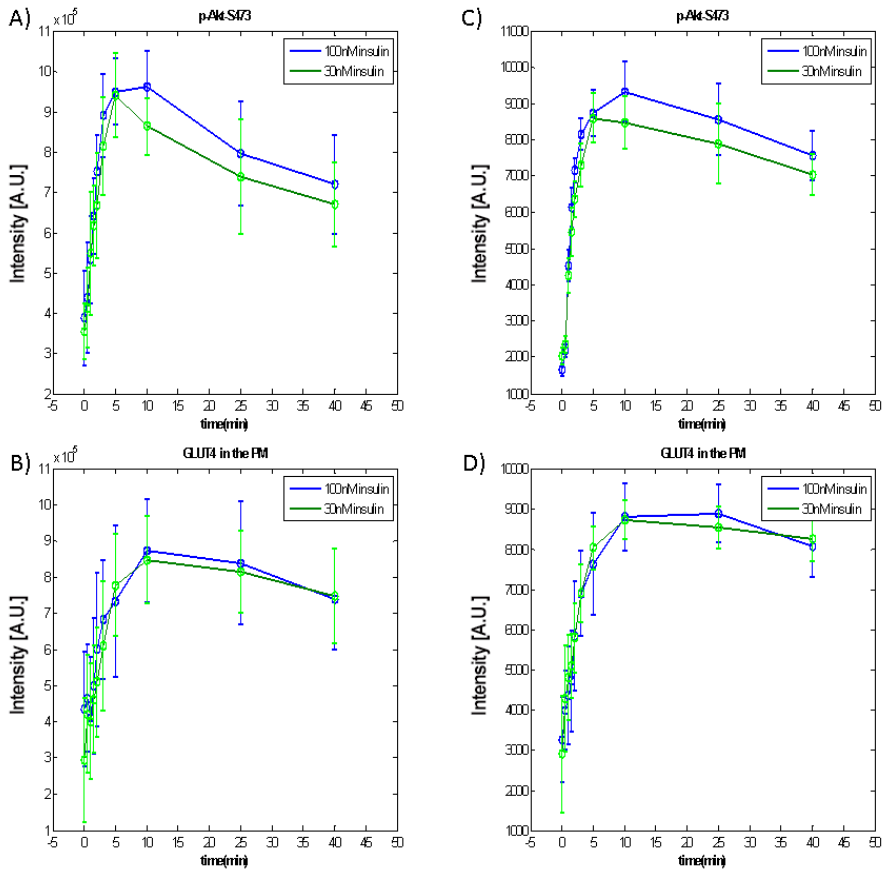
Figure 3.6: The quantified time course data of the phosphorylated proteins (p-Akt-S473 and GLUT4 protein in the PM) in insulin signalling cascade in L6-GLUT4 myotubes (Images were acquired in ImageXpress 5000) using A, B) pixel-based quantification method and C, D) intensity based quantification method where raw data is normalised with respect to the area of the tubes.

The intensity based quantification method allows us to obtain a better

approximation to the concentration of the phosphorylated proteins. On the other hand, thresholding in target staining leads to binary data neglecting the relationship between the strength of the fluorescent signal and the concentration. Fig. 3.6 shows the quantified time course data by both methods. It can be seen that the methods end up with slight change in the dynamics of protein activation. The proposed intensity based method leads to smaller standard deviations compared to the pixel based method.

3.4   Concluding remarks

In this chapter, we demonstrated the importance of the quantification of the data by using two different methods, namely, thresholding (pixel)-based and intensity-based quantification. The choice of the methodology used to quantify the raw images may lead to inconsistent results. In Section 3.3, we have shown that the thresholding method is subject to inaccuracies due to the manual selection of threshold value for the masks and the target proteins. As a result, this may lead to misinterpretation of the dynamics of the proteins. To overcome these drawbacks, In Section 3.4, we proposed an alternative method which extends the thresholding method with automatic determination of the masks by using region growing alghorithm and intensity-based protein quantification within these masks. We have shown on the experimental data, how this method provides a more accurate approximation of the concentration of the phosphorylated proteins in the insulin signalling pathway. In Chapter 4, the data that is quantified by using this proposed method will be presented.

Chapter 4

Image based decoding of the insulin signalling dynamics in rat skeletal muscle cells

Abstract

Insulin-mediated GLUT4 translocation depends on the insulin signalling pathway. Although many details of the underlying molecular mechanisms have been revealed, our understanding of the dynamics of the pathway in response to extracellular insulin changes is limited. We address the question to what extent differences in the extracellular change in insulin propagate into the pathway and result in different responses. In particular, we want to discriminate the effects that arise from different insulin input signals (external perturbation) from the differences due to possible internal variations. We also consider whether all the intermediates of the insulin signalling pathway exhibit the same dynamic behaviour upon insulin stimulation. We hypothesize that there could be (a)

representative protein(s) for studying the dynamics of the insulin signalling pathway.

We perturbed rat skeletal muscle cells with various insulin inputs and quantified the short term response of several intermediates. Immunocytochemistry assays for phosphorylation of (p-) IRS-1, Akt-S473, Akt-T308, AS160 and GLUT4 proteins in the plasma membrane were combined with high-throughput fluorescence microscopy in order to trace and quantify the temporal organisation of the proteins in the pathway. We show that all the measured intermediates exhibit consistent dynamic behaviour regardless of the inter-experimental variations. Correlation analysis shows that the temporal profile of p-Akt-S473 has high correlation with all the intermediates, particularly with GLUT4 protein in the plasma membrane. Based on these findings we conclude that p-Akt-S473 is the candidate to be the representative protein for insulin mediated GLUT4 translocation for further dynamics studies of the pathway.

4.1   Introduction

Living organisms respond to their surroundings by cellular signalling through which they maintain homeostasis or trigger developmental and adaptive responses. Signalling underlies crucial cellular decisions and administers the regulation needed for functionality of the multicellular organisms. Understanding cell signalling is pivotal because pathological alterations in cellular signalling are the main sources of diseases such as cancer, neurological diseases, cardiovascular diseases, and diabetes [45, 8, 125, 7, 73, 27, 28, 25]. Among cellular signalling cascades, insulin signalling plays an important role in the regulation of glucose uptake by cells for maintenance of glucose homeostasis. An impairment therein can lead to insulin resistance which is an early symptom of Type 2 Diabetes. Therefore, the identification of the insulin signalling pathway has received considerable interest from different fields such as cell biology, physiology, systems biology, and translational medicine [74, 69, 84, 77, 56].

The study of the insulin signalling pathway leading to GLUT4 translocation has focused on identifying the proteins that play a role in the signalling and their mechanisms and interactions. The illustration of the signalling pathway in Fig. 4.1 shows the identified intermediates of the insulin signalling pathway from insulin receptor to GLUT4 translocation from intracellular compartments to plasma membrane upon insulin stimuli. As insulin binds to its receptor, series of phosphorylation reactions occur subsequently. It starts with autophosphorylation of its receptor which in turn leads to tyrosine phosphorylation of IRS1. This adjoins activation of PI3-kinase (phosphoinositide 3-kinase) which converts PIP2 (phosphatidylinositol biphosphate) to PIP3 (phosphatidylinositol trisphosphate) in the plasma membrane and leads to phosphorylation of atypical protein kinase C (PKC) Phosphoinositide-dependent kinase-1 (PDK1), Phosphoinositide-dependent kinase-2 (PDK2) and Akt become associated with
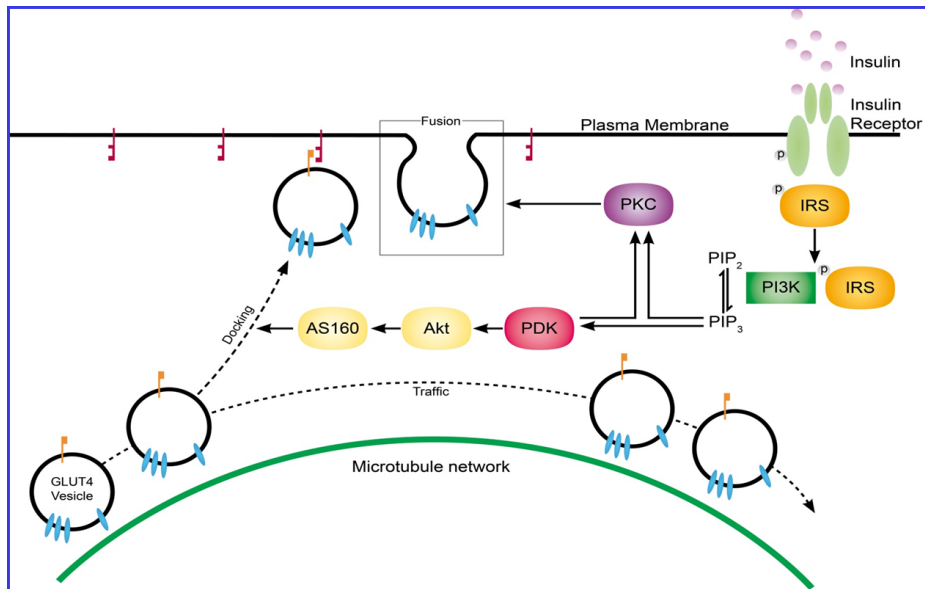
Figure 4.1: The scheme we propose for the insulin signalling pathway leading to GLUT4 translocation.

PIP3 and together induce the phosphorylation and activation of Akt [36]. The role of Ser473 phosphorylation in the COOH-terminal loop of Akt1/2 is controversial, but the emerging view is that Ser473 phosphorylation precedes and is required for Thr308 phosphorylation by PDK1. Dual phosphorylation of Akt is required for its full activation [104, 45]. Activated Akt then phosphorylates AS160 which is a Rab-GTPase-activating protein (GAP). This in return suppresses the target Rabs and mediates GLUT4 translocation to the PM. In the basal state, the GLUT4 vesicles which are trafficking near the PM weakly tether to the PM and rarely fuse into it, slowly exchanging GLUT4 with the PM. Upon insulin stimulation, it is proposed that the vesicles tether to the PM tighter and more vesicles dock by phosphorylation of AS160 [4, 103] and fuse into the PM by phosphorylation of atypical protein kinase C (PKC) [31, 69].

The signal from insulin receptor to the cell function (GLUT4 translocation) is regulated by the spatial and temporal organisation of the intermediates that are involved in the consecutive protein-protein and protein-lipid interactions [84]. To explore any impairments in the insulin signalling cascade, it is of crucial importance to reveal the functioning and the dynamics of the pathway composed of signalling complexes that transfer the signal [78]. One of the challenging aspects in investigating the dynamics of the intermediates in such complex systems is the

difficulty to trace the flow of information through proteins. How can cell process different inputs such as different shapes of input signal and multiple inputs? The challenge that cells in vivo face different shapes of the ligand input signal and proteins like Akt process (multiplex) signal from different receptors has not been introduced. In this study, we addressed the question to what extent differences in the extracellular change in insulin propagate into the pathway dynamics and result in different responses. In particular, we wanted to discriminate the effect due to different insulin input signals (external perturbation) from differences in response due to internal variations. In addition to this question the following questions directed the research: Are all the intermediates behaving in the same way in response to various insulin stimulations? How does the insulin dependent system switch off itself? Would the intermediates return to their basal levels when extracellular insulin level drops rapidly? How insulin-sensitive are these intermediates? Are there any representative proteins for studying the insulin mediated GLUT4 translocation?

The practical difficulty in enlightening the flow of information in complex systems is caused by the limitations in the experimental techniques. Widely used protein detection methods are western blotting, immunochemistry, spectroscopic procedures [50], measurement of the total protein content by colorimetry, and radiolabelling of proteins. The main body of experimental data accumulated thus far for the insulin signalling pathway is based on insulin dose response data showing the steady state responses of some of the intermediates of the cascade following insulin stimulation [48, 77, 56] and also perturbation/genetic variants/perturbed genes such as knockout and/or knockdown experiments [103, 101, 114, 69]. Time course data in long term (days) and short term (minutes-hours) have been collected for only a limited number of intermediates and/or data could only be sampled for limited time points due to practical restrictions in the current laborious methods [67, 98, 117, 77, 55, 89, 99, 18, 47]. Therefore, data on intermediate steps in signalling through GLUT4 translocation is still limited and the system level information on the short term dynamics of the intermediates of the insulin signalling pathway is lacking.

The expression of Green Fluorescent Protein (GFP) and variants [71] has become an extensively used methodology to study the spatial and temporal organisation of proteins. In parallel, high resolution, multi-mode and automated fluorescence microscopes have been developed for analyzing protein dynamics and interactions. The key to any high-throughput fluorescence microscopy approach is the development of an appropriate imaging assay that specifically reads out the biological function of interest and is robust enough to provide reproducible, quantitative data using high-throughput image acquisition and analysis. Unfortunately, there is no well-established methodology to investigate the dynamics of the multiple targets in fluorescence microscopy [80].

In this study, we explored the core dynamics of the insulin signalling pathway leading to GLUT4 translocation in skeletal muscle -via a combined platform of

high-throughput techniques in immunocytochemistry and fluorescence imaging. Skeletal muscle cells (rat L6-GLUT4myc myotubes) were exposed to multiple, different changes in extracellular insulin, including insulin washout. To study the short-term dynamics, frequently-sampled time course data was collected for several signalling intermediates. Immunocytochemistry assays for phosphorylation of (p-) IRS-1, p-Akt-S473, p-Akt-T308, p-AS160 and GLUT4 proteins in the plasma membrane were combined with high-throughput fluorescence microscopy to trace and quantify the spatial and temporal organisation of the proteins in the pathway. The metrics used to analyze the time course responses of the intermediates have revealed that all the measured intermediates show consistent dynamic behaviour regardless of the inter-experimental variations. Moreover, correlation analysis has shown that the temporal profile of p-Akt-S473 has high correlation with all the intermediates, particularly with GLUT4 protein in the plasma membrane. The results of this study will be comprehensively presented in the following sections.

4.2 Methods

Materials and reagents

The following reagents were used in cell culture for L6-Glut4myc cells: Dulbecco's modified Eagle medium (DMEM) (Sigma) containing 10 % fetal calf serum FCS (Gibco), 1 % Glutamax-1 (Gibco) and 1 % Pen/Strep (Sigma) as routine media; α-Minimal essential medium (α-MEM) (Invitrogen) containing 2 % FCS, 1 % Glutamax-1, and 1 % Pen/Strep as differentiation media, and α-MEM containing 1 % Glutamax-1 and 10 mM HEPES as serum starvation (depletion) media. Glycine, formaldehyde (FA), BSA and human insulin solution were bought from Sigma.

Antibodies

The primary antibodies against the following proteins were used: p-IRS1-Tyr989 (Santa Cruz), PI3-kinase p85α (Santa Cruz), p-Akt-T308 (ABCAM), p-Akt-S473 (Cell signalling Technology), p-AS160-Thr642 (Cell signalling Technology), GLUT4 myc (Sigma). The secondary antibody goat, anti-rabbit Alexa-488, (Molecular Probes # A11008) was used for all the primary antibodies. Furthermore, Hoechst 33342 (Invitrogen) and anti-β-tubulin mouse-Cy3 conjugated antibody (Sigma) were used for nuclei and tubulin detection respectively.

Cell culture

L6-GLUT4myc originated from Philip Bilan/ Amira Klip- (Department of Biochemistry, University of Toronto) and were purchased by AstraZeneca (Krister

Bamberg, Molndal). The cDNA was identified from a rat adipocyte library encoding the full length rat Glut4. This was cloned into the pCXN2 vector. (Neomycin resistance gene). Due to inability to select for neomycin resistant cells they co-transfected in an empty expression vector pSV2bls and selected for stable cells using blasticidin and use blasticidin through culture to maintain stable selection [115, 30]. All the experiments were performed at AstraZeneca facilities in UK. L6-Glut4myc cells of eighth passage number were used in the experiments. The cells were grown in T225 flasks in routine culture and plated into collagen coated clear bottomed/black walled 96 well plates at a density of 20000 cells/well (200 μl/well) in routine culture. After 24 hours, the routine culture was replaced by the differentiation media (200 μl/well). The cells differentiated optimally in 3 days with the formation of multinucleated myotubes. The cells were serum starved in depletion media (100 μl/well) 4 hours prior to experiments/insulin stimulation.

Antibody staining protocol

Following the specific insulin stimulation at predefined time points, cells were fixed at a time with FA (final concentration is 4 % FA). The plates were immediately placed on ice for 5 minutes, followed by 15 minutes at room temperature. Afterwards cells were washed once with PBS followed by a wash with 0.1 M Glycine in PBS. The antibody staining procedure started with permeabilizing the cells for all the target proteins with exception of GLUT4myc since it was aimed to detect myc tagged GLUT4 proteins in the cell surface. Cells were permeabilized with 0.1 % Triton-X (100 μl/well) for 5 minutes followed by a wash with PBS. The only difference in staining protocol for GLUT4 was the permeabilisation step which was done following incubation with the GLUT4 antibody. To reduce non-specific binding, cells were blocked with 3 % BSA in PBS (100 μl/well) for 1 hour at room temperature. After removing the blocking media, cells were incubated with the primary antibodies (25 μl/well) diluted in 3 % BSA for 2 hours at room temperature. The concentrations used for antibodies against p-IRS-1, p-Akt-S473, p-Akt-T308, p-AS160-Thr642, GLUT4 are as follows respectively: 4 μg/ml, 2 μg/ml, 10 μg/ml, 1 μg/ml, and 3.75 μg/ml. The cells were then washed with PBS (100 μl/well) followed by incubation of the cells with 25 μl/well fluorescent secondary antibody (4 μg/ml goat, anti-rabbit Alexa-488 along with 2 μg/ml Hoechst 33342 for 40 minutes to detect the target phosphorylated sites and nuclei respectively. After washing the cells with PBS twice, they were incubated with 25 μl/well anti-β-tubulin (5.5 μg/ml) mouse-Cy3 conjugated antibody for 1 hour at room temperature to detect tubulin which is the major constituent of microtubules. The cell plates were then washed with PBS three times and sealed. The plates were then imaged as described below.

Fluorescent image acquisition and quantification

Fluorescent images of the cells were acquired at 10x magnification (5 sites/well) using an ImageXpressTM Micro using the following excitation / emission settings; FITC labeled antibodies (482/536 nm), Cy5 labeled Tubulin antibody (628/692 nm), and Hoechst (377/477 nm). The fluorescent images were quantified in Matlab using intensity and pixel based quantification methods as described extensively in Chapter 3. The tubulin and target staining images were used in quantifying the phosphorylated proteins (p-IRS-1, p-Akt-S473, p-Akt-T308 and p-AS160) and the cell surface myc-GLUT4 protein.

Insulin signalling assays in L6-Glut4myc myotubes upon single dose insulin stimulation

Cells were grown and differentiated as described in the *Cell Culture* section. Due to plate effects, the outer edge wells were not used, leaving the inner 60 wells. Differentiated cells were serum starved and stimulated with either 10 nM or 100 nM insulin for a total of 60 minutes. The responses of the signalling intermediates (IRS-1, Akt-S473, Akt-T308, AS160, GLUT4) were sampled at frequent time intervals (0, 0.5, 1, 1.5, 2, 3, 5, 10, 30, and 60 minutes). 6 rows and 10 columns of wells in a 96 well plate were used in the experiments. 3 rows of a plate were exposed to a low dose of insulin (10 nM insulin) and the remaining 3 rows of the plate were exposed to a high dose of insulin (100 nM insulin). After fixing the cells following the insulin stimulation according to the plate map shown in Fig. 4.2, the Antibody Staining Protocols for p-IRS-1, p-Akt-S473, p-Akt-T308, p-AS160, GLUT4 were applied to the cells. Fluorescent image acquisition and quantification protocols were followed as described in Chapter 3.

Insulin signalling assays in L6-Glut4myc myotubes upon incremental insulin stimulation

Cells were grown and differentiated as described in the *Cell Culture* section. Cells were exposed to 1 nM insulin for 10 minutes, followed by 10 nM insulin for 60 minutes as shown in Fig. 4.3. After fixing the cells following insulin stimulations, the p-IRS1, p-Akt-S473 and GLUT4 staining protocols were applied. One plate was used for each target protein. Fluorescent image acquisition and quantification protocols were followed as described in Chapter 3.

Insulin signalling assays in Lean L6-Glut4myc myotubes upon insulin washout

Cells were grown and differentiated as described in the *Cell Culture* section. For staining of two antibodies one plate was used as shown in Fig. 4.4. Differentiated and serum starved cells were exposed to 100 nM insulin or media control for

Columns											
1	2	3	4	5	6	7	8	9	10	11	12
A	**Insulin stimulation exposure time [min]**										
	0	0.5	1	1.5	2	3	5	10	30	60	
B											
C				**10 nM insulin**							
D											
E											
F				**100 nM insulin**							
G											
H											

Figure 4.2: The plate map for insulin dosing and antibody staining

Columns											
1	2	3	4	5	6	7	8	9	10	11	12
At 70 minutes: Fixation of all cells at a time											
A	**Insulin stimulation exposure time [min]**										
	0	0.5	1	1.5	2	3	5	10	30	60	
	1 nM insulin injection: real time [min]										
	70	69.5	69	68.5	68	67	65	60	40	10	
B											
C				**1 nM insulin**							
D											
E											
F				**1 nM + 10 nM insulin**							
G											
H	**Insulin stimulation exposure time [min]**										
	0	0.5	1	1.5	2	3	5	10	30	60	
	1 nM insulin injection : real time [min]										
	60	59.5	59	58.5	58	57	55	50	30	0	
	10 nM insulin injection: real time [min]										
	70	69.5	69	68.5	68	67	65	60	40	10	

Figure 4.3: The plate map of incremental insulin dosing.

Figure 4.4: The plate map for insulin washout experiments.

10 minutes. At t=10 minutes, all the wells were washed with fresh media (100 μl/well), and fixed at specified times (2, 3, 5, 10, 20, 40 and 60 minutes after washout of the cells) with 8 % formaldehyde in PBS (100 μl/well, final concentration is 4 %.) for 15 minutes as shown in the plate map (Fig. 4.4). Then the Antibody Staining Protocols for p-IRS-1, p-Akt-S473, p-AS160, GLUT4 were applied to the cells/plates. Fluorescent image acquisition and quantification protocols were followed as described in Chapter 3.

Statistics

Independent data sets are expressed as mean $\pm$ standard deviation of the three replicates of each independent data sets. Statistical significance for the consecutive time points has been evaluated by one tailed student t-test, whereas statistical significance for dynamic characteristics of the time courses has been evaluated by two tailed student t-test. Values were considered significant when p >0.05. Pearson Correlation analysis has been performed for each couple of intermediates. Independent experiments have been used to calculate the correlation between two intermediates.

4.3 Results

In this study, skeletal muscle cells were exposed to various concentrations of insulin to study the short term dynamics of the intermediates of the insulin signalling pathway that leads to GLUT4 translocation. The antibody staining protocol was employed for labeling microtubules, nuclei, and the phosphorylated

proteins in response to insulin. Staining of tubulin, hoechst, and FITC was performed for detecting microtubules, nuclei and targeted phosphorylated protein, respectively, as shown in Fig. 4.5.A. High throughput fluorescent imaging was then used to detect the proteins. Each image shown in Fig. 4.5 represents a site from one of these experiments with an image size w (width) x h (height)=1392 x 1040 at 0.645 um/pixel of a 0.32 cm^2/well. In Fig. 4.6, it can be seen that the number of nuclei remains constant throughout the time course of the measurements which validates the assumption on the equal number of cells in each sample. In addition to the equal number of cells, differentiation of cells in each sample/well was required to be equal for the standardisation. The equal degree of differentiation of the cells in each well can be tracked in tubulin staining images in which the mean signal intensity for each well remains constant. The time course of phosphorylation was captured in short time intervals particularly in the beginning of the insulin signal to capture the difference in responses of the cascade intermediates, followed by wider intervals after 5 minutes. The time course of p-Akt-S473 can be qualitatively observed in Fig. 4.5.B. The overall staining intensity increased already in the consecutive early time points (0.5 min - 1 min) in p-Akt-S473 as well as in other intermediates. Specifically, in the case of p-Akt-S473, this increase in the intensity of fluorescense was also accompanied by a change in localisation of staining in the late time points, i.e. fluorescence intensity was localised around nuclei. Moving through the time course, the diffuse staining became more punctate and granular.

The differentiated cells were stimulated with 10 nM and 100 nM insulin for 60 minutes. The objective of using different doses was to evaluate the sensitivity of the intermediates of the cascade to insulin. We wanted to identify how strongly the intermediates respond to changes in extracellular insulin. The responses of the signalling intermediates (i.e. IRS-1, Akt-S473, Akt-T308, AS160, GLUT4) were sampled frequently in 60 minutes (0, 0.5, 1, 1.5, 2, 3, 5, 10, 30, and 60 minutes). The time courses of the intermediates to 10 nM and 100 nM insulin are shown in Fig. 4.7 - 4.8, respectively. The dynamic characteristics of the responses to two doses are reported in Table 4.1. In Fig. 4.7 - 4.8, it was observed that the system responded in a dose independent manner. The response profiles were the same and the difference in peak values (Table 4.1) did not linearly increase as the insulin dose was increased from 10 nM to 100 nM. The area under curve (Fig. 4.9 - 4.14) values of the intermediates' responses to different doses (Table 4.1) also support this observation. Based on these observations, it can be considered that the saturation point was almost reached for the response of the proteins with 10nM insulin stimulation. However, the significant difference in the peak values of phosphorylation of Akt-S473 site to different doses reveals that Akt-S473 can be the most insulin sensitive intermediate among the studied proteins in the cascade.
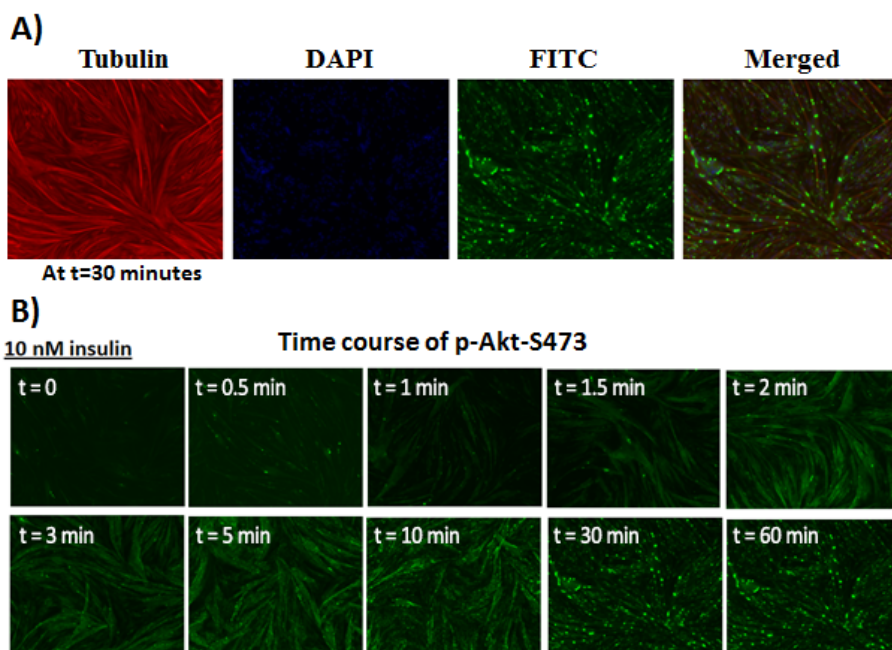
Figure 4.5: A)Microtubules (red), Nuclei (blue), Targeted Phosphorylated Protein (green) stainings, and the merged image of the first three from the same site. B) Time course of p-Akt-S473 in response to 10 nM insulin in raw images.

| Tubulin | Nuclei | p-Akt-S473 | Merged |
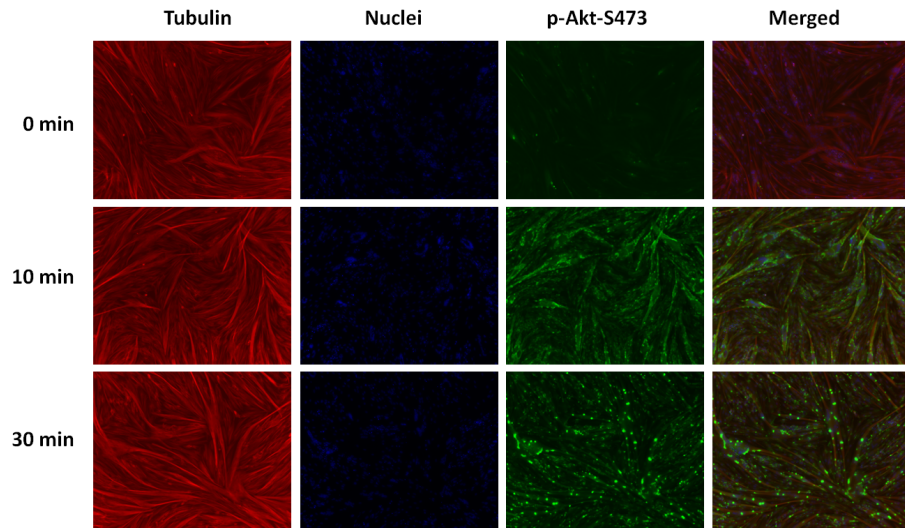
Figure 4.6: The number of nuclei and degree of differentiation remain
constant through the time course of phosphorylation of Akt-
S473 upon 10 nM insulin stimulation. The equal degree of
differentiation of the cells in each well can be tracked in tubulin
staining images in which the mean signal intensity for each
well remains constant.
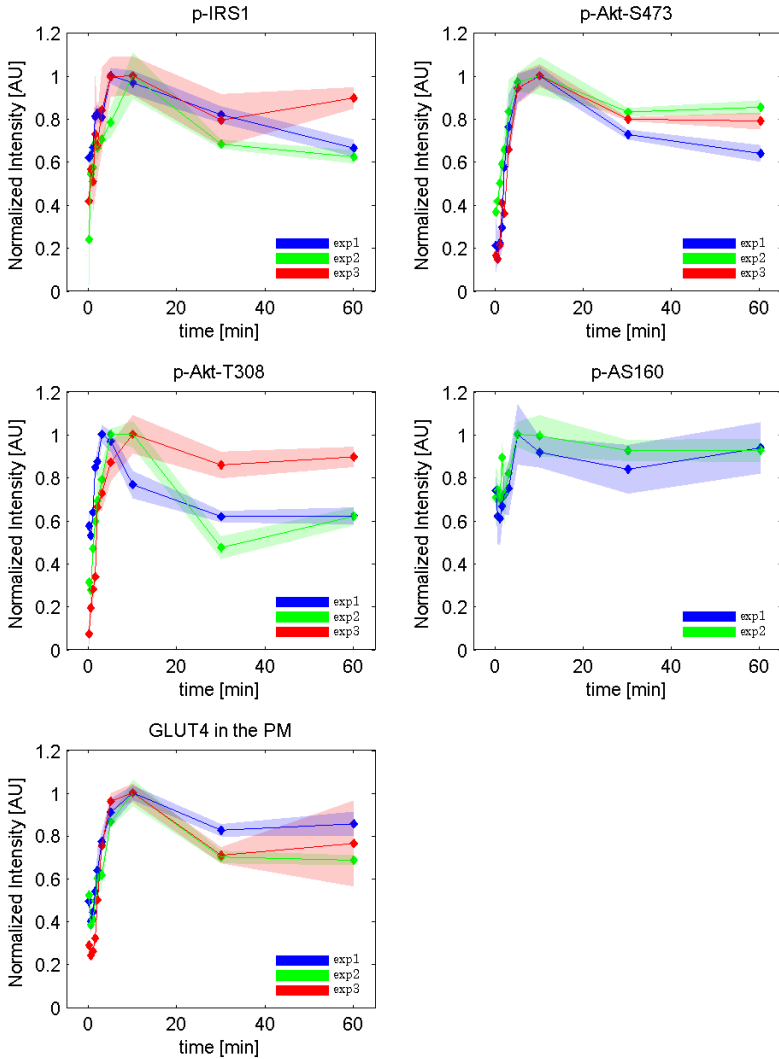
Figure 4.7: Time course responses of the signalling intermediates (p-IRS1, p-Akt-S473, p-Akt-T308, p-AS160 and GLUT4 in the PM respectively) upon 10 nM insulin stimulation. Each independent experiment presented in different colours is obtained by averaging 3 replicates per time point (3 wells /time point) and normalised with respect to the peak value. Note that each replicate (well) represents the average of 5 sites per well. The standard deviations of the replicates are shown in light colour shaded area.
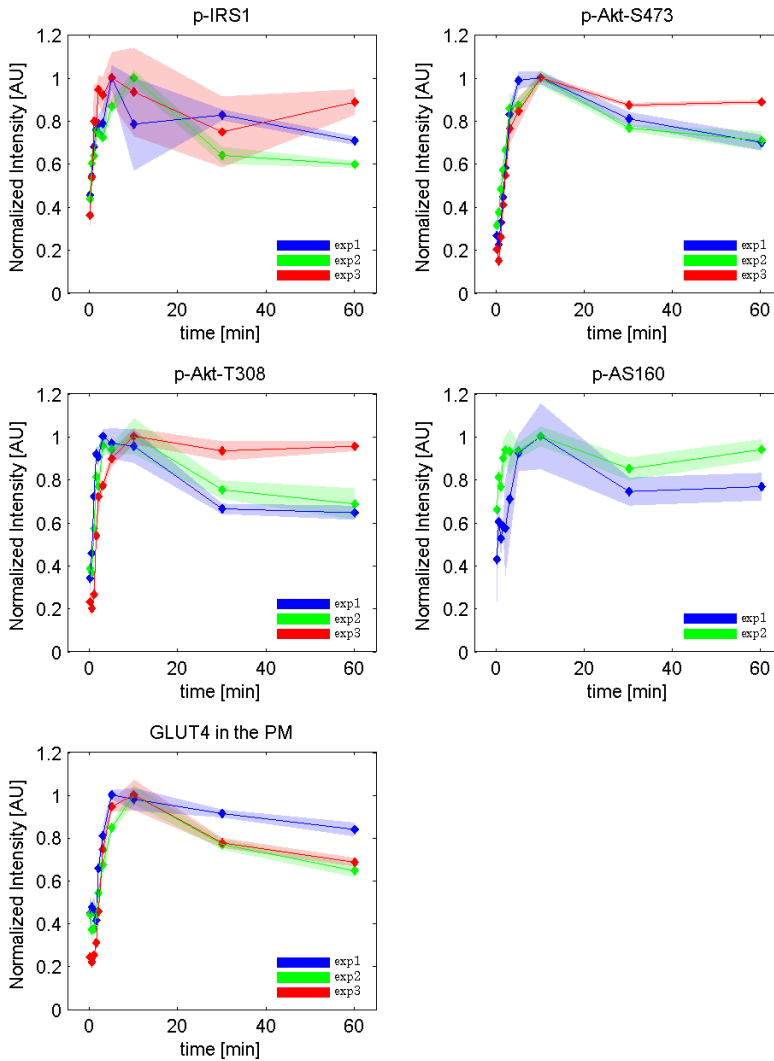
Figure 4.8: Time course responses of the signalling intermediates (p-IRS1, p-Akt-S473, p-Akt-T308, p-AS160 and GLUT4 in the PM respectively) upon 100 nM insulin stimulation. Each independent experiment presented in different colours is obtained by averaging 3 replicates per time point (3 wells /time point) and normalised with respect to the peak value. Note that each replicate (well) represents the average of 5 sites per well. The standard deviations of the replicates are shown in light colour shaded area.

Table 4.1: Dynamic characteristics of the insulin signalling intermediates' responses to single doses

| Target	Insulin [nM]	Area Under Curve [AU*e-8]	Rise Time [min]	Peak Time [min]	Fold Increase	Overshoot [AU]	Peak Value [AU*e-7]
p-IRS1	10	7.78 ± 1.99	1.33 ± 1.14	8.33 ± 2.89	1.68 ± 0.49	41.51 ± 25.18	11.69 ± 2.71
	100	7.89 ± 1.14	0.87 ± 0.35	6.67 ± 2.89	1.67 ± 0.51	41.02 ± 28.30	11.58 ± 1.06
p-Akt-S473	10	6.79 ± 1.05	2.17 ± 0.51	10.00 ± 0.00	4.15 ± 1.91	35.82 ± 25.18	12.63 ± 3.33
	100	7.89 ± 1.14	2.18 ± 0.99	8.33 ± 2.89	4.03 ± 2.17	33.74 ± 17.61	14.45 ± 3.19
p-Akt-T308	10	6.88 ± 1.12	1.64 ± 1.55	8.33 ± 2.89	5.92 ± 7.19	46.90 ± 29.74	11.72 ± 3.34
	100	8.24 ± 0.94	1.79 ± 1.73	8.33 ± 2.89	3.48 ± 2.61	35.43 ± 26.09	12.67 ± 2.36
p-AS160	10	6.26 ± 0.11	2.45 ± 0.90	7.50 ± 3.54	1.34 ± 0.04	7.27 ± 1.69	8.53 ± 0.56
	100	6.76 ± 0.20	2.14 ± 0.35	10.00 ± 0.00	1.46 ± 0.15	20.01 ± 18.38	9.78 ± 1.96
GLUT4	10	6.29 ± 0.41	2.00 ± 0.41	10.00 ± 0.00	2.19 ± 0.82	33.48 ± 15.09	10.95 ± 0.93
	100	6.82 ± 0.44	1.56 ± 0.12	8.33 ± 2.89	2.27 ± 0.87	41.80 ± 18.36	11.98 ± 0.90

The results are expressed as mean ± SD of 2 independent experiments for p-AS160 and 3 independent experiments for the other targets. *Area Under Curve*: The area under the curve in a plot of phosphorylated state of a protein over time. *Rise time*: The time required to increase the phosphorylated/activated state from 0.2 to 0.9 of the normalised peak value. *Peak time*: The time required to reach the peak phosphorylated/activated state. *Fold Increase*: The steady state value after stimulation over the basal state value. *Overshoot*: Percentage of the difference between the peak and the settling value. *Peak Value*: The value of the peak phosphorylated/activated state.

Table 4.2: Correlation analysis of the insulin signalling intermediates' responses to 10 nM insulin stimulation

	Pearson Correlation Coefficient	R^2
Akt-S473 vs GLUT4	0.94	0.88
IRS1 vs GLUT4	0.82	0.67
Akt-S473 vs AS160	0.82	0.67
IRS1 vs Akt-T308	0.79	0.62
Akt-T308 vs GLUT4	0.78	0.61
Akt-S473 vs Akt-T308	0.78	0.60
GLUT4 vs AS160	0.76	0.58
IRS1 vs Akt-S473	0.74	0.54
Akt-T308 vs AS160	0.52	0.27
IRS1 vs AS160	0.42	0.18

Upon single insulin dose stimulations, all the intermediates showed similar transient response whereas the steady state levels of the proteins and dynamic characteristics (Fig. 4.9 - 4.14) showed considerable variation in absolute values in each independent experiments. Therefore, we chose not to merge the data of the independent experiments, but to analyse the results individually. This approach is substantiated by the fact that the replicates within each independent experiment provide measurements that could be used to get data on the pathway dynamics expressed as mean values and a standard deviation. The heterogeneity in the independent experiments is a general challenge in proteomics that still requires new techniques and standardisation to generate reproducible data. To overcome the heterogeneity between independent experiments and to identify the common patterns in the pathway, correlation analysis was employed. The correlations of the intermediates are reported in Table 5.1 which shows that the intermediates of the cascade responses are correlated. In Fig. 4.10, the linear regression of the time courses of phosphorylation of Akt-S473 and translocation of GLUT4 protein to the PM upon insulin stimulation is shown. Correlation analysis has identified that the responses of p-IRS1, p-Akt-S473, p-Akt-T308, p-AS160, and GLUT4 proteins are similar. The metrics used to analyse and compare the dynamic profiles of the different intermediates between independent experiments capture a consistent dynamic behaviour of the pathway despite the inter-experiment differences in the data (Table 5.1).

Moreover, we also examined whether the previous insulin stimuli would have an impact on the response of the pathway to the subsequent insulin stimuli. In other words, we addressed the question of whether the pathway has a hysterisis behaviour such that its response to a current stimulus is dependent on the past stimuli. In addition to that, we explored the sensitivity of the intermediates. In
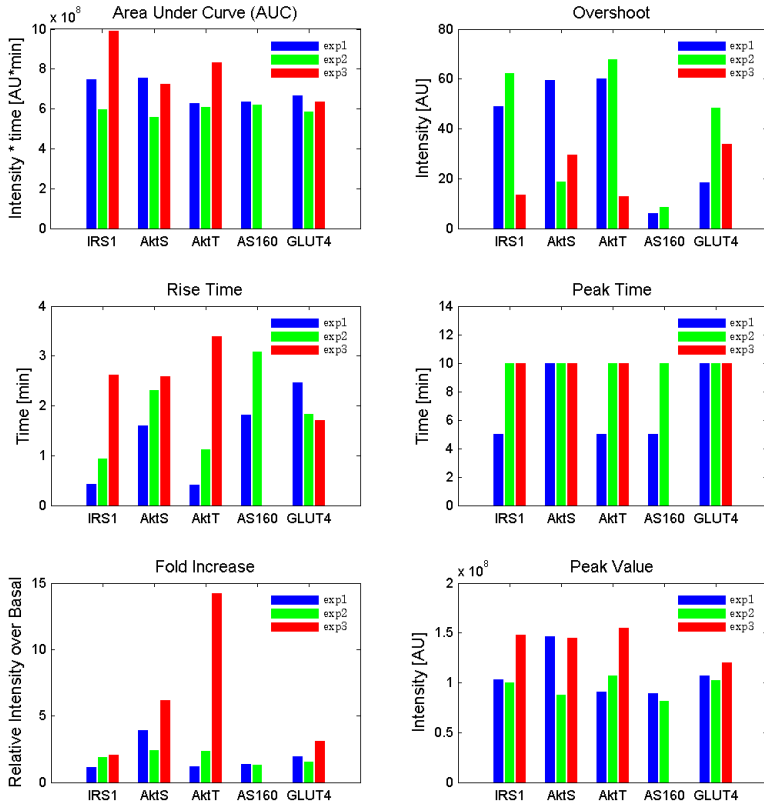
Figure 4.9: Dynamic analysis of the protein responses to 10nM insulin stimulation in 3 independent experiments. *Area Under Curve*: The area under the curve in a plot of phosphorylated state of a protein over time. *Overshoot*: Percentage of the difference between the peak and the settling value. *Rise time*: The time required to increase the phosphorylated/activated state from 0.2 to 0.9 of the normalised peak value. *Peak time*: The time required to reach the peak phosphorylated/activated state. *Fold Increase*: The steady state value after stimulation over the basal state value. *Peak Value*: The value of the peak phosphorylated/activated state.
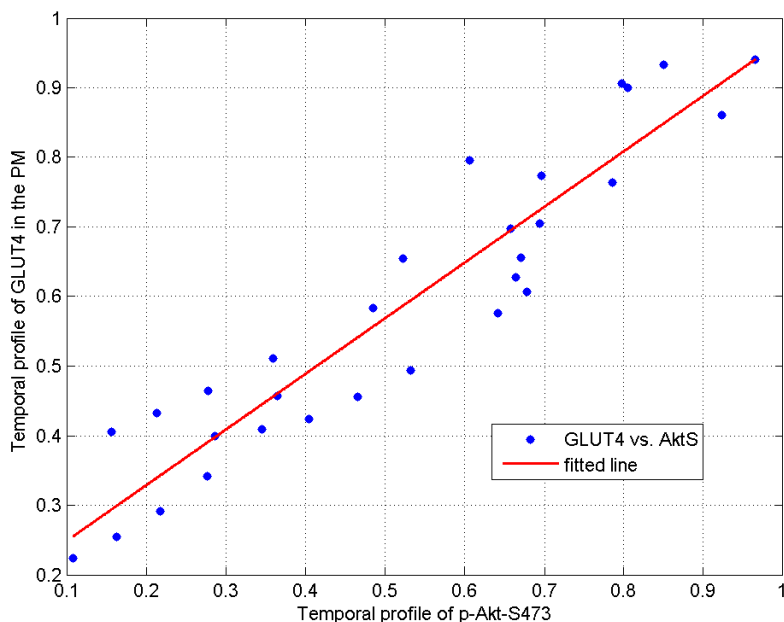
Figure 4.10: Linear regression of temporal profile of GLUT4 in the PM vs
that of p-Akt-S473 in response to 10 nM insulin stimulation.

order to investigate the system response to incremental insulin stimulation, the
differentiated cells were exposed to 10 nM stimulation for 60 minutes followed
by 1 nM insulin stimulation for 10 minutes. The response of the intermediates
are shown in Fig. 4.11. Incremental insulin stimulations (Fig. 4.11) revealed
that IRS-1 as well as Akt-S473 can also be very responsive to small increases in
insulin doses when the insulin concentration does not exceed 10 nM.

We have observed that the insulin signal is transmitted through the pathway
upon insulin stimulation. However, from a physiological point of view, it is also of
great importance to study switching off the insulin signalling pathway by insulin
washout. We hypothesized that the stimulated intermediates would return to
their basal lines when insulin would be removed from the media. Besides, we
addressed how fast they would react to switching off and whether the dynamic
profile of the reverse functioning (deactivation) would be similar to that of
activation. As we have observed maximum activation within 10 minutes for
all the proteins in single dose insulin assays, the cells were exposed to 100nM
insulin specifically for 10 minutes before insulin washout. This way we could
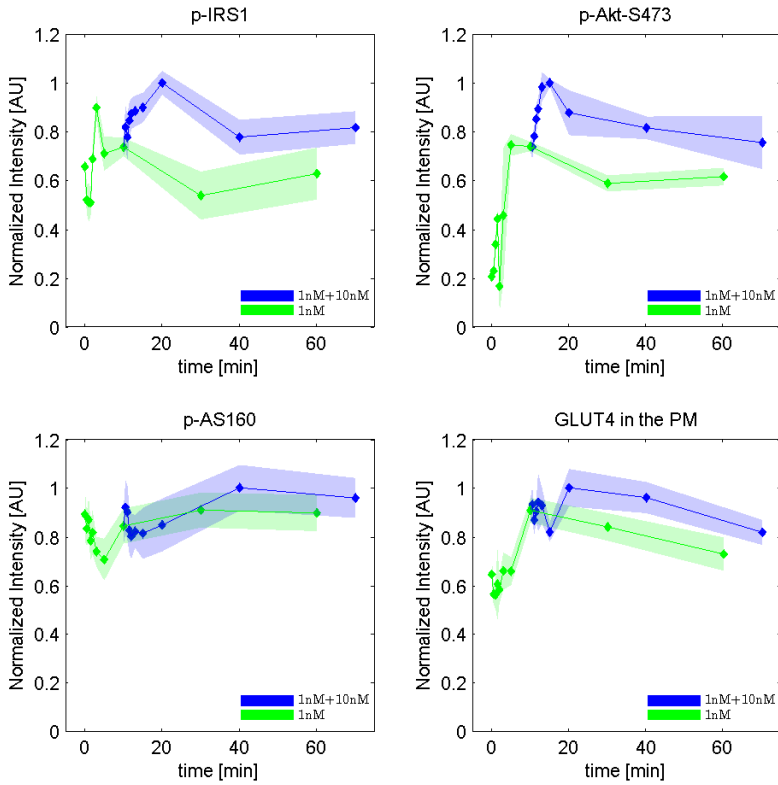
Figure 4.11: Time course responses of p-IRS1, p-Akt-S473 and GLUT4
proteins in the plasma membrane upon incremental insulin
stimulation. At t=0, 1 nM was given to the cells and at t=10
minutes, an additional 10nM insulin was given to the cells.
Data is obtained by averaging 3 replicates per time point (3
wells /time point) and normalised with respect to the peak
value. Note that each replicate (well) represents the average
of 5 sites per well. The standard deviations of the replicates
are shown in light colour shaded area.

observe switching off (deactivation of) the intermediates after full activation
(switching on). The response of the intermediates to insulin washout are shown
in Fig. 4.12. In Fig. 4.12, it was observed that the upstream insulin signalling
intermediates rapidly dephosphorylated and returned to their basal levels within

$\sim$ 10 minutes after insulin washout. However, GLUT4 proteins, in contrast to the others, stayed in the plasma membrane for a longer period and reached the basal level in 20 minutes after insulin washout.
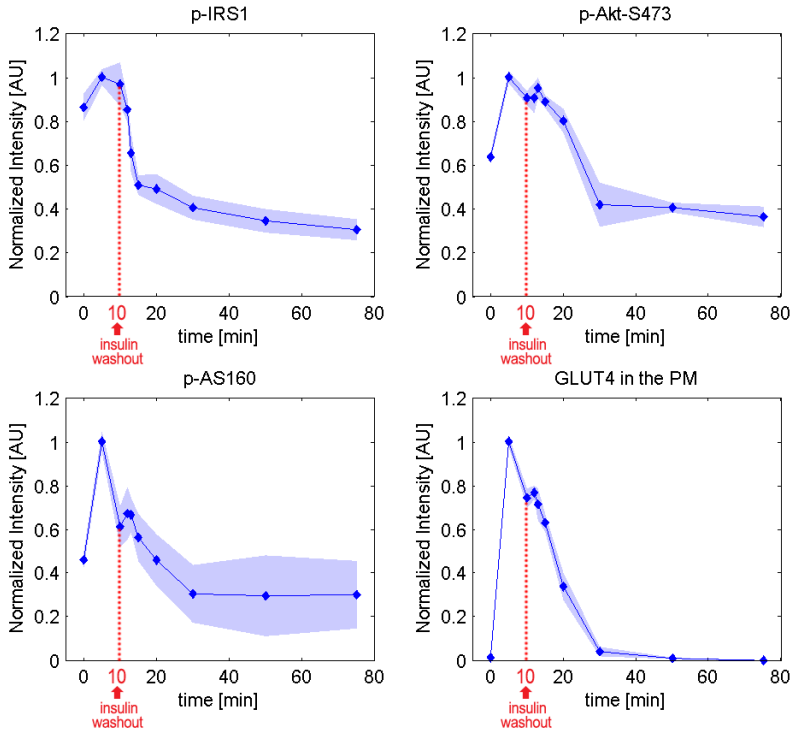
Figure 4.12: Time course responses of p-IRS1, p-Akt-S473, p-AS160, and GLUT4 in the PM upon insulin washout after 10 minutes insulin stimulation. Data is obtained by averaging 3 replicates per time point (3 wells /time point) and normalised with respect to the peak value. Note that each replicate (well) represents the average of 5 sites per well. The standard deviations of the replicates are shown in light colour shaded area.

4.4 Discussion

To understand any impairments in the insulin signalling cascade, it is of crucial importance to reveal the functioning/dynamics of the pathway composed of signalling complexes. In the literature, dose responses of the insulin signalling pathway have been studied to investigate the fold increase of the intermediates of the signalling cascade. However, the dynamic responses of the system to multiple doses have not been studied for several intermediates [48, 77, 56]. In vivo cells are continuously exposed to changing insulin levels, understanding the pathway characteristics requires dynamic data in response to diverse insulin perturbations. Therefore, in this study, we stimulated skeletal muscle cells with various insulin doses and observed the temporal response of several intermediates of the insulin signalling pathway. We addressed the question to what extent differences in the extracellular change in insulin propagate into the pathway and result in different responses. For this purpose, functional immunocytochemistry assays were designed to quantify the dynamic response of several intermediates, namely; IRS-1, Akt-S473, Akt-T308, AS160 and GLUT4 in the PM upon insulin stimulation in different doses in rat skeletal muscle cells (L6-Glut4myc cells).

Upstream intermediates can easily be dephosphorylated and be ready for the next insulin signal. Upstream signalling intermediates (p-IRS-1, p-Akt-S473 and p-Akt-T308) showed distinctive overshoot behaviours (decrease in activation following a peak) and reached steady states with a value close to their basal levels. This may be due to the presence of negative feedback mechanisms affecting the mentioned intermediates. Particularly, p-Akt-S473 and p-Akt-T308 having the highest overshoot values (Table 4.1) is a good indicator for being affected by a negative feedback from other intermediates or cross-linked pathways. Studies show that Akt-S473 is regulated by mTOR [45, 51]. On the other hand p-AS160 showed a slight decrease after reaching the peak value and GLUT4 proteins mostly remained in the plasma keeping the stimulated level for a longer period than the upstream signalling intermediates. These results are also in agreement with the insulin washout experiments. The upstream signalling intermediates rapidly responded to insulin washout by dephosphorylation and reached their basal lines within 10 minutes whereas GLUT4 redistribution took longer than dephosphorylation of the upstream signalling proteins. In the view of these observations, we can conclude that upstream intermediates can easily be dephosphorylated and be ready for the next insulin signal.

GLUT4 translocation is the rate determining step. As the insulin signalling pathway is a complex system involving many intermediates and cross-links to other pathways, time delays in the responses of consecutive intermediates were expected in the early signalling period [39]. However, in single dose insulin stimulations, most of the proteins rapidly phosphorylated and reached their maximum activity within 10 minutes followed by a gradual decrease and reached steady state in 50-60 minutes as shown in Fig. 4.7 - 4.8. Moreover, no time

delays were recorded in the phosphorylation of the observed proteins as the signal propagated through GLUT4 translocation. However, we observed variations among the phosphorylation rates of the intermediates before they all reach their peak values. By comparing the rates of phosphorylation with the rise times of the intermediate responses in Table 4.1 we can conclude that the response of GLUT4, downstream signalling mediate, is slower than that of the upstream signalling intermediates. Although the signal is transmitted very fast it is possible to track the rate of transmission through rise times of the intermediates. The fastest phosphorylations were observed in the phosphorylation of IRS1 and T308 site of Akt with the smallest rise times to both 10 and 100nM insulin stimulation whereas phosphorylation of Akt-S473 and translocation of GLUT4 to the PM were slower. In consecutive insulin stimulation experiments, we addressed how the pathway would respond to variations in extracellular insulin and if the previous insulin concentration would have an impact on the following insulin stimulation. All the intermediates showed a rapid increase in their phosphorylation rates after the second dose of stimulation (Fig. 4.11). But the rate of increase was lowered as the signal passed through the downstream signalling intermediates (i.e. GLUT4 proteins in the plasma membrane). Insulin washout experiments showed that signalling intermediates follow the same trend was also observed in the switching off the signalling caswashout experiments. In Fig. 4.12, it was observed that the upstream insulin signalling intermediates rapidly dephosphorylated and reached basal levels within ∼10 minutes after insulin washout. However, GLUT4 proteins, in contrast to the others, stayed in the plasma membrane for a longer period and returned to the basal level in 20 minutes after insulin washout. It is evident from these observations that the rate-determining step of the insulin signal transmission is GLUT4 translocation. This may be due to the fact that GLUT4 translocation involves intracellular sorting, vesicular transport to the cell surface along cytoskeletal elements, and finally, docking, priming, and fusion of the GLUT4 storage vesicles with the cell surface. There is good evidence that the rate-determining step(s) of the insulin signal transmission from the receptor to GLUT4 translocation is/are the docking and/or fusion of the GLUT4 vesicles with the plasma membrane [4, 64, 74].

The power of the methodology. Large scale projects using high-throughput microscopy that have been reported so far almost exclusively used fixed-cell assays which do not provide any temporal information. Using live-cell assays and high-throughput time-lapse microscopy can overcome this problem [71, 74] since they provide much more temporal information than fixed-cell assays. However, the high-throughput automated fluorescence imaging of biological processes in living cells is currently technically challenging. Because the quantification of sudden and short-term events is challenging, and live imaging is prone to such errors that depend on the speed of the imaging equipment [14, 92]. Besides, live cell assays require robust and simple fluorescent labelling techniques since fluorescent labelling of intermediates in live cells could affect the physiology. The high

throughput fluorescent imaging of fixed myotubes and quantification methods used in this study provided reproducible, high quality proteomics data with small standard deviations. The data shows both qualitatively and quantitatively how the insulin signal propagates through each intermediate in a short time interval not only when insulin is exposed in different and incremental doses but also when it is removed from the media. This way the activation and inactivation dynamics of the proteins were investigated. This study also conceptually demonstrates that immunocytochemistry together with high throughput techniques can be used as an efficient way of protein detection. This approach offers the opportunity to generate qualitative and quantitative data sets with high spatial and temporal resolution. Compared to western blotting and mass spectrometry, this technique enables to study the localisation of the proteins in addition to the dynamics of the proteins. Local organisation of the proteins is also important for their activity levels which in turn effects the functioning of the proteins. However, in this study, localisation of the proteins was not comprehensively studied.

Distinct behaviour of AS160 from the pathway. The metrics used to analyse and compare the dynamic profiles of the different intermediates between independent experiments capture a consistent dynamic behaviour of the pathway despite the inter-experimental differences in the data (Table 5.1) due to the cell variability. IRS1, Akt-S473, Akt-T308 and GLUT4 have coordinated action in responding to insulin stimulation with well defined profiles. In Fig. 4.10, it can be seen that there is a very strong correlation especially between p-Akt-S473 and GLUT4 in the PM (Corr. Coef = 0.94). It implies that measuring one of these two targets is sufficient to get information about both under these experimental conditions. However, among the coupled intermediates, p-IRS1 & p-AS160 and p-Akt-T308 & p-AS160 have relatively lower correlation than the other couples. This evidence can be considered as AS160 has the weakest correlation with the well-established members of the upstream signalling cascade Table 5.1. AS160 is one of the more recently discovered intermediates of which the mechanism is not fully known. We can speculate that its role in transmission of the signal may not be direct but indirect by looking at the distinct dynamic response to insulin stimuli. Recent knockout and knockdown studies of AS160 focus on its role in GLUT4 translocation. The involvement of AS160 in the insulin signalling pathway was proved with knockout studies in mice [69]. Studies with 3T3-L1 adipocytes expressing AS160 phosphorylation site mutants (AS160-4A) placed the point of AS160 action upstream of GLUT4 vesicle fusion with the plasma membrane [119, 69] and at the docking of GLUT4 vesicles to the plasma membrane [4]. A recent in vitro study using GLUT4 vesicles and plasma membranes isolated from rat adipocytes further supports a role for AS160 in GLUT4 vesicle fusion with the plasma membrane [65].

Robust and/or Isodynamic system behaviour of insulin signalling pathway. The presented study contributes comprehensive frequent time course data for the phosphorylation and activation of the selected proteins (shown in
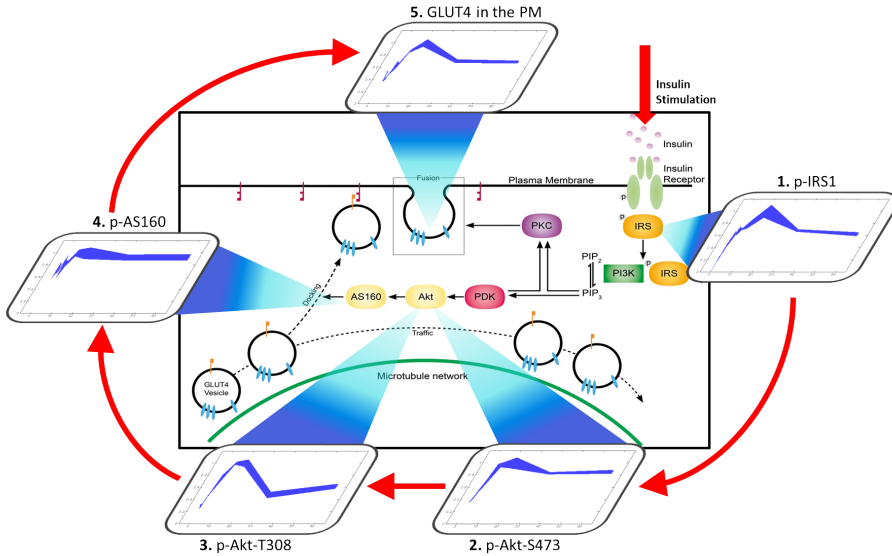
Figure 4.13: **The insulin signal propagation from insulin receptor to GLUT4 translocation.** The insulin signal can be tracked through the insulin signalling pathway on phosphorylation of IRS1, two sites of Akt, (S473 and T308 respectively), AS160, and GLUT4 in the PM.

Fig. 4.13) in the insulin signalling pathway leading to GLUT4 translocation. Thereby, it reveals the dynamics of the intermediates that play a role in the signalling through insulin mediated GLUT4 translocation. The analyses confirm that the signal propagates through the pathway, but time delays are small and the dynamic profiles of the different intermediates are very similar in responding to various insulin stimulations. They persist the consistent dynamic profile in response to various insulin perturbations. They show iso-dynamic profile in response to different insulin stimulations. In conclusion, we propose that the insulin signalling pathway leading to GLUT4 translocation can be an isodynamic system although the intermediates respond differently between experiments, they show the same overall behaviour. This property/observation can be used to capture fundamental interactions and ease the understanding of other signalling pathways.

4.5   Conclusion

In this study, we have generated unique data revealing the short term dynamics of the insulin signalling pathway in skeletal muscle cell lines. We used techniques that allow spatial and temporal organisation of the proteins. The data analysis approach employed to the time course data sets facilitated to identify common patterns in the time courses despite the heterogeneity caused by cell variability. We have shown that there is significant correlation between the dynamic profiles of the intermediates except p-AS160which has a distinct behaviour. We propose that the dynamic profile of the phosphorylation of Akt-S473 is a good candidate for representing the dynamics of the insulin signalling through GLUT4 translocation for further dynamics studies of the pathway.

In the following chapter the integration of the data into the mathematical model is presented. These data are an essential resource for systems biology studies of signal transduction pathways to further study the underlying mechanisms of the pathways. The computational model will be used as a tool to test different hypotheses about possible roles of the intermediates and crosstalks in regulation of insulin-induced GLUT4 translocation.

4.6   Appendix
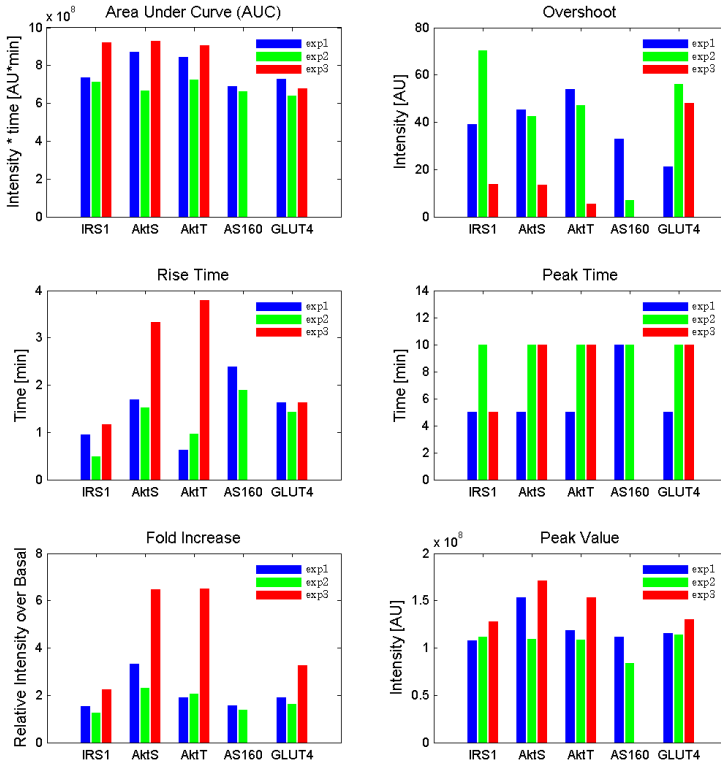
Figure 4.14: Dynamic analysis of the protein responses to 100nM insulin
stimulation in 3 independent experiments. *Area Under
Curve*: The area under the curve in a plot of phosphory-
lated state of a protein over time. *Overshoot*: Percentage
of the difference between the peak and the settling value.
Rise time: The time required to increase the phosphory-
lated/activated state from 0.2 to 0.9 of the normalised peak
value. *Peak time*: The time required to reach the peak
phosphorylated/activated state. *Fold Increase*: The steady
state value after stimulation over the basal state value. *Peak
Value*: The value of the peak phosphorylated/activated state.

Chapter 5

The eINDHOVEN model - Insulin sigNalling Dynamics for Hypotheses, Observations and Virtual ExperimeNts

Abstract

To understand possible impairments in the GLUT4 translocation in skeletal muscle, it is essential to study the functioning and therefore the dynamics of the insulin signalling pathway that leads to the GLUT4 translocation. In this chapter, we utilize a systems biology approach and combine mathematical modeling and experimental work to study the regulations in the insulin signalling pathway that describe the core dynamic behaviour of the signalling from insulin receptor to GLUT4 translocation in skeletal muscle. Here, we build the eINDHOVEN model of the insuling signalling pathway by integrating our high resolution temporal data of the intermediates of the pathway in rat skeletal muscle. The model is refined through a process that consists of several iterations of model

development and testing of the hypotheses. Based on the analyses of our model, we propose that the phosphorylation of IRS is regulated by a delayed negative feedback from Akt. Subsequently, we use our model of the insulin signalling pathway to test the hypotheses formulated in the previous chapter. We have shown that the measured intermediates of the insulin signalling pathway have a consistent dynamic behaviour among each other regardless of the variations between the independent experiments. However, the dynamics of the other intermediates is still not fully known. Here we investigate whether they also exhibit consistent dynamics upon insulin stimulation despite the cell variability. We also study whether the insulin signalling pathway can be considered as an *isodynamic* system. Based on the analyses of the model that is parameterised for each independent data set, we find that the insulin signalling intermediates have consistent dynamics. Furthermore, the eINDHOVEN model is used to conduct virtual experiments based on the hypotheses on insulin resistance in skeletal muscle. The effect of the impaired p-IRS, p-AktS, and the fusion of GSVs on the GLUT4 translocation is then quantified. It is seen that the effect of an impairment in p-IRS on the system output is larger than that of an impairment in p-AktS. This indicates that p-IRS dominates the behaviour of the whole system including GLUT4 translocation.

5.1   Introduction

Studying the dynamics of the pathway helps us to understand the functioning of the insulin signalling pathway that leads to the GLUT4 translocation and therewith, aids our understanding of the malfunction of the pathway which leads to insulin resistance in skeletal muscle. Insulin resistance in skeletal muscle is the primary defect to glucose homeostasis, leading to Type 2 diabetes, since it accounts for 75 - 80 % of whole body insulin-stimulated glucose uptake [29]. In this chapter, we utilize a systems biology approach that combines mathematical modeling and experimental work to study the regulations in the insulin signalling pathway that describe the core dynamic behaviour of the signalling from insulin receptor to GLUT4 translocation. Our main goal is to develop a mathematical model that can represent the dynamical behaviour of the insulin signalling pathway in skeletal muscle; in order to gain a better understanding of their complex interactions and to develop quantitative descriptions of its dynamics in skeletal muscle. To build such a mathematical model, the cycle of systems biology is repeated several times such that a more reliable mathematical model of the system is obtained. The method consists of iterative cycles of experiments and mathematical modelling both of which feed each other.

In the scope of this approach, we start as basis with the mathematical models in Chapter 2 based on the data gathered from the literature. The model structure has been developed based on the KEGG model and the hypotheses on the interactions of the intermediates of the insulin signalling pathway. The
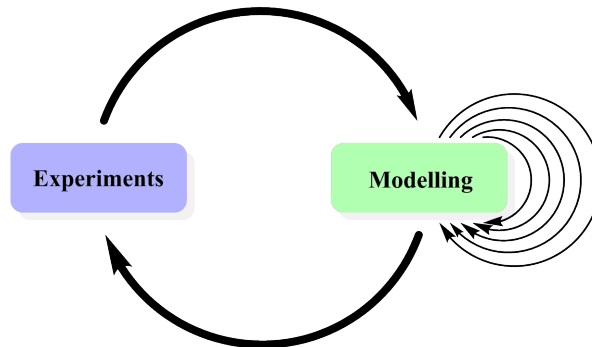
Figure 5.1: The cycle of systems biology.

model is parameterised by using the composite data set. However, uncertainty analysis of the model reveals that the model contains high uncertainty given the composite data set. To overcome the uncertainty of the model predictions reflected from the uncertainty of the composite data set, a favorable solution is to generate a high resolution temporal data set for a broader subset of intermediates from the same cell type in order to develop an identifiable model that can provide predictions with higher certainty. In Chapter 4, such data from skeletal muscle cells has been generated by a combined platform of high-throughput techniques of immunocytochemistry and fluorescence imaging. The pieces of the puzzle come together in this chapter to construct our mathematical model for the insulin signalling pathway that leads to GLUT4 translocation in rat skeletal muscle cell.

In this chapter, the data and hypothesis driven modelling approach described in Chapter 2 is re-utilized to construct a new model based on the new data sets generated in Chapter 4. Initially, the data is integrated into *Model II*. However, the results obtained from this model do not coincide with the time course data with the given model structure. This indicates that the model is not complete with the given mechanisms of the intermediates. To identify the required modifications in the model, several iterative cycles of model development, hypothesis testing and refining of mathematical models is used as presented in the modelling part of the systems biology cycle (Fig. 5.1). This will be further explained in the model development section. Resnorm analysis and correlation analysis are used together to select the model structure among others. The selected model is called the eINDHOVEN model which is an abbreviation of Insulin sigNalling Dynamics for Hypotheses, Observations and Virtual ExperimeNts. Multi Parametric Sensitivity Analysis is then applied to the eINDHOVEN model to assess the identifiability of the parameters and to determine the critical steps in GLUT4 translocation.

In Chapter 4, we have shown that the measured intermediates of the insulin signalling pathway have a consistent dynamic behaviour among each other

regardless of the inter-experimental behaviour. We define the systems that display this property as *isodynamic systems*. Herewith, we investigate if the estimated dynamic response of all intermediates of the insulin signalling pathway to insulin stimulation remains identical despite the variety in their magnitudes and if the insulin signalling pathway can be considered as an isodynamic system. For this purpose, we apply correlation analysis on the eINDHOVEN model which is separately parameterised for each independent experiment.

Moreover, the eINDHOVEN model is used to conduct virtual experiments based on the hypotheses about insulin resistance in skeletal muscle. The effect of the impaired phosphorylation (p-) IRS, p-AktS, and the fusion of GSVs on GLUT4 translocation is quantified.

5.2   Results

Model development

In this chapter, we present the eINDHOVEN model which is an extension of the earlier presented model in Chapter 2 by incorporating the outcomes of the experiments that were performed. The mathematical model developed in Chapter 2; namely *Model II* (shown in Fig. 5.2), was parameterised based on a composite data set that was obtained from the literature. In this chapter, we show how we integrate the experimental data of Chapter 4 with *Model II* and parameterise this model to build the eINDHOVEN model. As each independent experiment that was carried out is presented individually in the previous chapter, the model is parameterised separately for each independent experiment which consists of time courses of insulin responses of the intermediates. Model parameters are estimated by fitting the model to the experimental data by using a weighted least square estimation algorithm. To this end, a cost function to be minimized is defined as follows:

$$\chi^2(\theta) = \sum_{i=1}^{n} \sum_{j=1}^{d_i} \left(\frac{y_i(t_j) - y_i(t_j|\theta)}{\sigma_{ij}} \right)^2, \tag{5.1}$$

where $y_i(t_j)$ denotes the data-point for the ith observable state, measured at time point t_j, $y_i(t_j|\theta)$ stands for the ith observable state predicted by the parameters θ at t_j, and σ_{ij} represents the standard deviation of the jth data-point of the ith observable state. The standard deviations (σ_{ij}) of the experimental data-points are used as the weighting criteria for the error between the corresponding data point and the estimated observable state. A higher standard deviation of a data-point results in a lower weighting coefficient for the corresponding error (between the estimated state and the actual data-point). The normalised data with respect to the maximum stimulated states of the corresponding protein is introduced into the optimization routine. The nonlinear recursive least squares
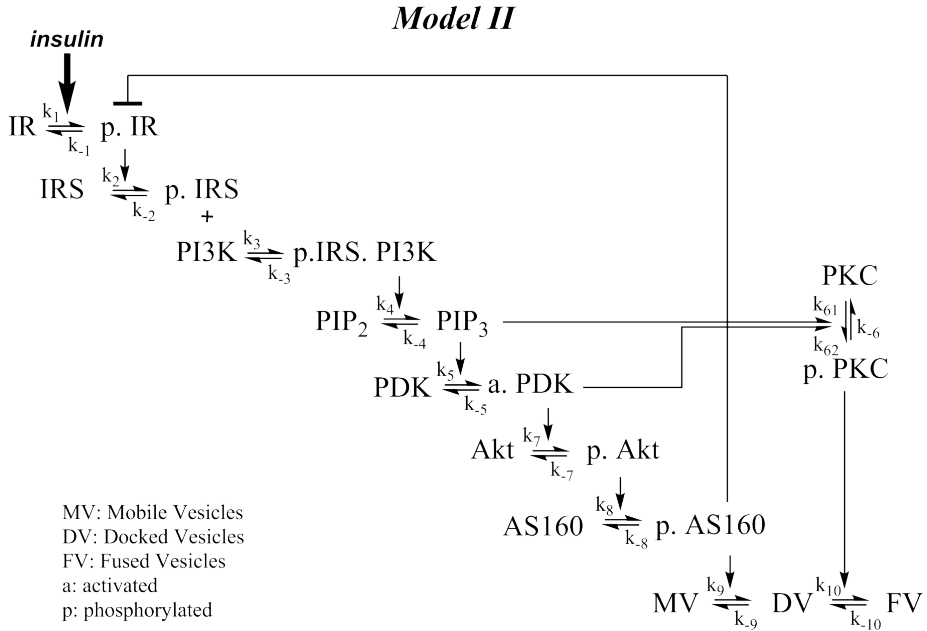
Figure 5.2: The scheme of the reactions in *Model II*.

based on the differences of the normalised individual data set and the normalised model output are solved by the routine *lsqnonlin* found in Matlab optimization toolbox. The further details of the implementation are explained in the Appendix.

From Fig. 5.3 we conclude that *Model II* is not able to fully describe the time course data with the given model structure; in particular, the GLUT4 translocation is not described accurately. This indicates that the model is not complete with the given mechanisms of the intermediates. This addresses the need to adjust the computational model such that the experimental data can be reproduced by the model. An overshoot behaviour is observed in all time-course data as seen in Fig. 5.3, however, the estimated time course of p-AS160 and GLUT4 translocation do not display this overshoot behaviour. This observation hints to a model mismatch in the feedback mechanism descriptions or their sources. We therefore, first focus our attention in adjusting the negative feedback source and their targeted proteins.
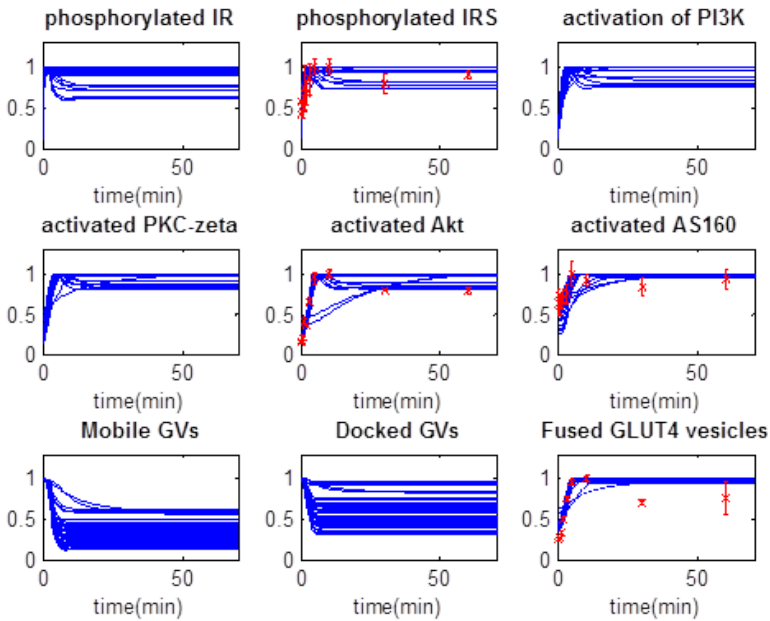
Figure 5.3: Simulations of the parameterised *Model II* based on the new
experimental data. *Model II* cannot fully describe the time
course data. Simulations are shown in blue lines whereas the
data is shown in red dots.

Hypothesis testing

As an initial step to adjust the model, we repeat the hypothesis testing for several
sources (PKC, Akt, AS160, and GLUT4) of single negative feedback as described
in Chapter 2. In Chapter 2, several feedback scenarios were tested to produce the
overshoot behaviour of p-IR and p-IRS. There, we have found that a feedback to
p-IR is required to produce the overshoot behaviour and p-AS160 is the most
likely source of this feedback. This time as a target protein that is regulated by
the feedback, p-IRS is tested as well as p-IR. The model with a negative feedback
to p-IRS from p-AS160 (See Fig. 5.4) gives the minimum sum of squared error
among the others. The simulation results with respect to 10 best parameter
sets are shown in blue lines. The experimental data is shown in red dots. The
data except p-AS160 can be described by the model. However, the estimated
p-AS160 shows a delayed response to insulin. In order to overcome the delay

that is displayed in p-AS160, first a parameter space for the rate constants of the (de)phosphorylation of AS160 is examined to obtain a fitting model to the experimental data. As a result, the time constant of the p-AS160 decreases, however the overshoot behaviour in the p-AS160 disappears. This result directs us to investigate the existence of a delay mechanism in the negative feedback path to p-IRS that originates from p-AS160.

Introducing delay on the feedback

In continuous systems, discrete time delays are introduced via continuous approximation methods such as padé approximation or linear chain approximation. The idea is to add extra states to the system to create the delay on the feedback path. We find that a 4-th order delay should be introduced on the feedback from p-AS160 to p-IRS (See Fig. 5.5). This model can describe the overshoot behaviour in each time course. Then all potential feedback sources are tested again with the given delayed feedback structure. It is found out that they all can describe the data to the same extent. However, the resnorms of each scenario vary in the range of 80-100 which can be considered high. To investigate the underlying reason of high resnorms, resnorm analysis is carried out. Furthermore, to select the feedback source, correlation analysis in combination with resnorm analysis are applied for each model.

Resnorm Analysis

The cost function (Eqn. 5.1) that is used in the parameter estimation is based on the difference between the data points and the estimated values of the state variables at the corresponding time points. Fig. 5.6 depicts the contribution of each data point on the total resnorm (i.e. weighted sum of squared error) in the model with a delayed feedback from pAkt to p-IRS. The top figure shows the absolute value of the error between the estimate and the data per data point. The bottom figure shows the weighted squared error per data point. Each 10 of the total 40 data points refer to the time course of p-IRS, p-AktS, p-AS160, and GLUT4 proteins in the PM, respectively. It is clear that the biggest portion of the resnorm is formed due to the combined effect of low standard deviation and relatively higher error of the first time points of p-IRS and p-AktS. The contribution of each data point to the resnorm shown in this model do not vary between that in the models with different scenarios (See Fig. 5.12, 5.13, 5.14 in the Appendix). The models are all capable of reproducing the whole time course of p-AS160 and GLUT4 proteins in the PM, except the first time points of p-IRS and p-AktS. Since we are mainly interested in the dynamic profile of the intermediates, the models are found to be acceptable regardless of their
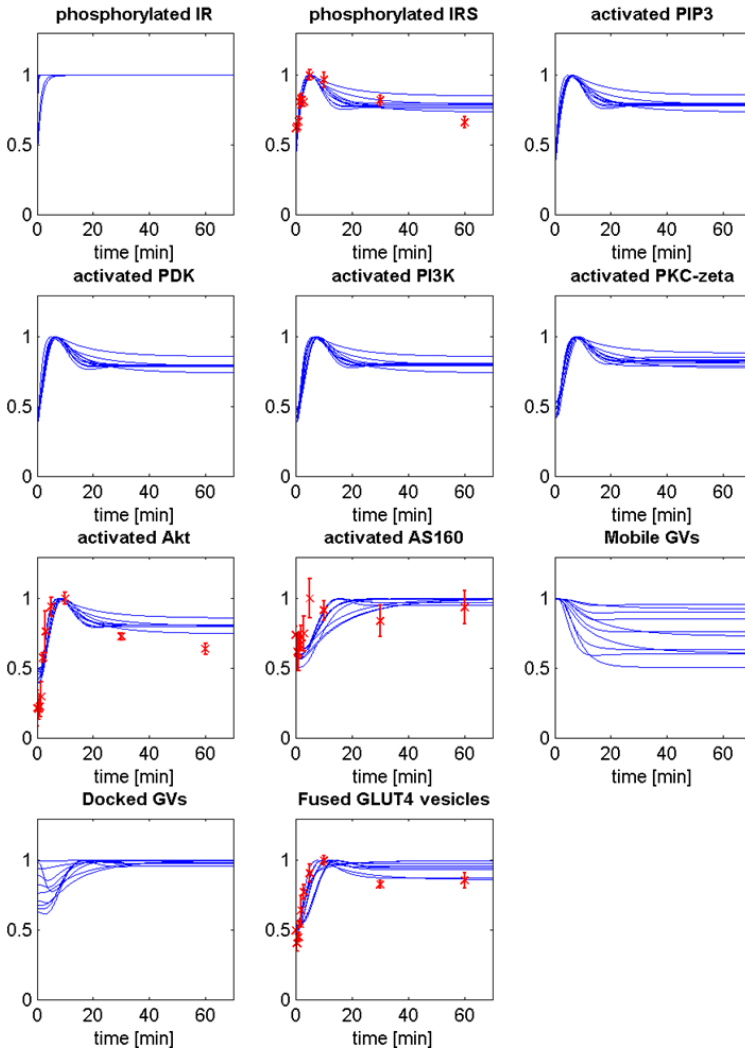
Figure 5.4: Simulations of the model with a feedback to p-IRS from p-AS160. The simulation results with respect to 10 best parameter sets are shown in blue lines. The experimental data is shown in red dots. The model can produce the overshoot behaviour in the time course of p-IRS, p-Akt, and GLUT4 in the PM but not in that of p-AS160. The estimated p-AS160 shows a delayed response to insulin stimulation.
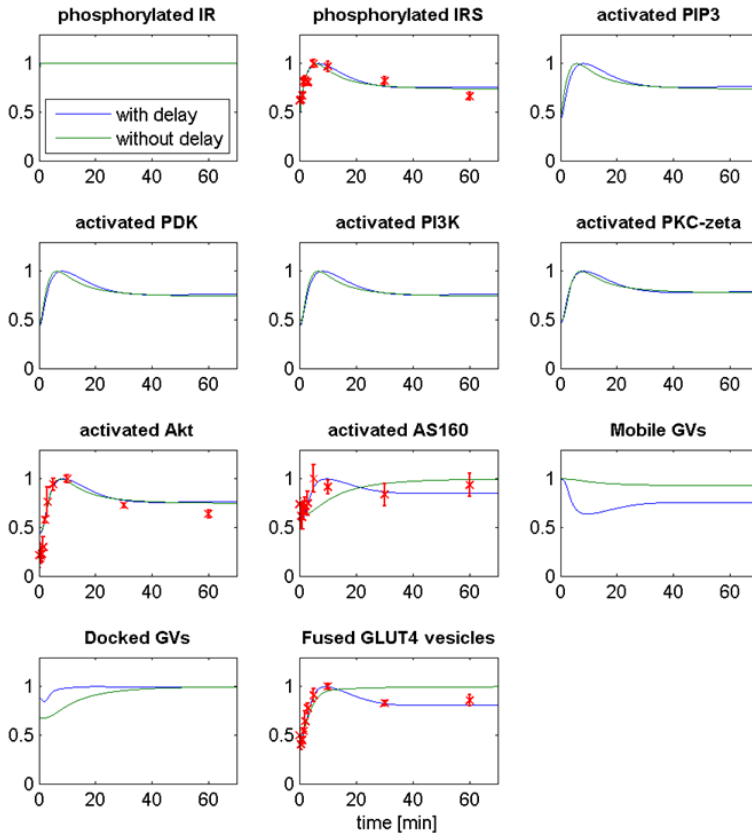
Figure 5.5: Simulations of the model with a delayed feedback to p-IRS from p-AS160 are shown in blue lines, whereas the simulations shown in green refer to the results of the best fit shown in Fig. 5.4 (the model with a feedback without delay). The data is shown in red dots.

relatively high resnorms. The resnorm could be lowered by eliminating the first time points which would lead to biased estimation of the model parameters. In order to reduce the resnorms, one could introduce the basal levels of the 4 intermediates as the initial conditions of these intermediates in the parameter estimation routine. However, as the basal levels of the most intermediates of the pathway are not known, this approach may lead to biased results. Therefore, we adopt an additional criteria to select the feedback source. As an additional
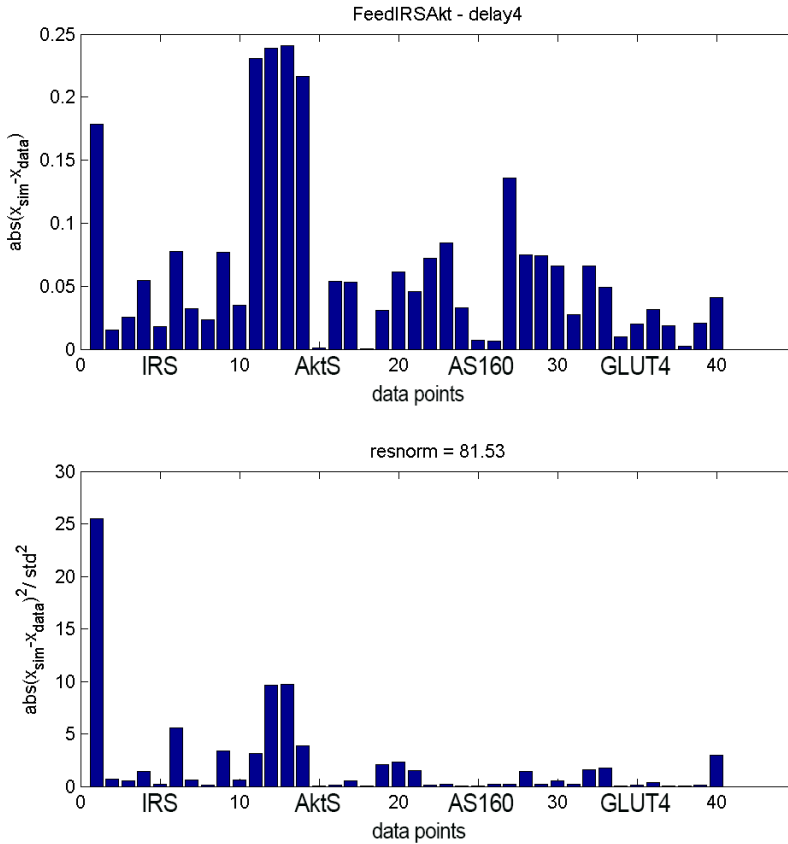
Figure 5.6: Resnorm Analysis for the model with feedback to p-IRS from
pAkt. The top figure shows the absolute value of the error
between the estimate and the data per data point. The bottom
figure shows the weighted squared error per data point. Each
10 of the total 40 data points refer to p-IRS, p-AktS, p-AS160,
and GLUT4 proteins in the PM, respectively.

criteria, we use correlation analysis.

Correlation Analysis

In Chapter 4, linear correlation analysis was employed to the insulin signalling assays. Pearson correlation coefficient was calculated for each couple of intermediates. Independent experiments have been used to calculate the correlation between two intermediates. Here, the correlation analysis is used as an additional criteria to select the optimum model since the resnorm of each scenario lies in the same range. Each model is parameterised separately for each independent data set. The Pearson correlation coefficient for the state variables that are estimated based on each independent data set are calculated. The correlation of the state variables estimated by the models is compared with the correlation of measured state variables that were obtained in Chapter 4. The cost function for the correlation analysis is determined as the summation of the differences between the correlation based on the experimental data and the correlation based on the model prediction; and defined as the weighted sum of errors. The correlations of the estimated intermediates by each model and the corresponding cost functions (i.e. weighted sum of errors) are summarized in Table 5.1. Based on this criteria, the model with a delayed negative feedback from Akt to IRS (Weighted SE=0.47) has been selected as the best among the others. This model is called the eINDHOVEN model for referring Insulin sigNalling Dynamics for Hypotheses, Observations and Virtual ExperimeNts; and its scheme is shown in Fig. 5.7. The simulation results of the eINDHOVEN model which is parameterised based on each independent set are shown in Fig. 5.15, 5.16, and 5.17 separately.

Table 5.1: Correlation analysis of the insulin signalling intermediates' responses to 10 nM insulin stimulation

	Model Feedback from PKC	Model Feedback from Akt	Model Feedback from AS160	Model Feedback from GLUT4	Exp. Data
Akt-S473 vs GLUT4	0.50	0.89	0.92	0.94	0.94
IRS1 vs GLUT4	0.50	0.77	0.65	0.64	0.82
Akt-S473 vs AS160	0.83	0.82	0.72	0.80	0.82
GLUT4 vs AS160	0.24	0.71	0.64	0.79	0.76
IRS1 vs Akt-S473	0.51	0.54	0.64	0.59	0.74
IRS1 vs AS160	0.43	0.42	0.50	0.55	0.42
Weighted SE	1.89	0.47	0.83	0.78	

Furthermore, we utilize the correlation analysis on the model predictions to quantify the correlation among the non-measured states of the pathway and
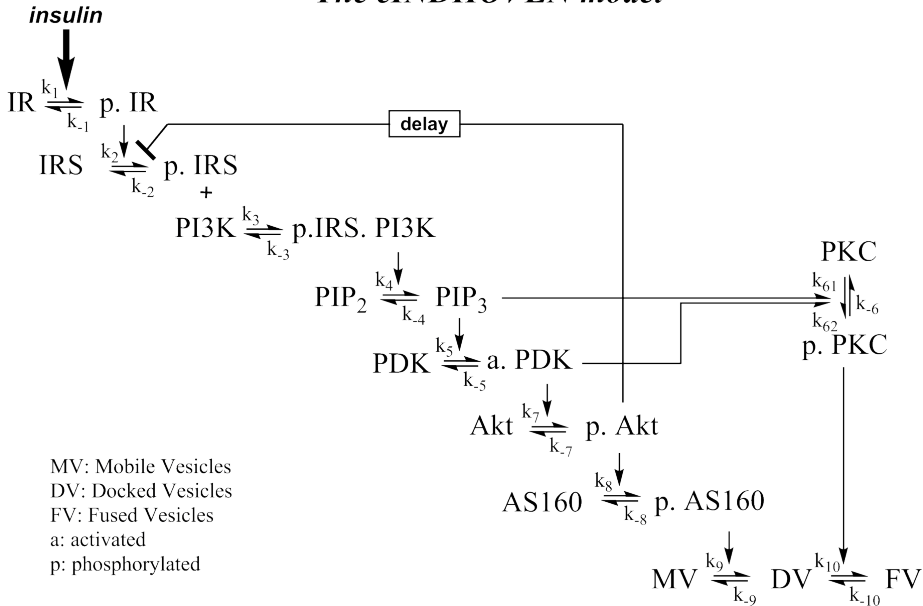
Figure 5.7: The scheme of the eINDHOVEN model.

to test the hypotheses generated in Chapter 4. Linear correlation analysis was employed to the independent insulin signalling assays in Chapter 4. Pearson correlation coefficient was calculated for each couple of the intermediates. Independent experiments have been used to calculate the correlation between two intermediates. We have shown that the measured intermediates of the insulin signalling pathway have a consistent dynamic behaviour among each other regardless of the inter-experimental behaviour. Herewith, we investigate if the dynamic response of the whole insulin signalling pathway to insulin stimulation remains identical despite the variety in their magnitudes (i.e. is isodynamic). The correlations of the paired state variables that are estimated based on each independent data set are presented in a pseudocolour plot shown in Fig. 5.8. We see that the non observed state variables; PI3K, PIP3, and PKC are also highly correlated with other, whereas AS160 maintains the distinct behaviour from the other intermediates. The correlation analysis for the other scenarios (Feedback from AS160, PKC, and GLUT4) are presented in Fig. 5.18 in the Appendix.
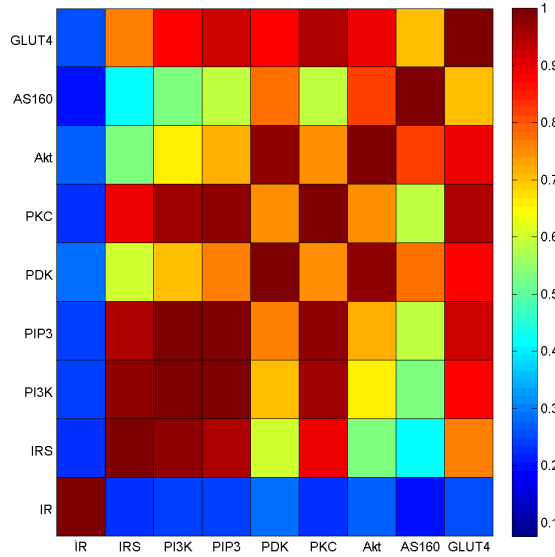
Figure 5.8: Correlations of the estimated state variables via the eIND-HOVEN model.

Multi Parametric Sensitivity Analysis

Multi Parametric Sensitivity Analysis is performed on the selected model; firstly, to assess the identifiability of the parameters; and secondly, to determine the critical steps in GLUT4 translocation. In order to quantify the identifiability of the parameters in the model, the model fitness to the total experimental data upon the perturbations of the model parameters is used as a cost function. On the other hand, to determine the critical steps in GLUT4 translocation that is the output of the system, the fitness of the model to the GLUT4 time course data is used as the cost function. The method is performed as explained in *Multi Parametric Sensitivity Analysis* section in Chapter 2. The results of the MPSA based on the model fitness and the GLUT4 translocation are shown in Fig. 5.9b. MPSA based on the model fitness (Fig. 5.9b) shows that the most of the parameters of the developed model are sensitive (above the threshold) and hence, are identifiable unlike the *Model II* developed in Chapter 2 in which more than half of the parameters displayed no significant impact on the overall system behaviour. However, a few parameters (i.e. k_{62}, k_{-2}) are found to be non-identifiable. k_{62} is the rate constant of the phosphorylation of PKC by PDK.

When we knockout this branch in the model, we see no significant change in the overall system behaviour (See Fig. 5.19). Therefore, we propose that the significant activation of PKC occurs only via PIP3 but not PDK [107]. The PDK branch [107] could be excluded from the model. However, k_{-2} is the rate constant of dephosphorylation of IRS which is also required since the phosphorylation of IRS is considered to be a reversible reaction.
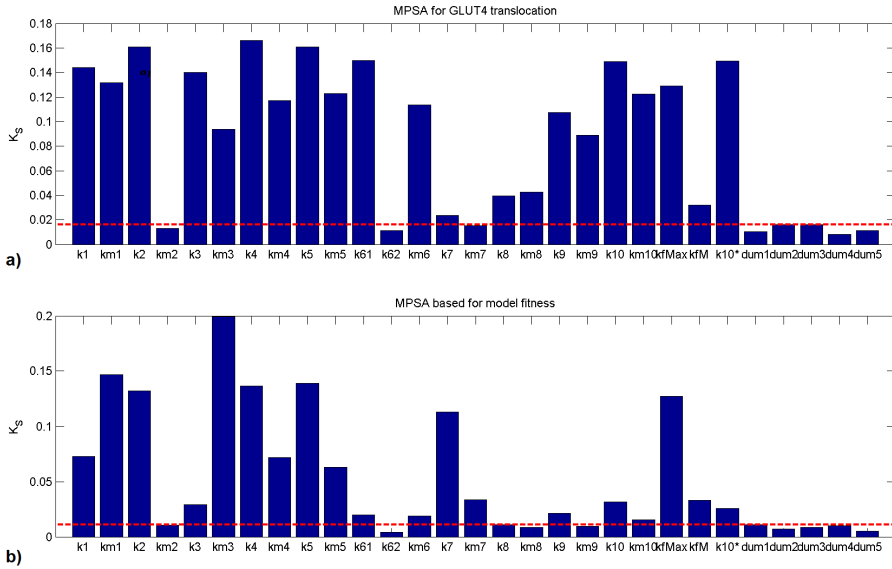
Figure 5.9: MPSA results for *Model III* based on **a)** GLUT4 translocation and **b)** the model fitness. The horizontal dotted line indicates the maximum sensitivity of the dummy parameters. Note that the parameters represent different reactions/interactions in the model.

MPSA based on the GLUT4 translocation (Fig. 5. 9b) reveals that almost all the interactions in the signalling pathway leading to GLUT4 translocation are essential for GLUT4 translocation. This result indicates that the intermediate steps in signal transmission are also critical for GLUT4 translocation as well as docking and fusion of GLUT4 carrying vesicle to the plasmam membrane and therefore, the model with the given intermediates and their interactions cannot be reduced.

Identifiability Analysis

Profile likelihood is performed as described in *Identifiability* section in Chapter 2 to assess the identifiability of the model parameters. In Fig. 5.10, we can see that profile likelihood of the parameters of the model with a delayed feedback from Akt to IRS. The results are in agreement with the results of MPSA based on the model fitness. The values of the parameters (θ_{ref}) are listed in Table 5.3 in the Appendix.
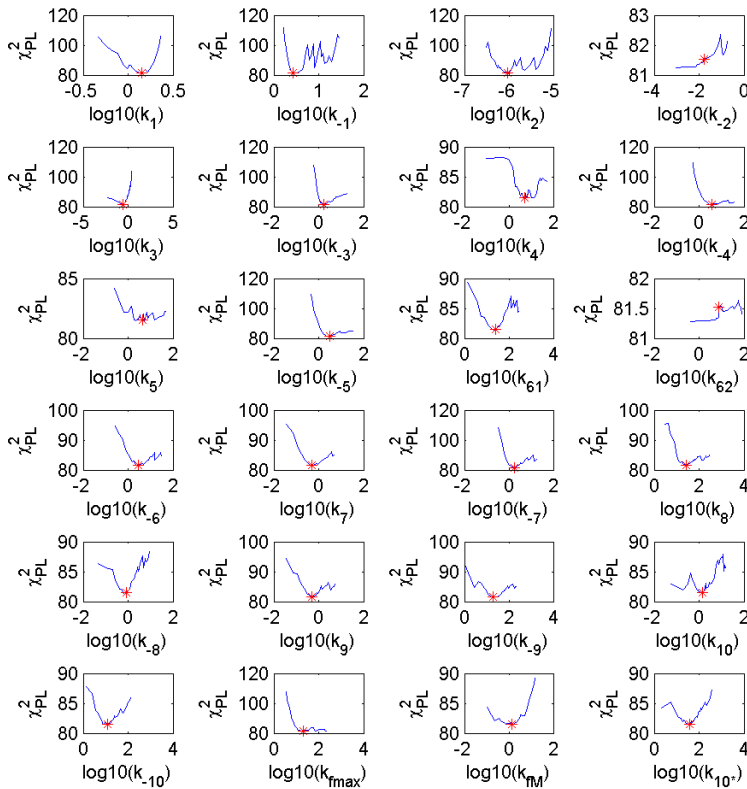
Figure 5.10: Profile likelihood of the parameters of the eINDHOVEN model that is parameterised with the independent data set 1. Red stars represent the calibrated parameter values θ_{ref}.

Virtual experiments

There are several hypotheses on lipid induced insulin resistance in skeletal muscle in the literature. When fatty acid flux into cells exceeds the ability of these pathways to dispose of fatty acyl-CoAs, intermediaries of fatty acid metabolism (e.g., DAG, PA, LPA, ceramide) accumulate. In turn, the mTOR/p70S6K, JNK, IKK, and/or the novel PKC/conventional PKC (nPKC/cPKC; e.g. , PKC-θ) can be activated. The serine kinases phosphorylates serine sites of IRS, and therefore tyrosine phosphorylation of IRS is impaired [94, 23, 24, 118]. In addition to impaired p-IRS, ceramide can also impair insulin action through interactions with PKB/Akt [94, 24, 82]. Moreover, the SNARE proteins (SNAP23) play role in the fusion of both lipid droplets and GLUT4 carrying vesicles (GSVs) to the PM in skeletal muscle [12]. As cells are overloaded with lipid, lipid droplets tend to grow in size by fusion of lipid droplets. In these circumstances, it is hypothesized that the Snap23 proteins that exist in the plasma membrane are hi-jacked by the lipid droplets to be able to grow. In turn, the fusion of the GSVs with the PM is down-regulated in skeletal muscle [13].

Table 5.2: Virtual experiments based on hypotheses on insulin resistance.

Rate of p-IRS (%)	GLUT4 in PM (%)	Rate of p-AktS (%)	GLUT4 in PM (%)	Rate of p-IRS& p-AktS (%)	GLUT4 in PM (%)	Rate of GSV fusion (%)	GLUT4 in PM (%)
100	100.00	100	100	100	100	100	100
75	82.24	75	94.37	75	78.01	75	75
50	62.26	50	86.46	50	55.53	50	50
25	38.86	25	73.78	25	32.54	25	25
10	22.09	10	59.96	10	18.50	10	10
1	10.17	1	42.22	1	9.98	1	1

Herewith, we use our model to conduct virtual experiments based on the hypotheses on lipid induced insulin resistance. The aim of these experiments is to quantify the effect of the impaired p-IRS, p-AktS, and the fusion of GSVs on the cell function that is GLUT4 translocation in our system. The rate constants of phosphorylation of the (p-) IRS, p-AktS, and fusion of GSVs to the PM are decreased to % 75, 50, 25, 10, and 1. The steady state values of GLUT4 proteins in the PM (i.e. the output of the system) upon insulin stimulation (10nM insulin) in case of the impaired p-IRS, p-AktS, p-IRS in combination with p-AktS, and fusion of GSVs are recorded. Table 5.2 summarizes the results of these virtual experiments. It can be seen that the decrease in the rate of both p-IRS and p-AktS influences the system significantly in a nonlinear way. Furthermore, the effect of an impairment in p-IRS on the system output is larger than that of

an impairment in p-AktS. This indicates that p-IRS dominates the behaviour of the whole system including GLUT4 translocation. The added value of the impaired p-AktS in combination with p-IRS on the system output is relatively small despite the fact that its own effect is more substantial. On the other hand, we observe a linear decrease in the GLUT4 proteins, as the fusion of GSVs is the final step of the insulin signalling pathway.

5.3 Discussion and Concluding Remarks

Studying the dynamics of the pathway helps us to understand the functioning of the insulin signalling pathway that leads to the GLUT4 translocation and therewith, aids our understanding of the malfunction of the pathway which leads to insulin resistance in skeletal muscle. In this chapter, we utilize a systems biology approach that combines mathematical modeling and experimental work to study the regulations in the insulin signalling pathway that describe the core dynamic behaviour of the insulin signalling pathway from insulin receptor to GLUT4 translocation. The main goal in this work is to create a mathematical model that can represent the dynamical behaviour of the insulin signalling pathways in order to gain a better understanding of their complex interactions and to develop quantitative descriptions of its dynamics. In order to build such mathematical models, the widely known cycle of systems biology is repeated several times such that a more reliable mathematical model of the system is obtained. The method consists of iterative cycles of experiments and mathematical modelling both of which feed each other.

The overshoot behaviour of the signalling intermediates that is observed in the insulin signalling assays presented in Chapter 4 indicates that a negative feedback mechanism is required for the model. We have found out that the feedback originates from the downstream signalling intermediates (i.e. starting from PKC) by testing each intermediate of the signalling pathway. Further analyses were applied to PKC, Akt, AS160, and GLUT4. Based on the residual analysis and correlation analysis, we propose that Akt is the strongest candidate for being the source of the mentioned feedback. Furthermore, we observe that the feedback is delayed. It may be due to the localisation of the downstream signalling intermediates or due to the involvement of a scaffold protein(s) that regulate(s) signal transduction and facillitates the localisation of the intermediates. Scaffold proteins play a role in co-ordinating this cascade, and may influence cellular responses through effects on signal intensity and duration, localisation of complexes and recruitment of modulatory proteins. such as phosphatases and ubiquitin ligases [96].

In a recently published work by Gray and Foster, a reduced version of Sedaghat model is presented [37]. However, this model lacks the information on the intermediate steps of the insulin signalling pathway. On the other hand, the parameters of the model that we presented in this chapter are found to be

identifiable and sensitive based on Profile likelihood and MPSA. Furthermore, MPSA based on the system output which is the GLUT4 translocation reveals that the intermediates of the insulin signalling and their interactions are essential for GLUT4 translocation as well as the docking and fusion of GLUT4 carrying vesicles to the plasma membrane. Hence, the model reduction is not required for our developed model. It is due to the added value of combining the novel experimental data with modelling. It provides means of studying the intermediate steps in insulin signalling as well.

In Chapter 4, the metrics used to analyse and compare the dynamic profiles of the different intermediates between independent experiments captured a consistent dynamic behaviour of the pathway despite the inter-experimental differences in the data (Table 5.1) due to the cell variability. IRS1, Akt-S473, Akt-T308 and GLUT4 have coordinated action in responding to insulin stimulation with well defined profiles. In conclusion, we propose that the insulin signalling pathway leading to GLUT4 translocation can be an isodynamic system although the intermediates respond differently between experiments, they show the same overall behaviour. This property/observation can be used to capture fundamental interactions and ease the understanding of other signalling pathways. Herewith, we investigate if the dynamic response of the whole insulin signalling pathway to insulin stimulation remains identical despite the variety in their magnitudes. The correlations of the paired state variables that are estimated based on each independent data set are presented in a pseudocolour plot shown in Fig. 5.8. We see that the non observed state variables; PI3K, PIP3, and PKC are also highly correlated with each other, whereas AS160 maintains the distinct behaviour from the other intermediates. The correlation analysis for the other scenarios (Feedback from AS160, PKC, and GLUT4) are presented in Fig. 5.18 in the Appendix.Our model also depicts that as well as the observed intermediates, non observed intermediates are highly correlated with each other despite the variability among the models based on independent experiments. Therefore, our hypothesis on dynamics of the pathway cannot be rejected with model analyses: The insulin signalling pathway that leads to GLUT4 translocation can be proposed to be an isodynamic system.

Furhermore, by conducting virtual experiments, we present an application of the model to increase our understanding in the effect of impaired activity of the intermediates of insulin signalling. Herewith, we use our model to conduct virtual experiments based on the hypotheses on lipid induced insulin resistance. The aim of these experiments is to quantify the effect of the impaired p-IRS, p-AktS, and the fusion of GSVs on the cell function that is GLUT4 translocation in our system. The rate constants of phosphorylation of the (p-) IRS, p-AktS, and fusion of GSVs to the PM are decreased to % 75, 50, 25, 10, and 1. The steady state values of GLUT4 proteins in the PM (i.e. the output of the system) upon insulin stimulation (10nM insulin) in case of the impaired p-IRS, p-AktS, p-IRS in combination with p-AktS, and fusion of GSVs are recorded. Table 5.2

summarizes the results of these virtual experiments. It can be seen that the decrease in the rate of both p-IRS and p-AktS influences the system significantly in a nonlinear way. Furthermore, the effect of an impairment in p-IRS on the system output is larger than that of an impairment in p-AktS. This indicates that p-IRS dominates the behaviour of the whole system including GLUT4 translocation. The added value of the impaired p-AktS in combination with p-IRS on the system output is relatively small despite the fact that its own effect is more substantial. On the other hand, we observe a linear decrease in the GLUT4 proteins, as the fusion of GSVs is the final step of the insulin signalling pathway.

5.4   Appendix

Parameter Estimation

Normalisation: Each time course data generated is normalised with respect to the peak value in the time course. Standard deviations are also normalised with respect to the peak value of the time course. To calculate the error function of the model, the simulated time course is normalised with respect to its peak value in the time course. The difference of the normalised data point and the normalised estimated value of the states at the given time point, is divided by the standard deviation of the data point.

Presimulation: The initial conditions of the state variables are determined via a presimulation process. Here, steady state response of the system to 1 nM is supplied as the initial conditions of the real simulations. As each independent experiment that is carried out is presented individually in the previous chapter, the model is parameterised separately for each independent experiment which consists of time courses of insulin responses of the five intermediates. The normalised data with respect to the maximum stimulated states of the corresponding protein was introduced into the optimization routine. The nonlinear recursive least squares based on the differences of the normalised individual data set and the normalised model output are solved by the *lsqnonlin* routine found in Matlab optimization toolbox. The parameter space (with a size of n x p, where n is the sample size of each of p parameters) was constructed by Latin hypercube sample ($(X = lhsdesign(n, p)$ found in Matlab Statistics toolbox. The lower bound of the parameters is set to zero whereas there set to be no upper bound. Optimization routine ended with different dynamic behaviors for each models based on each independent experiments.

Implementation

All algorithms were implemented in Matlab (Natrick, MA). Numerical integration was performed using compiled MEX files using numerical integrators from the SUNDIALS CVode package (Lawrence Livermore National Laboratory, Livermore, CA). To perform the initial large scale search, we performed random sampling using a uniform hypercube to obtain initial parameter values. These were subsequently optimized using the Levenberg-Marquardt minimizer from the MATLAB optimization toolbox. The best fit was subsequently selected and used for determining the PL.

Model Equations

$$\dot{x}_2 = -k_1 x_1 x_2 + k_{-1} x_3$$

$$\dot{x}_3 = k_1 x_1 x_2 - k_{-1} x_3$$

$$\dot{x}_4 = -k_2 x_3 x_4 + k_{-2} x_5 + \frac{k_{fmax} x_5 x_{15}(t-\tau)}{x_{15}(t-\tau) + k_{fM}}$$

$$\dot{x}_5 = k_2 x_3 x_4 - k_{-2} x_5 - \frac{k_{fmax} x_5 x_{15}(t-\tau)}{x_{15}(t-\tau) + k_{fM}} - k_3 x_5 x_6 + k_{-3} x_7$$

$$\dot{x}_6 = -k_3 x_5 x_6 + k_{-3} x_7$$

$$\dot{x}_7 = k_3 x_5 x_6 - k_{-3} x_7$$

$$\dot{x}_8 = -k_4 x_7 x_8 + k_{-4} x_9$$

$$\dot{x}_9 = k_4 x_7 x_8 - k_{-4} x_9$$

$$\dot{x}_{10} = -k_5 x_9 x_{10} + k_{-5} x_{11}$$

$$\dot{x}_{11} = k_5 x_9 x_{10} - k_{-5} x_{11}$$

$$\dot{x}_{12} = -k_{6f1} x_{11} x_{12} - k_{-6f2} x_9 x_{12} + k_{-6} x_{13}$$

$$\dot{x}_{13} = k_{6f1} x_{11} x_{12} + k_{-6f2} x_9 x_{12} - k_{-6} x_{13}$$

$$\dot{x}_{14} = -k_7 x_{11} x_{14} + k_{-7} x_{15}$$

$$\dot{x}_{15} = k_7 x_{11} x_{14} - k_{-7} x_{15}$$

$$\dot{x}_{16} = -k_8 x_{15} x_{16} + k_{-8} x_{17}$$

$$\dot{x}_{17} = k_8 x_{15} x_{16} - k_{-8} x_{17}$$

$$\dot{x}_{18} = -k_9 x_{17} x_{18} + k_{-9} x_{19}$$

$$\dot{x}_{19} = k_9 x_{17} x_{18} - k_{-9} x_{19} - k_{10} x_{19} - k_{10,branch} x_{19} x_{13} + k_{-10} x_{20}$$

$$\dot{x}_{20} = k_{10} x_{19} x_{13} - k_{-10} x_{20}$$

where x stands for the model state variables.

For mathematically introducing delay τ represented in $x_{15}(t-\tau)$ into the models, linear chain approximation is used. Extra states are incorporated to the model. These states are assumed to go through the following reaction.

$$Z \rightleftharpoons Z^* \tag{5.3}$$

Fig. 5.11 shows the profile of the extra states which are called as the delay states. The ordering of the delay states (Z) with different time constansts is important in generating the desired dynamic profile of the delayed feedback source. At least 2 states with fast dynamics are required to generate the desired S-shaped profile. 2 states with slow dynamics followed by 2 states with fast dynamics are incorporated into the model to produce the delay in the feedback path.

The ODEs for these extra states are given as follows:

$$\dot{Z}_1 = -k_{11}x_{15}Z_1 + k_{-11}Z_1^*$$
$$\dot{Z}_1^* = k_{11}x_{15}Z_1 - k_{-11}Z_1^*$$
$$\dot{Z}_2 = -k_{12}Z_1^*Z_2 + k_{-12}Z_2^*$$
$$\dot{Z}_2^* = k_{12}Z_1^*Z_2 - k_{-12}Z_2^*$$
$$\dot{Z}_3 = -k_{13}Z_2^*Z_3 + k_{-13}Z_3^*$$
$$\dot{Z}_3^* = k_{13}Z_2^*Z_3 - k_{-13}Z_3^*$$
$$\dot{Z}_4 = -k_{13}Z_3^*Z_4 + k_{-13}Z_4^*$$
$$\dot{Z}_4^* = k_{13}Z_3^*Z_4 - k_{-13}Z_4^*$$

Model state variables

x_1	= insulin input	x_{11}	= activated PDK
x_2	= unphosphorylated IR	x_{12}	= unactivated PKC
x_3	= phosphorylated IR	x_{13}	= activated PKC
x_4	= unphosphorylated IRS-1	x_{14}	= unphosphorylated Akt
x_5	= phosphorylated IRS-1	x_{15}	= phosphorylated Akt
x_6	= unactivated PI3K	x_{16}	= unphosphorylated AS160
x_7	= IRS-1/PI3K complex	x_{17}	= phosphorylated AS160
x_8	= PI(3,4)P2	x_{18}	= mobile GLUT4 vesicles (MV)
x_9	= PI(3,4,5)P3	x_{19}	= docked GLUT4 vesicles (DV)
x_{10}	= unactivated PDK	x_{20}	= fused GLUT4 vesicles (FV)

Model parameters

p_1	$= k_1$	p_{13}	$= k_{-6}$
p_2	$= k_{-1}$	p_{14}	$= k_7$
p_3	$= k_2$	p_{15}	$= k_{-7}$
p_4	$= k_{-2}$	p_{16}	$= k_8$
p_5	$= k_3$	p_{17}	$= k_{-8}$
p_6	$= k_{-3}$	p_{18}	$= k_9$
p_7	$= k_4$	p_{19}	$= k_{-9}$
p_8	$= k_{-4}$	p_{20}	$= k_{10}$
p_9	$= k_5$	p_{21}	$= k_{-10}$
p_{10}	$= k_{-5}$	p_{22}	$= k_{fmax}$
p_{11}	$= k_{61}$	p_{23}	$= k_{fM}$
p_{12}	$= k_{62}$	p_{24}	$= k_{10,branch}$

Table 5.3: The parameter values for the eINDHOVEN model parame-
terised for the independent data set 1. θ_{ref} denotes the values
of the reference parameters.

Parameters	θ_{ref} $[\text{min}]^{-1}$	Parameters	θ_{ref} $[\text{min}]^{-1}$
k_1	1.4159	k_8	26.5692
k_{-1}	2.6335	k_{-8}	0.8551
k_2	9.38E-07	k_9	0.5106
k_{-2}	0.0163	k_{-9}	19.1401
k_3	0.2454	k_{10}	1.4317
k_{-3}	1.7026	k_{-10}	12.4977
k_4	4.9529	k_{10*}	37,1937
k_{-4}	3.5722	k_{fmax}	21.1644
k_5	4.3687	k_{fM}	1.4070
k_{-5}	3.2239	k_{11}	1.49E-05
k_{61}	24.8683	k_{-11}	0.0265
k_{62}	7.4088	k_{12}	0.7117
k_{-6}	2.9858	k_{-12}	0.2108
k_7	0.4777	k_{13}	3.5595
k_{-7}	1.8035	k_{-13}	7.9937
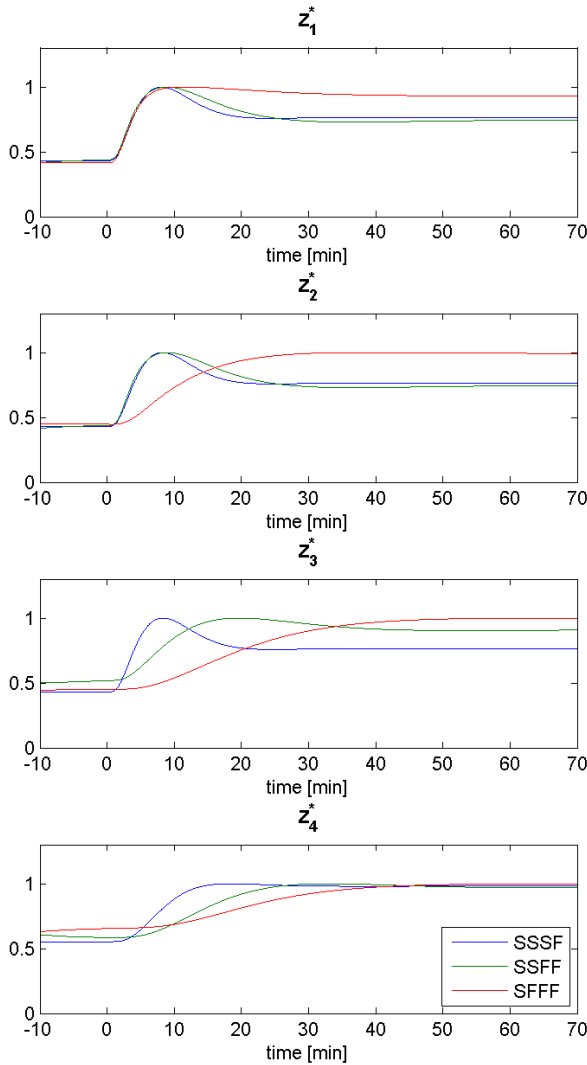
Figure 5.11: The ordering of the delay states (Z) with different time
constansts is important in generating the desired dynamic
profile of the feedback source. At least 2 states with fast
dynamics are required to generate the desired S-shaped profile.
In the legend of the curves, S represents slow dynamics,
whereas F denotes fast dynamics of the delay states.

Figure 5.12: Resnorm Analysis for the model with feedback to p-IRS from p-PKC. The top figure shows the absolute value of the error between the estimate and the data per data point. The bottom figure shows the weighted squared error per data point. Each 10 of the total 40 data points refer to p-IRS, p-AktS, p-AS160, and GLUT4 proteins in the PM, respectively.
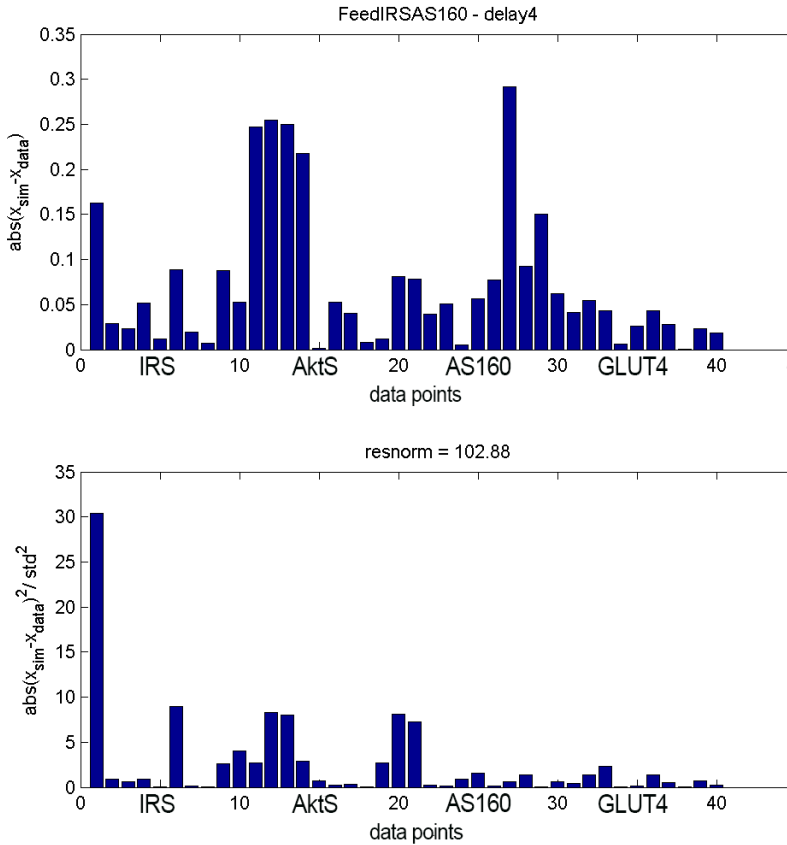
Figure 5.13: Resnorm Analysis for the model with feedback to p-IRS from p-AS160. The top figure shows the absolute value of the error between the estimate and the data per data point. The bottom figure shows the weighted squared error per data point. Each 10 of the total 40 data points refer to p-IRS, p-AktS, p-AS160, and GLUT4 proteins in the PM, respectively.
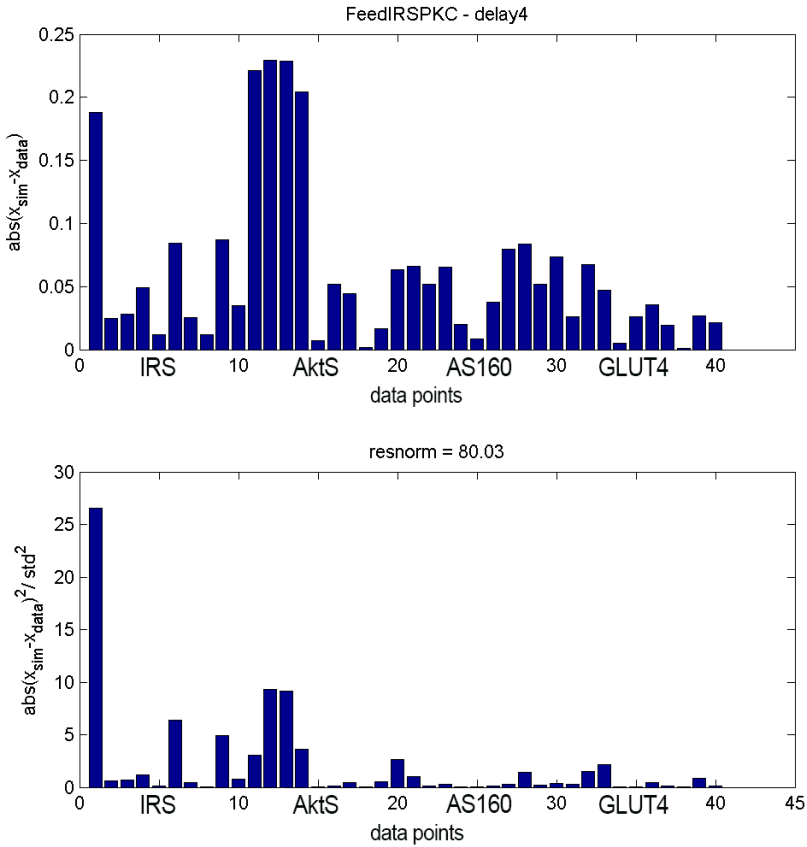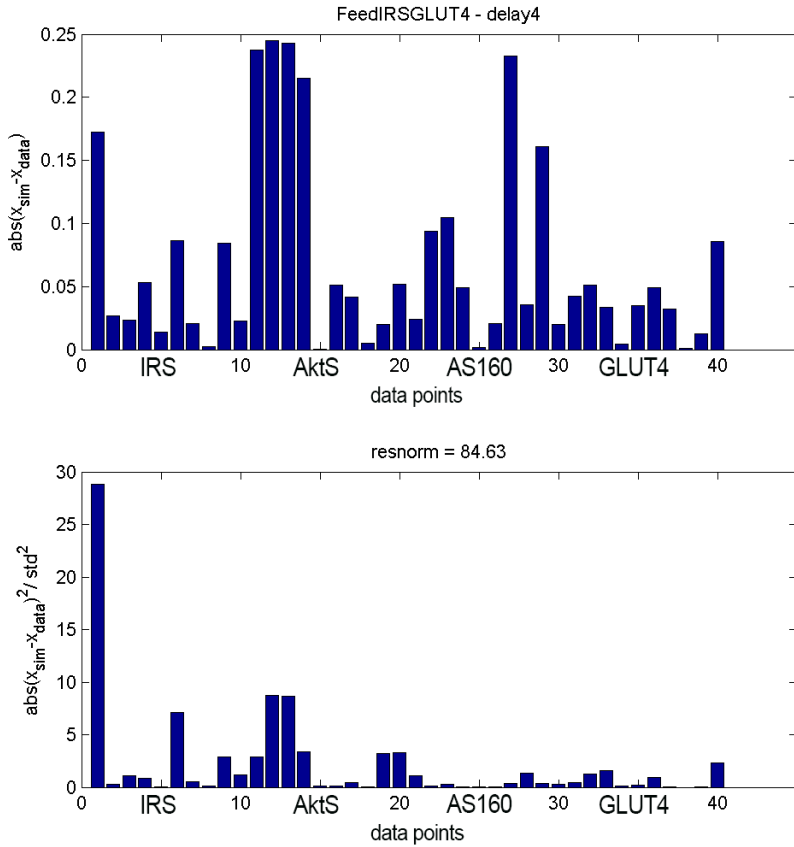
Figure 5.14: Resnorm Analysis for the model with feedback to p-IRS from GLUT4. The top figure shows the absolute value of the error between the estimate and the data per data point. The bottom figure shows the weighted squared error per data point. Each 10 of the total 40 data points refer to p-IRS, p-AktS, p-AS160, and GLUT4 proteins in the PM, respectively.
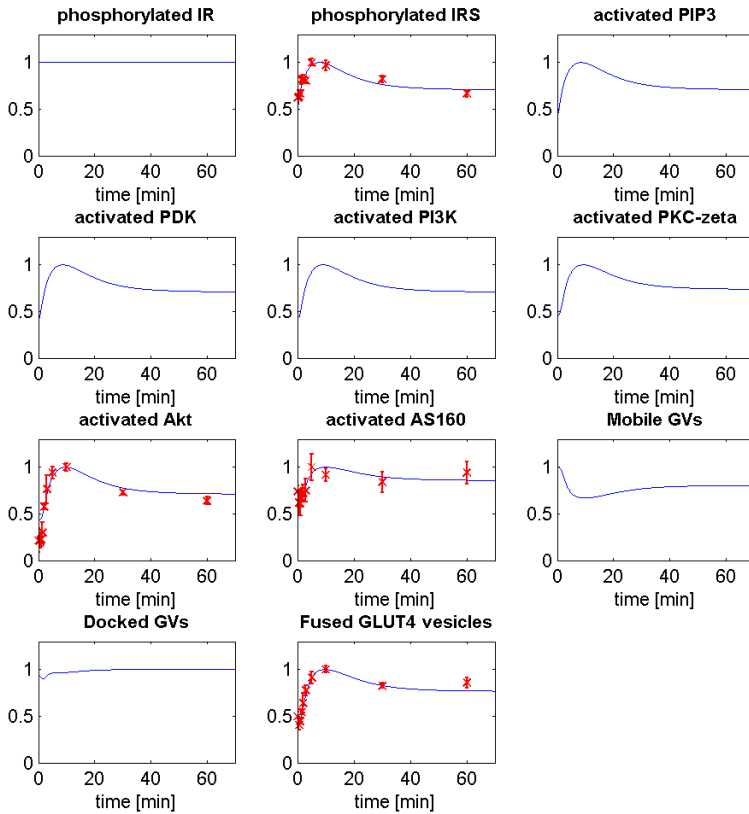
Figure 5.15: Simulation results of the eINDHOVEN model parameterised
based on independent data set 1. The data is shown in red
dots and the model is shown in blue lines.
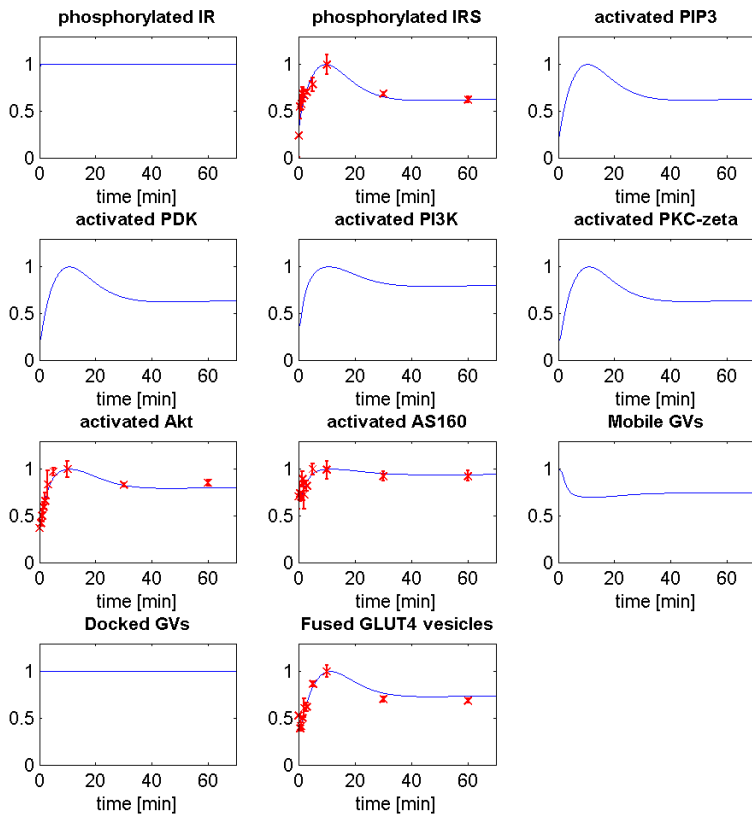
Figure 5.16: Simulation results of the eINDHOVEN model parameterised based on independent data set 2. The data is shown in red dots and the model is shown in blue lines.
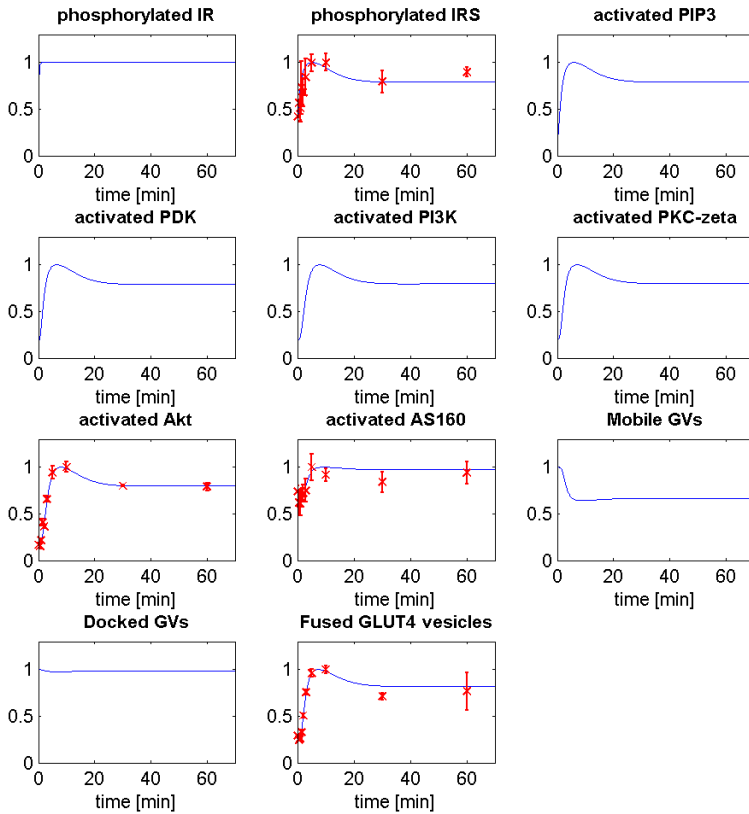
Figure 5.17: Simulation results of the eINDHOVEN model parameterised
based on independent data set 3. The data is shown in red
dots and the model is shown in blue lines.
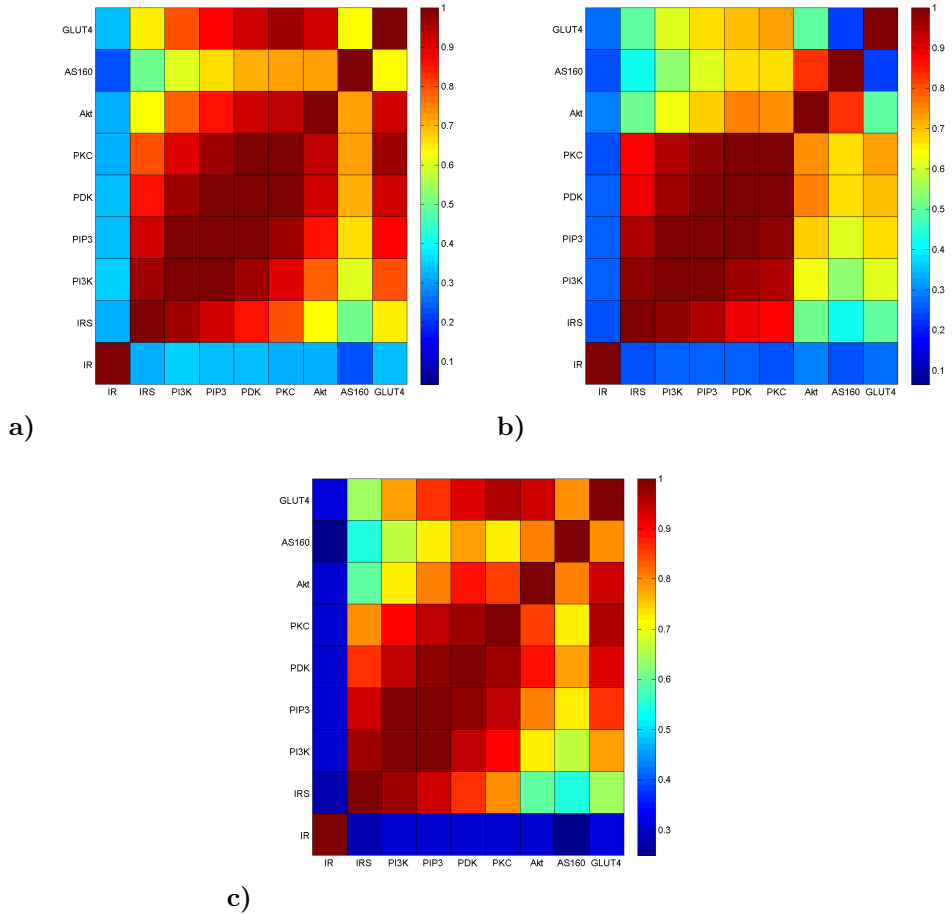
Figure 5.18: Correlations of the estimated state variables via a) the model with a delayed feedback from AS160 to IRS, b) the model with a delayed feedback from PKC to IRS, and c)the model with a delayed feedback from GLUT4 to IRS.
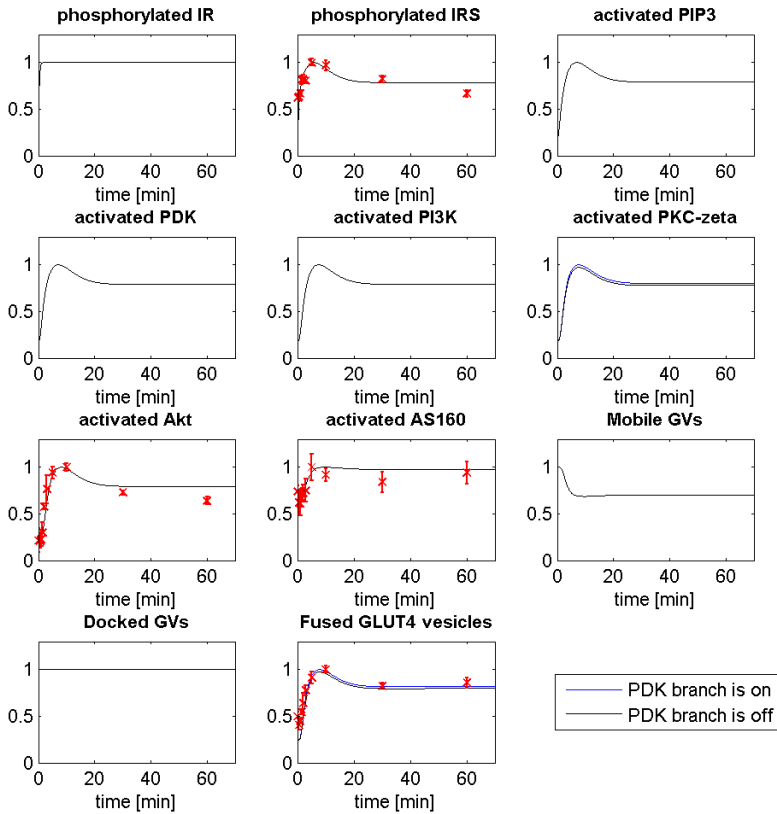
Figure 5.19: When PKC activation by PDK is knocked out in the model,
simulation results show that there is no significant change in
the overall behaviour of the system.

Chapter 6

Summary and Outlook

6.1   Summary and Main Conclusions

The insulin signalling pathway that leads to GLUT4 translocation is a prerequisite of the insulin-stimulated glucose uptake and therefore is an important element of glucose homeostasis. An impairment in the insulin signalling leads to insulin resistance which is an early symptom of Type 2 diabetes. To develop strategies for reestablishing normal glucose homeostasis in people with type 2 diabetes, understanding of the functioning and the dynamics of the insulin signal leading to GLUT4 translocation is essential. Skeletal muscle is considered as one of the primary tissues among insulin-sensitive tissues, because it accounts for 75 - 80 % of whole body insulin-stimulated glucose uptake. In this thesis, to study the functioning and the dynamics of the insulin signalling pathway in skeletal muscle, we adopt a Systems Biology framework in which we combine in silico and in vitro studies. The main goal of this thesis is to create the eINDHOVEN model that can represent the dynamical behaviour of insulin signalling from insulin receptor to GLUT4 translocation in rat skeletal muscle cells. In each chapter, we presented a step towards our main goal.

The insulin signalling pathway has been studied for decades for identifying the intermediates and their interactions. However, our understanding of the key mechanisms in the insulin signalling pathway and how the insulin signalling pathway interfaces with the GLUT4 storage compartments are still limited. In

chapter 2, we use a data-hypothesis driven modelling approach to study the missing regulations in the insulin signalling pathway that describe the core dynamic behaviour of the insulin signalling pathway from insulin receptor to GLUT4 translocation. The parameters of the developed model (*Model II*) are estimated based on the composite data set which combines heterogenous studies. These studies were conducted by using Western blotting methods for different cell types under different experimental conditions. Most of the parameters in *Model II* have been observed to be non-identifiable which might be caused by combining different data sources due to the fact that the kinetic parameters of interactions of proteins in a signalling cascade are highly dependent on the cell type. Each study provides data for only a limited number of intermediates and data could only be sampled for limited time points due to practical restrictions in the Western blotting method. Therefore, understanding of the intermediate steps in signalling through GLUT4 translocation is still limited and the system level information on the short term dynamics of the intermediates of the insulin signalling pathway is lacking. The nonidentifiability of most of the model parameters in *Model II* is a cause for the uncertainty of the model predictions. The underlying reason of identifiability problems of the developed model is the mismatch between the available data and the data required to uniquely identify the model parameters. A solution for overcoming this limitation is to generate a high resolution temporal data set for a broader subset of intermediates from the same cell type in order to parameterise a model that can provide predictions with higher certainty. In Chapter 4 such data from skeletal muscle cells is generated by a combined platform of high-throughput techniques in immunocytochemistry and fluorescence imaging.

In Chapter 3, the methodology for the quantification of the generated data is presented. We demonstrated the importance of the quantification of the data by using two different methods, namely, thresholding (pixel)-based and intensity-based quantification. The choice of the methodology used to quantify the raw images may lead to inconsistent results. We have shown that the thresholding method is subject to inaccuracies due to the manual selection of threshold value for the masks and the target proteins. As a result, this may lead to misinterpretation of the dynamics of the proteins and also limited reproducibility of the data. To overcome these drawbacks, we proposed an alternative method which extends the thresholding method with automatic determination of the masks by using a region growing algorithm and intensity-based protein quantification within these masks. We have shown for the experimental data, how this method provides a more accurate approximation of the concentration of the phosphorylated proteins in the insulin signalling pathway. The proposed method was used to quantify our fluorescence data.

Chapter 4 represents our in vitro studies obtained by a combined platform of high-throughput techniques in immunocytochemistry and fluorescence imaging. Skeletal muscle cells (rat L6-GLUT4myc myotubes) were exposed to multiple,

different changes in extracellular insulin, including insulin washout. To study the short-term dynamics, frequently-sampled time course data was collected for several signalling intermediates. Immunocytochemistry assays for phosphorylation of (p-) IRS-1, Akt-S473, Akt-T308, AS160 and GLUT4 proteins in the plasma membrane were combined with high-throughput fluorescence microscopy to trace and quantify the spatial and temporal organisation of the proteins in the pathway. The metrics used to analyze the time course responses of the intermediates have revealed that all the measured intermediates show consistent dynamic behaviour regardless of the inter-experimental variations. Moreover, correlation analysis has shown that the temporal profile of p-Akt-S473 has high correlation with all the intermediates, particularly with GLUT4 protein in the plasma membrane. The presented study contributes a comprehensive frequent time course data for the phosphorylation and activation of the selected proteins (shown in Fig. 4.13) in the insulin signalling pathway leading to GLUT4 translocation. Thereby, it reveals the dynamics of the intermediates that play a role in the signalling through insulin mediated GLUT4 translocation in rat skeletal muscle cells. The analyses confirm that the signal propagates through the pathway, but time delays are small and the dynamic profiles of the different intermediates are very similar in responding to various insulin stimulations. They persist the consistent dynamic profile in response to various insulin perturbations. The cellular signalling pathways can respond to the same perturbation with a similar profile although the magnitude of the responses can display variations due to the cellular variability and the cross-links to other pathways. We define the systems that display this property as *isodynamic systems* as a novel concept for cellular signalling pathways. This property can be used to capture fundamental interactions and ease the understanding of cellular signalling pathways. Although the intermediates of the insulin signalling pathway respond differently between experiments, they show the same overall behaviour. Based on these observations, we hypothesize that the insulin signalling pathway leading to GLUT4 translocation can be an isodynamic system. This hypothesis is further investigated in silico, in Chapter 5.

Chapter 5 represents the integration of the generated data into the model developed in Chapter 2. The model is refined through a process that consists of several iterations of model development, testing of the hypotheses and virtual experiments. The overshoot behaviour of the signalling intermediates that is observed in the insulin signalling assays presented in Chapter 4 indicates that a negative feedback mechanism is required. Based on residual analysis and correlation analysis, we propose that the phosphorylation of IRS is regulated by a delayed negative feedback from Akt-S473. The delay on the feedback may be due to the localisation of the downstream signalling intermediates or due to the involvement of a scaffold protein(s) that regulate(s) signal transduction and facillitates the localisation of the intermediates. Subsequently, we use our model of the insulin signalling pathway to test the hypotheses formulated in Chapter

4. We have shown that the measured intermediates of the insulin signalling pathway have a consistent dynamic behaviour among each other regardless of the variations between the independent experiments. Profile likelihood and MPSA show that the model parameters are identifiable and sensitive. Furthermore, MPSA based on the system output, which is the GLUT4 translocation, reveals that the intermediates of the insulin signalling pathway and their interactions are essential for GLUT4 translocation. Hence, the model reduction is not required for our developed model. Our model also depicts that, as well as the observed intermediates, non observed intermediates are highly correlated with each other despite the variability among the independent experiments and models. Therefore, our hypothesis on dynamics of the pathway cannot be rejected with model analyses: The insulin signalling pathway that leads to GLUT4 translocation can be proposed to be an isodynamic system.

6.2   Outlook and Future Perspectives

Throughout the thesis, we assessed the insulin signalling pathway as an isolated pathway from the signalling network. We developed the eINDHOVEN model for the insulin signalling to GLUT4 translocation in rat skeletal muscle and focused on the interactions among the intermediates that have been discovered so far. In developing our model, we aimed to build the bridge between the insulin signalling which involves phoshphorylation and activation reactions; and the GLUT4 translocation which involves physical processes such as intracellular sorting GLUT4 translocation involves intracellular sorting, vesicular transport to the cell surface along cytoskeletal elements, and finally, docking, priming, and fusion of the GLUT4 storage vesicles with the cell surface. There might be the need for incorporating more detailed physical processes that would require more proteins and elements (e.g. SNARE proteins that play role in fusion of the vesicles, AS160 interacting protein 14-3-3.) incorporated into the model. However, as models get larger, one would be confronted with more identifiability issues since there is limited dynamic data on the mentioned physical processes.

The spatial organisation of the proteins influences the dynamic characteristics of insulin signalling as well as the other signalling pathways. In our model, we could not investigate the effect of the spatial organisation of the proteins, as we studied the insulin signalling pathway in cell lines which allow to generate frequently sampled data. Skeletal muscle also consists of different types of fibers (i.e. Type I, Type IIa, TypeIIb). The GLUT4 translocation shows variety between the types of fibers [15]. Besides, insulin resistance is also considered as a fiber specific characteristics. However, we have considered the overall behaviour in skeletal muscle by using skeletal muscle cell lines in our experimental studies.

Zoom out from the insuling signalling pathway via ADAPT

Furthermore, it is known that the signalling part is in reality not isolated. Instead, it is cross-linked to other pathways and open to regulations and crosstalks. However, the intersection points of the pathway with the complex signalling network are not fully known. For zooming out from the insulin signalling pathway, here we present a short study as an outlook. To find out the possible modulation points in the insulin signalling pathway, we employ the Analysis of Dynamic Adaptations in Parameter Trajectories (ADAPT) which is recently developed by Tiemann *et.al.* [105]. The parameter trajectories can provide valuable information in classical modelling approaches that study short term dynamics and involve the development of mathematical models containing time-constant parameters. We apply ADAPT on the eINDHOVEN model to infer missing network interactions by using parameter trajectories.

Dynamic parameters to identify missing regulations

Identifying missing regulatory mechanisms in mathematical models is quite challenging. However, ADAPT can aid in this task by providing targeted directions for the mechanisms to be changed. The ADAPT method is based on a time-dependent evolution of model parameters. Here we use ADAPT to find out the possible modulation points in the eINDHOVEN model.

Cubic smoothening splines which depict the dynamic profile of the time course data were calculated and used as input for ADAPT. Time dependent parameters are introduced to account for missing regulation interactions or inappropriate kinetic equations in the computational model. Therefore, a model simulation was divided in N_t steps with Δt time periods by using the following discretization:

$$\begin{aligned}
\vec{X}\,[n] &= \vec{x}(\Delta t, \vec{\theta}\,[n]) \text{ with } \quad \vec{x}(0) = \vec{X}\,[n-1]\,, \\
\vec{Y}\,[n] &= \vec{g}(X\,[n]\,, \vec{\theta}\,[n]\,, \vec{u}), \\
\vec{X}\,[0] &= \vec{x_{ss}}(\vec{\theta}\,[0])
\end{aligned} \tag{6.1}$$

with $0 \leq n \leq N_t$ and $N_t \Delta t$ being the time period of the entire model simulation. The simulation is initiated ($n = 0$) using the steady state values of the model states $\vec{x_{ss}}$ which are obtained with parameter set $\vec{\theta}\,[0]$. Subsequently for each step $n > 0$ the system is simulated for a period of a time period Δt using the final values of the model states of the previous step $n-1$ as initial conditions. Parameters $\vec{\theta}\,[n]$ were estimated by minimizing the difference between the data interpolants and corresponding model outputs $\vec{Y}\,[n]$. Here, the previously estimated parameter

set $\vec{\theta}\,[n-1]$ was provided as initial set for the optimization algorithm. The parameter optimization problem is given by:

$$\vec{\theta}\,[n] = \arg\min_{\vec{\theta}\,[n]} \chi_d^2(\vec{\theta}\,[n]) \tag{6.2}$$

$$\chi_d^2(\vec{\theta}\,[n]) = \sum_{i=1}^{N_y} \left(\frac{Y_i\,[n] - d_{m,i}(n\Delta t)}{\sigma_{m,i}(n\Delta t)} \right)^2 \tag{6.3}$$

where $\vec{\theta}\,[n]$ represents the optimized parameter set.
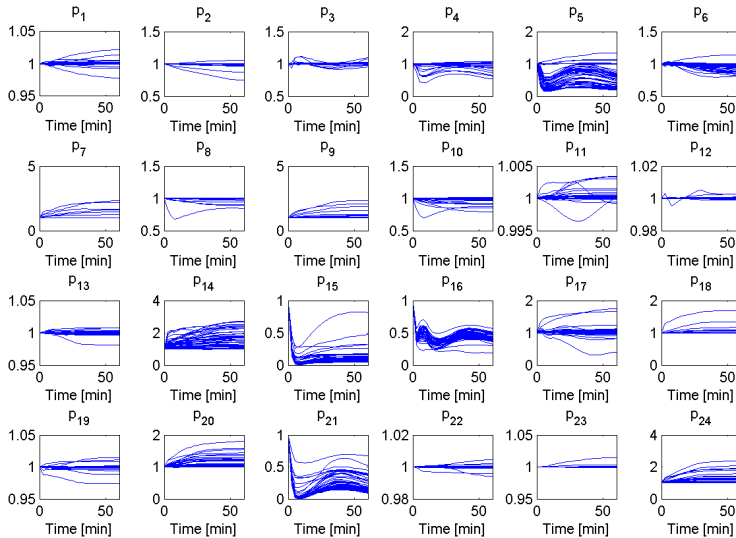
Figure 6.1: Parameter trajectories in time. All parameters are free to change such that the model reproduces the time course data.

Fig. 6.1 shows the estimated parameter trajectories in time that are obtained via ADAPT. All parameters are set free to change such that the model fully reproduces the time course data (Resnorm = 1). It can be observed that the parameters p5, p15, p16, and p21 change in time to describe the data, whereas the rest of the parameters remain constant in time. This result points out that the reactions corresponding to these four parameters are open to external regulations. The profile of the trajectories of these parameters, gives hints on the type of these regulations (i.e. inhibition or activation). If the values of a parameter change in

negative direction, it indicates an inhibition effect on the corresponding reaction whereas a change in a positive direction indicates an activation. As all four parameters are decreasing in time, an inhibition mechanism is required for all the corresponding reactions. To double check if these parameters form the sufficient set of parameters to be changed to have a fitting model, only p5, p15, p16, and p21 are set free to change such that the model reproduces the time course data in Fig. 6.2. The simulation results of the Eindhoven model by using ADAPT algorithm can be seen in Fig. 6.4.
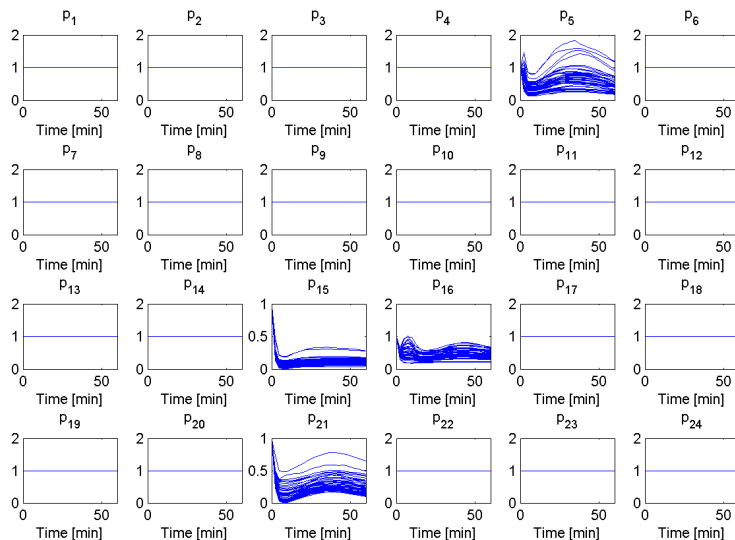
Figure 6.2: Parameter trajectories in time. p5, p15, p16, and p21 are free to change such that the model reproduces the time course data.

By using ADAPT, we determine the possible modulation points of the eIND-HOVEN model as shown in Fig. 6.4. This, in turn, has revealed the reactions of which mechanisms to be changed. The modulation points of the isolated pathway can be listed as follows:

- 1.Activation of PI3K
- 2.Dephosphorylation of Akt
- 3.Phosphorylation of AS160
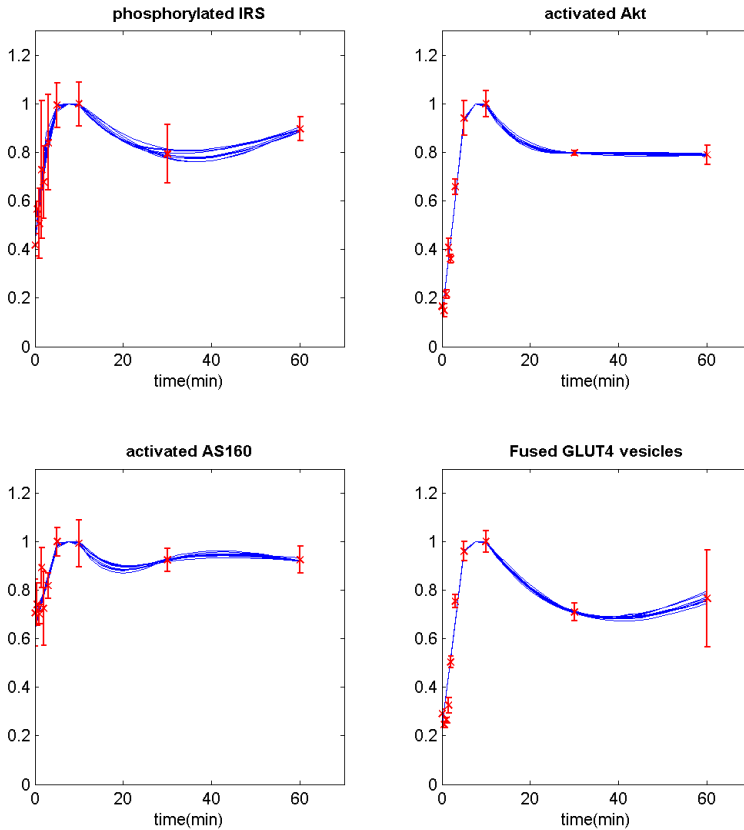
Figure 6.3: Result of ADAPT with free p5(k3=Activation of PI3K), p15
(km7=Deactivation of Akt), p16(k8=Activation of AS160),
and p21(km10=Defusion/Endocytosis of GLUT4).

- 4.Defusion/Endocytosis of GSVs

The modulation points of the insulin signalling pathway that are found via
ADAPT can be supported with the following studies from the literature.

The modulation point 1 (i.e. Activation of PI3K): Inhibition of mTOR
kinase relieves feedback inhibition of receptor tyrosine kinases (RTK), leading
to subsequent phosphoinositide 3-kinase activation and rephosphorylation of
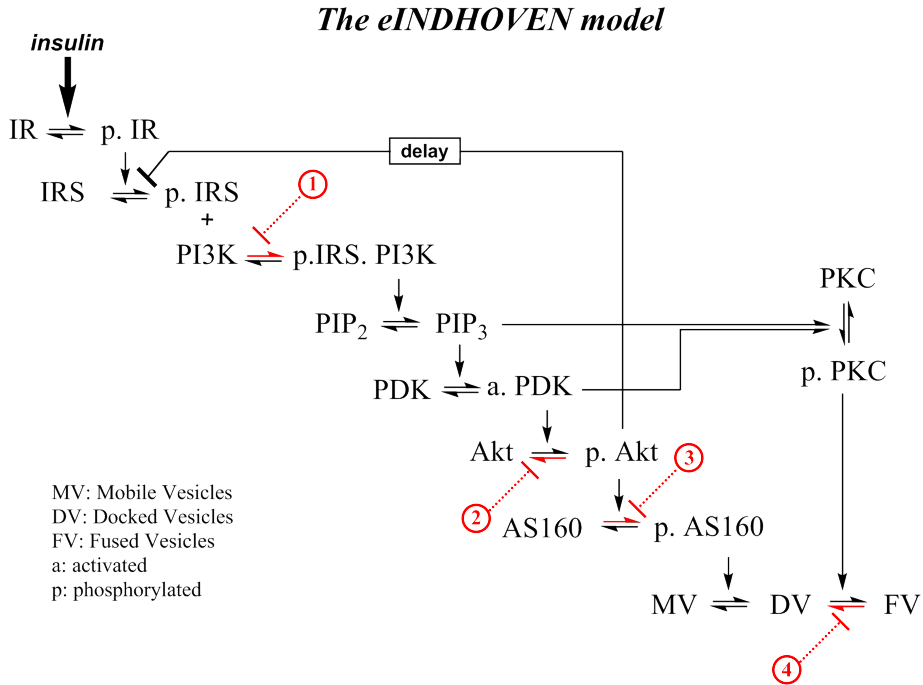
Figure 6.4: ADAPT addresses the modulation points. Red lines refer to the parameters that should be decreased. 1.Activation of PI3K, 2.Deactivation of Akt, 3.Activation of AS160, 4.Defusion/Endocytosis of GLUT4 vesicles.

Akt-T308 sufficient to reactivate Akt activity and signalling [90]. A negative feedback loop has been described, whereby mTOR/S6K1 activation attenuates PI3K signalling by suppressing insulin receptor substrate-1 (IRS1) function, a mediator of insulin receptordependent activation of PI3K [17].

The modulation point 2 (i.e. Dephosphorylation of Akt): The serine threonine protein kinase, Akt, is at the central hub of signalling pathways that regulates cell growth, differentiation, and survival. The reciprocal relation that exists between the two activating phosphorylation sites of Akt, T308 and S473, and the two mTOR complexes, C1 and C2, forms the central controlling hub that regulates these cellular functions [108]. Inhibition of mTORC2 leads to Akt serine 473 (S473) dephosphorylation and a rapid but transient inhibition of Akt-T308 phosphorylation and Akt signalling [90].

The modulation point 3 (i.e. Phosphorylation of AS160) may be the link to the regulation of multisite phosphorylation and 14-3-3 binding of AS160 in response to IGF-1 (insulin-like growth factor- 1), EGF (epidermal growth factor), PMA and AICAR. Upon insulin stimulation, AS160 is phosphorylated, which leads to its binding to 14-3-3 proteins and the inactivation of the RabGAP activity of AS160 and/or its dissociation from GSVs, thereby promote GLUT4 translocation. Thus GSV- associated Rabs are thought to become loaded with GTP and promote events that lead to expression of GLUT4 at the cell surface, thereby mediating the influx of glucose. The IGF-1, EGF, PMA and AICAR induce distinct patterns of multisite phosphorylation and 14-3-3 binding of AS160, involving at least four protein kinases [35].

The modulation point 4 (i.e. Defusion of GSVs): Fusion of GLUT4-containing vesicles with the plasma membrane of insulin-sensitive cells involves the SM protein Munc18c, and is regulated by the formation of syntaxin 4/SNAP23/VAMP2 SNARE complexes. The findings of the study ascertain a direct inhibitory role for Munc18c in regulating membrane fusion mediated by syntaxin 4/SNAP23/VAMP2 SNARE complex formation [16].

Here we present the application of ADAPT to identify the modulation points of the insulin signalling pathway with signalling network. For future studies, the next step would be to incorporate the proposed modulations into the eINDHOVEN model.

Bibliography

[1] B. B. Aldridge, J. M. Burke, D. A. Lauffenburger, and P. K. Sorger. Physicochemical modelling of cell signalling pathways. *Nature cell biology*, 8(11):1195--1203, 2006.

[2] J. Anderson and A. Papachristodoulou. On validation and invalidation of biological models. *BMC bioinformatics*, 10:132, Jan. 2009.

[3] D. Angeli, J. E. Ferrell, and E. D. Sontag. Detection of multistability, bifurcations, and hysteresis in a large class of biological positive-feedback systems. *Proceedings of the National Academy of Sciences of the United States of America*, 101(7):1822--1827, 2004.

[4] L. Bai, Y. Wang, J. Fan, Y. Chen, W. Ji, A. Qu, P. Xu, D. E. James, and T. Xu. Dissecting multiple steps of GLUT4 trafficking and identifying the sites of insulin action. *Cell metabolism*, 5(1):47--57, 2007.

[5] D. S. Baskin, M. A. Widmayer, and M. A. Sharpe. Quantification and calibration of images in fluorescence microscopy. *Analytical Biochemistry*, 404(2):118--126, 2010.

[6] K. S. Bell, C. Schmitz-Peiffer, M. Lim-Fraser, T. J. Biden, G. J. Cooney, and E. W. Kraegen. Acute reversal of lipid-induced muscle insulin resistance is associated with rapid alteration in pkc-θ localization. *American Journal of Physiology-Endocrinology And Metabolism*, 279(5):E1196--E1201, 2000.

[7] R. K. P. Benninger, M. S. Remedi, W. S. Head, a. Ustione, D. W. Piston, and C. G. Nichols. Defects in beta cell Ca+ signalling, glucose metabolism and insulin secretion in a murine model of K(ATP) channel-induced neonatal diabetes mellitus. *Diabetologia*, 54(5):1087--97, May 2011.

[8] M. Berridge. Cell Signalling Biology: Module 12 - Signalling Defects and Disease. *Biochemical Journal*, pages 1--75, Apr. 2012.

[9] M. Berridge. Cell Signalling Biology: Module 2 - Cell signalling pathways. *Biochemical Journal*, pages 1--138, Apr. 2012.

[10] M. Berridge. Cell Signalling Biology: Module 6 - Spatial and Temporal Aspects of Signalling. *Biochemical Journal*, pages 1--52, Apr. 2012.

[11] U. S. Bhalla and R. Iyengar. Robustness of the bistable behavior of a biological signaling feedback loop. *Chaos: An Interdisciplinary Journal of Nonlinear Science*, 11(1):221--226, 2001.

[12] P. Boström, L. Andersson, M. Rutberg, J. Perman, U. Lidberg, B. R. Johansson, J. Fernandez-Rodriguez, J. Ericson, T. Nilsson, J. Borén, and S.-O. Olofsson. SNARE proteins mediate fusion between cytosolic lipid droplets and are implicated in insulin sensitivity. *Nature cell biology*, 9(11):1286--93, 2007.

[13] P. Boström, L. Andersson, B. Vind, L. Håversen, M. Rutberg, Y. Wickström, E. Larsson, P.-A. Jansson, M. K. Svensson, R. Brånemark, et al. The snare protein snap23 and the snare-interacting protein munc18c in human skeletal muscle are implicated in insulin resistance/type 2 diabetes. *Diabetes*, 59(8):1870--1878, 2010.

[14] J. Boulanger, A. Gidon, C. Kervran, and J. Salamero. A patch-based method for repetitive and transient event detection in fluorescence imaging. *PloS one*, 5(10):e13190, Jan. 2010.

[15] H. Bradley, C. S. Shaw, P. L. Worthington, S. O. Shepherd, M. Cocks, and A. J. M. Wagenmakers. Quantitative immunofluorescence microscopy of subcellular GLUT4 distribution in human skeletal muscle: effects of endurance and sprint interval training. *Physiological reports*, 2(7):1--16, July 2014.

[16] F. M. Brandie, V. Aran, A. Verma, J. a. McNew, N. J. Bryant, and G. W. Gould. Negative regulation of syntaxin4/SNAP-23/VAMP2-mediated membrane fusion by Munc18c in vitro. *PloS one*, 3(12):e4074, Jan. 2008.

[17] M. Breuleux, M. Klopfenstein, C. Stephan, C. A. Doughty, L. Barys, S.-M. Maira, D. Kwiatkowski, and H. A. Lane. Increased AKT S473 phosphorylation after mTORC1 inhibition is rictor dependent and does not predict tumor cell response to PI3K/mTOR inhibition. *Molecular cancer therapeutics*, 8(4):742--53, Apr. 2009.

[18] M. D. Bruss, E. B. Arias, G. E. Lienhard, and G. D. Cartee. Increased phosphorylation of Akt substrate of 160 kDa (AS160) in rat skeletal muscle in response to insulin or contractile activity. *Diabetes*, 54(1):41--50, Jan. 2005.

[19] N. J. Bryant, R. Govers, and D. E. James. Regulated transport of the glucose transporter GLUT4. *Nature reviews. Molecular cell biology*, 3(4):267--77, Apr. 2002.

[20] G. Cedersund, J. Roll, E. Ulfhielm, A. Danielsson, H. Tidefelt, and P. Strålfors. Model-based hypothesis testing of key mechanisms in initial phase of insulin signaling. *PLoS computational biology*, 4(6):e1000096, 2008.

[21] J. A. Chavez and S. A. Summers. Lipid oversupply, selective insulin resistance, and lipotoxicity: molecular mechanisms. *Biochimica et biophysica acta*, 1801(3):252--65, Mar. 2010.

[22] W. W. Chen, B. Schoeberl, P. J. Jasper, M. Niepel, U. B. Nielsen, D. a. Lauffenburger, and P. K. Sorger. Input-output behavior of ErbB signaling pathways as revealed by a mass action model trained against dynamic data. *Molecular systems biology*, 5(239):239, Jan. 2009.

[23] L. Chow, A. From, and E. Seaquist. Skeletal muscle insulin resistance: the interplay of local lipid excess and mitochondrial dysfunction. *Metabolism: clinical and experimental*, 59(1):70--85, 2010.

[24] P. M. Coen, J. J. Dubé, F. Amati, M. Stefanovic-Racic, R. E. Ferrell, F. G. Toledo, and B. H. Goodpaster. Insulin resistance is associated with higher intramyocellular triglycerides in type i but not type ii myocytes concomitant with higher ceramide content. *Diabetes*, 59(1):80--88, 2010.

[25] S. W. Cole and A. K. Sood. Molecular pathways: beta-adrenergic signaling in cancer. *Clinical cancer research : an official journal of the American Association for Cancer Research*, 18(5):1201--6, Mar. 2012.

[26] M. Cvijovic, J. Almquist, J. Hagmar, S. Hohmann, H. M. Kaltenbach, E. Klipp, M. Krantz, P. Mendes, S. Nelander, J. Nielsen, A. Pagnani, N. Przulj, A. Raue, J. Stelling, S. Stoma, F. Tobin, J. A. H. Wodke, R. Zecchina, and M. Jirstrand. Bridging the gaps in systems biology. *Molecular genetics and genomics : MGG*, 289(5):727--34, Oct. 2014.

[27] G. V. De Ferrari and N. C. Inestrosa. Wnt signaling function in Alzheimers disease. *Brain Research Reviews*, 33(1):1--12, Aug. 2000.

[28] R. A. DeFronzo. Insulin resistance, lipotoxicity, type 2 diabetes and atherosclerosis: the missing links. The Claude Bernard Lecture 2009. *Diabetologia*, 53(7):1270--87, July 2010.

[29] R. A. DeFronzo and D. Tripathy. Skeletal muscle insulin resistance is the primary defect in type 2 diabetes. *Diabetes care*, 32 Suppl 2:S157--63, Nov. 2009.

[30] B. Di Ventura, C. Lemerle, K. Michalodimitrakis, and L. Serrano. From in vivo to in silico biology and back. *Nature*, 443(7111):527--33, Oct. 2006.

[31] R. V. Farese, M. P. Sajan, and M. L. Standaert. Atypical protein kinase C in insulin action and insulin resistance. *Biochemical Society transactions*, 33(Pt 2):350--3, Apr. 2005.

[32] K. P. Foley and A. Klip. Dynamic GLUT4 sorting through a syntaxin-6 compartment in muscle cells is derailed by insulin resistance-causing ceramide. *Biology open*, pages 1--12, Apr. 2014.

[33] T. Forster, D. Roy, and P. Ghazal. Experiments using microarray technology: limitations and standard operating procedures. *The Journal of endocrinology*, 178(2):195--204, Aug. 2003.

[34] M. Freeman. Feedback control of intercellular signalling in development. *Nature*, 408(6810):313--319, 2000.

[35] K. M. Geraghty, S. Chen, J. E. Harthill, A. F. Ibrahim, R. Toth, N. a. Morrice, F. Vandermoere, G. B. Moorhead, D. G. Hardie, and C. MacKintosh. Regulation of multisite phosphorylation and 14-3-3 binding of AS160 in response to IGF-1, EGF, PMA and AICAR. *The Biochemical journal*, 407(2):231--41, Oct. 2007.

[36] E. Gonzalez and T. E. Mcgraw. Insulin Signaling Diverges into Akt-dependent and -independent Signals to Regulate the Recruitment / Docking and the Fusion of GLUT4 Vesicles to the Plasma Membrane . *Molecular biology of the cell*, 17(October):4484--4493, 2006.

[37] C. W. Gray and A. C. Coster. A receptor state space model of the insulin signalling system in glucose transport. *Mathematical Medicine and Biology*, page dqv003, 2015.

[38] M. E. Griffin, M. J. Marcucci, G. W. Cline, K. Bell, N. Barucci, D. Lee, L. J. Goodyear, E. W. Kraegen, M. F. White, and G. I. Shulman. Free fatty acid-induced insulin resistance is associated with activation of protein kinase c theta and alterations in the insulin signaling cascade. *Diabetes*, 48(6):1270--1274, 1999.

[39] T. Grimmsmann, K. Levin, M. M. Meyer, H. Beck-Nielsen, and H. H. Klein. Delays in insulin signaling towards glucose disposal in human skeletal muscle. *The Journal of endocrinology*, 172(3):645--51, Mar. 2002.

[40] D. Haasch, C. Berg, J. E. Clampit, T. Pederson, L. Frost, P. Kroeger, and C. M. Rondinone. PKCtheta is a key player in the development of insulin resistance. *Biochemical and biophysical research communications*, 343(2):361--8, May 2006.

[41] E. Hajduch, A. Balendran, I. Batty, G. Litherland, A. Blair, C. Downes, and H. Hundal. Ceramide impairs the insulin-dependent membrane recruitment of protein kinase b leading to a loss in downstream signalling in l6 skeletal muscle cells. *Diabetologia*, 44(2):173--183, 2001.

[42] N. Hamilton. Quantification and its applications in fluorescent microscopy imaging. *Traffic (Copenhagen, Denmark)*, 10(8):951--61, Aug. 2009.

[43] Y.-P. Han, T. L. Tuan, H. Wu, M. Hughes, and W. L. Garner. Tnf-alpha stimulates activation of pro-mmp2 in human skin through nf-(kappa) b mediated induction of mt1-mmp. *Journal of cell science*, 114(1):131--139, 2001.

[44] M. Hatakeyama, S. Kimura, T. Naka, T. Kawasaki, N. Yumoto, M. Ichikawa, J.-H. Kim, K. Saito, M. Saeki, M. Shirouzu, S. Yokoyama, and A. Konagaya. A computational model on the modulation of mitogen-activated protein kinase (MAPK) and Akt pathways in heregulin-induced ErbB signalling. *The Biochemical journal*, 373(Pt 2):451--63, July 2003.

[45] I. Hers, E. E. Vincent, and J. M. Tavaré. Akt signalling in health and disease. *Cellular signalling*, 23(10):1515--27, Oct. 2011.

[46] A. Hoffmann, A. Levchenko, M. L. Scott, and D. Baltimore. The iκb-nf-κb signaling module: temporal control and selective gene activation. *Science*, 298(5596):1241--1245, 2002.

[47] A. J. Hoy, A. E. Brandon, N. Turner, M. J. Watt, C. R. Bruce, G. J. Cooney, and E. W. Kraegen. Lipid and insulin infusion-induced skeletal muscle insulin resistance is likely due to metabolic feedback and not changes in IRS-1, Akt, or AS160 phosphorylation. *American journal of physiology. Endocrinology and metabolism*, 297(1):E67--75, July 2009.

[48] C. Huang, R. Somwar, N. Patel, W. Niu, D. Torok, and Klip. Sustained exposure of L6 myotubes to high glucose and insulin decreases insulin-stimulated GLUT4 translocation but upregulates GLUT4 activity. *Diabetes*, 51(July), 2002.

[49] S. Huang and M. P. Czech. The GLUT4 glucose transporter. *Cell metabolism*, 5(4):237--52, Apr. 2007.

[50] S. J. Humphrey, G. Yang, P. Yang, D. J. Fazakerley, J. Stöckli, J. Y. Yang, and D. E. James. Dynamic adipocyte phosphoproteome reveals that Akt directly regulates mTORC2. *Cell metabolism*, 17(6):1009--20, June 2013.

[51] T. Ijuin and T. Takenawa. Regulation of insulin signaling and glucose transporter 4 (GLUT4) exocytosis by phosphatidylinositol 3,4,5-trisphosphate (PIP3) phosphatase, skeletal muscle, and kidney enriched inositol polyphosphate phosphatase (SKIP). *The Journal of biological chemistry*, 287(10):6991--9, Mar. 2012.

[52] M. Ishiki and A. Klip. Minireview: recent developments in the regulation of glucose transporter-4 traffic: new signals, locations, and partners. *Endocrinology*, 146(12):5071--8, Dec. 2005.

[53] M. Kanehisa and S. Goto. Kegg: kyoto encyclopedia of genes and genomes. *Nucleic acids research*, 28(1):27--30, 2000.

[54] M. Kanehisa, S. Goto, Y. Sato, M. Kawashima, M. Furumichi, and M. Tanabe. Data, information, knowledge and principle: back to metabolism in kegg. *Nucleic acids research*, 42(D1):D199--D205, 2014.

[55] H. K. R. Karlsson, A. V. Chibalin, H. A. Koistinen, J. Yang, F. Koumanov, H. Wallberg-henriksson, J. R. Zierath, and G. D. Holman. Skeletal Muscle. *PRism*, 58(April), 2009.

[56] H. K. R. Karlsson, K. Hällsten, M. Björnholm, H. Tsuchida, A. V. Chibalin, K. a. Virtanen, O. J. Heinonen, F. Lönnqvist, P. Nuutila, and J. R. Zierath. Effects of metformin and rosiglitazone treatment on insulin signaling and glucose uptake in patients with newly diagnosed type 2 diabetes: a randomized controlled study. *Diabetes*, 54(5):1459--67, May 2005.

[57] D. E. Kelley, M. A. Mintun, S. C. Watkins, J.-A. Simoneau, F. Jadali, A. Fredrickson, J. Beattie, and R. Thériault. The effect of non-insulin-dependent diabetes mellitus and obesity on glucose transport and phosphorylation in skeletal muscle. *Journal of Clinical Investigation*, 97(12):2705, 1996.

[58] B. N. Kholodenko. Cell-signalling dynamics in time and space. *Nature reviews Molecular cell biology*, 7(3):165--176, 2006.

[59] H. Kitano. Systems Biology : A Brief Overview. *Science*, 295(5560):1662--1665, 2002.

[60] H. Kitano. Towards a theory of biological robustness. *Molecular systems biology*, 3(137):137, Jan. 2007.

[61] A. Klip. The many ways to regulate glucose transporter 4. *Applied physiology, nutrition, and metabolism = Physiologie appliquée, nutrition et métabolisme*, 34(3):481--7, June 2009.

[62] A. Klip, T. Ramlal, P. Bilan, G. Cartee, E. Gulve, and J. Holloszy. Recruitment of glut-4 glucose transporters by insulin in diabetic rat skeletal muscle. *Biochemical and biophysical research communications*, 172(2):728--736, 1990.

[63] E. Klipp and W. Liebermeister. Mathematical modeling of intracellular signaling pathways. *BMC neuroscience*, 7 Suppl 1:S10, Jan. 2006.

[64] F. Koumanov, B. Jin, J. Yang, and G. D. Holman. Insulin signaling meets vesicle traffic of GLUT4 at a plasma-membrane-activated fusion step. *Cell metabolism*, 2(3):179--89, Sept. 2005.

[65] F. Koumanov, J. D. Richardson, B. a. Murrow, and G. D. Holman. AS160 phosphotyrosine-binding domain constructs inhibit insulin-stimulated GLUT4 vesicle fusion with the plasma membrane. *The Journal of biological chemistry*, 286(19):16574--82, May 2011.

[66] E. W. Kraegen, P. W. Clark, A. B. Jenkins, E. A. Daley, D. J. Chisholm, and L. H. Storlien. Development of muscle insulin resistance after liver insulin resistance in high-fat--fed rats. *Diabetes*, 40(11):1397--1403, 1991.

[67] A. Krook, M. Björnholm, D. Galuska, X. J. Jiang, R. Fahlman, M. G. Myers, H. Wallberg-Henriksson, and J. R. Zierath. Characterization of signal transduction and glucose transport in skeletal muscle from type 2 diabetic patients. *Diabetes*, 49(2):284--92, Feb. 2000.

[68] A. Krook, R. A. Roth, X. J. Jiang, J. R. Zierath, and H. Wallberg-Henriksson. Insulin-stimulated akt kinase activity is reduced in skeletal muscle from niddm subjects. *Diabetes*, 47(8):1281--1286, 1998.

[69] M. N. Lansey, N. N. Walker, S. R. Hargett, J. R. Stevens, and S. R. Keller. Deletion of Rab GAP AS160 modifies glucose uptake and GLUT4 translocation in primary skeletal muscles and adipocytes and impairs glucose homeostasis. *American journal of physiology. Endocrinology and metabolism*, 303(10):E1273--86, Nov. 2012.

[70] Y. Leng, H. K. R. Karlsson, and J. R. Zierath. Insulin signaling defects in type 2 diabetes. *Reviews in endocrine & metabolic disorders*, 5(2):111--7, May 2004.

[71] J. Lippincott-Schwartz and G. H. Patterson. Development and use of fluorescent protein markers in living cells. *Science (New York, N.Y.)*, 300(5616):87--91, Apr. 2003.

[72] H. Liu. Interacted regulation of GLUT4 cycling and insulin signaling transduction. Master's thesis, Eindhoven University of Technology, the Netherlands, 2010.

[73] Y. Liu, F. Liu, I. Grundke-Iqbal, K. Iqbal, and C.-X. Gong. Deficient brain insulin signalling pathway in Alzheimer's disease and diabetes. *The Journal of pathology*, 225(1):54--62, Sept. 2011.

[74] V. A. Lizunov, H. Matsumoto, J. Zimmerberg, S. W. Cushman, and V. A. Frolov. Insulin stimulates the halting, tethering, and fusion of mobile GLUT4 vesicles in rat adipose cells. *The Journal of cell biology*, 169(3):481--9, May 2005.

[75] S. Marino, I. B. Hogue, C. J. Ray, and D. E. Kirschner. A methodology for performing global uncertainty and sensitivity analysis in systems biology. *Journal of theoretical biology*, 254(1):178--96, Sept. 2008.

[76] J. Min, S. Okada, M. Kanzaki, J. S. Elmendorf, K. J. Coker, B. P. Ceresa, L.-J. Syu, Y. Noda, A. R. Saltiel, and J. E. Pessin. Synip: A novel insulin-regulated syntaxin 4--binding protein mediating glut4 translocation in adipocytes. *Molecular cell*, 3(6):751--760, 1999.

[77] Y. Ng, G. Ramm, J. G. Burchfield, A. C. F. Coster, J. Stöckli, and D. E. James. Cluster analysis of insulin action in adipocytes reveals a key role for Akt at the plasma membrane. *The Journal of biological chemistry*, 285(4):2245--57, 2010.

[78] F. H. Nystrom and M. J. Quon. Insulin signalling: metabolic pathways and mechanisms for specificity. *Cellular signalling*, 11(8):563--74, Aug. 1999.

[79] D. Pan, S. Lillioja, A. Kriketos, M. Milner, L. Baur, C. Bogardus, A. B. Jenkins, and L. Storlien. Skeletal muscle triglyceride levels are inversely related to insulin action. *Diabetes*, 46(6):983--988, 1997.

[80] R. Pepperkok and J. Ellenberg. High-throughput fluorescence microscopy for systems biology. *Nature Reviews Molecular Cell Biology*, 7(September):690--696, 2006.

[81] N. Perrimon and A. P. McMahon. Negative feedback mechanisms and their roles during pattern formation. *Cell*, 97(1):13--16, 1999.

[82] L. Pickersgill, G. J. Litherland, A. S. Greenberg, M. Walker, and S. J. Yeaman. Key role for ceramides in mediating insulin resistance in human muscle cells. *The Journal of biological chemistry*, 282(17):12583--9, Apr. 2007.

[83] A. Pujol, R. Mosca, J. Farrés, and P. Aloy. Unveiling the role of network and systems biology in drug discovery. *Trends in pharmacological sciences*, 31(3):115--123, 2010.

[84] K. Radhakrishnan, A. Halász, D. Vlachos, and J. S. Edwards. Quantitative understanding of cell signaling: the importance of membrane organization. *Current opinion in biotechnology*, 21(5):677--82, Oct. 2010.

[85] M. Rathinam, L. R. Petzold, Y. Cao, and D. T. Gillespie. Stiffness in stochastic chemically reacting systems: The implicit tau-leaping method. *The Journal of Chemical Physics*, 119(24):12784, 2003.

[86] A. Raue, C. Kreutz, T. Maiwald, J. Bachmann, M. Schilling, U. Klingmüller, and J. Timmer. Structural and practical identifiability analysis of partially observed dynamical models by exploiting the profile likelihood. *Bioinformatics (Oxford, England)*, 25(15):1923--9, Aug. 2009.

[87] L. Ravichandran and H. Chen. Phosphorylation of PTP1B at Ser50 by Akt impairs its ability to dephosphorylate the insulin receptor. *Molecular Endocrinology*, 15(January):1768--1780, 2001.

[88] L. V. Ravichandran, D. L. Esposito, J. Chen, and M. J. Quon. Protein kinase C-zeta phosphorylates insulin receptor substrate-1 and impairs its ability to activate phosphatidylinositol 3-kinase in response to insulin. *The Journal of biological chemistry*, 276(5):3543--9, Feb. 2001.

[89] E. Rodríguez, N. Pulido, R. Romero, F. Arrieta, A. Panadero, and A. Rovira. Phosphatidylinositol 3-kinase activation is required for sulfonylurea stimulation of glucose transport in rat skeletal muscle. *Endocrinology*, 145(2):679--85, Feb. 2004.

[90] V. S. Rodrik-Outmezguine, S. Chandarlapaty, N. C. Pagano, P. I. Poulikakos, M. Scaltriti, E. Moskatel, J. Baselga, S. Guichard, and N. Rosen. mTOR kinase inhibition causes feedback-dependent biphasic regulation of AKT signaling. *Cancer discovery*, 1(3):248--59, Aug. 2011.

[91] J. Russell, G. Shillabeer, J. Bar-Tana, D. Lau, M. Richardson, L. Wenzel, S. Graham, and P. Dolphin. Development of insulin resistance in the jcr: La-cp rat: role of triacylglycerols and effects of medica 16. *Diabetes*, 47(5):770--778, 1998.

[92] P. Ruusuvuori, L. Paavolainen, K. Rutanen, A. Mäki, H. Huttunen, and V. Marjomäki. Quantitative analysis of dynamic association in live biological fluorescent samples. *PloS one*, 9(4):e94245, Jan. 2014.

[93] J. Schaber, R. Baltanas, A. Bush, E. Klipp, and A. Colman-Lerner. Modelling reveals novel roles of two parallel signalling pathways and homeostatic feedbacks in yeast. *Molecular Systems Biology*, 8(622):1--17, Nov. 2012.

[94] S. Schenk, M. Saberi, and J. M. Olefsky. Insulin sensitivity: modulation by nutrients and inflammation. *The Journal of clinical investigation*, 118(9):2992, 2008.

[95] A. R. Sedaghat, A. Sherman, and M. J. Quon. A mathematical model of metabolic insulin signaling pathways. *American journal of physiology. Endocrinology and metabolism*, 283(5):E1084--101, Nov. 2002.

[96] K. Siddle. Signalling by insulin and igf receptors: supporting acts and new players. *Journal of molecular endocrinology*, 47(1):R1--R10, 2011.

[97] R. Somwar, D. Y. Kim, G. Sweeney, C. Huang, W. Niu, C. Lador, T. Ramlal, and a. Klip. GLUT4 translocation precedes the stimulation of glucose uptake by insulin in muscle cells: potential activation of GLUT4 via p38 mitogen-activated protein kinase. *The Biochemical journal*, 359(Pt 3):639--49, Nov. 2001.

[98] R. Somwar, S. Sumitani, C. Taha, G. Sweeney, and A. Klip. Temporal activation of p70 S6 kinase and Akt1 by insulin: PI 3-kinase-dependent and -independent mechanisms. *The American journal of physiology*, 275(4 Pt 1):E618--25, Oct. 1998.

[99] X. M. Song, J. W. Ryder, Y. Kawano, A. V. Chibalin, A. Krook, J. R. Zierath, X. M. E. I. Song, and X. Mei. Muscle fiber type specificity in insulin signal transduction Muscle fiber type specificity in insulin signal transduction. *The American journal of physiology*, 277:R1690--R1696, 1999.

[100] C. Souchier, C. Brisson, B. Batteux, M. Robert-Nicoud, and P.-A. Bryon. Data reproducibility in fluorescence image analysis. *Methods in cell science : an official journal of the Society for In Vitro Biology*, 25(3-4):195--200, Jan. 2003.

[101] J. Stöckli, D. J. Fazakerley, and D. E. James. GLUT4 exocytosis. *Journal of cell science*, 124(Pt 24):4147--59, Dec. 2011.

[102] S. A. Summers. Ceramides in insulin resistance and lipotoxicity. *Progress in lipid research*, 45(1):42--72, Jan. 2006.

[103] S. X. Tan, Y. Ng, J. G. Burchfield, G. Ramm, D. G. Lambright, J. Stöckli, and D. E. James. The Rab GTPase-activating protein TBC1D4/AS160 contains an atypical phosphotyrosine-binding domain that interacts with plasma membrane phospholipids to facilitate GLUT4 trafficking in adipocytes. *Molecular and cellular biology*, 32(24):4946--59, Dec. 2012.

[104] F. S. L. Thong, C. B. Dugani, and A. Klip. Turning signals on and off: GLUT4 traffic in the insulin-signaling highway. *Physiology (Bethesda, Md.)*, 20:271--84, Aug. 2005.

[105] C. A. Tiemann, J. Vanlier, M. H. Oosterveer, A. K. Groen, P. A. J. Hilbers, and N. A. W. van Riel. Parameter trajectory analysis to identify treatment effects of pharmacological interventions. *PLoS computational biology*, 9(8):e1003166, Jan. 2013.

[106] S. Timmers, P. Schrauwen, and J. de Vogel. Muscular diacylglycerol metabolism and insulin resistance. *Physiology & behavior*, 94(2):242--251, 2008.

[107] A. Toker. Pdk-1 and protein kinase c phosphorylation. In *Protein Kinase C Protocols*, pages 171--189. Springer, 2003.

[108] L. Vadlakonda, A. Dash, M. Pasupuleti, K. Anil Kumar, and P. Reddanna. The Paradox of Akt-mTOR Interactions. *Frontiers in oncology*, 3(June):165, Jan. 2013.

[109] N. A. W. van Riel. Dynamic modelling and analysis of biochemical networks: mechanism-based models and model-based experiments. *Briefings in bioinformatics*, 7(4):364--74, 2006.

[110] N. A. W. van Riel. Speeding up simulations of ODE models in Matlab using CVode and MEX files. *Bioinformatics*, 8(28):1130--5, 2012.

[111] J. Vanlier, C. A. Tiemann, P. A. J. Hilbers, and N. A. W. van Riel. A Bayesian approach to targeted experiment design. *Bioinformatics (Oxford, England)*, 28(8):1136--42, Apr. 2012.

[112] J. Vanlier, C. A. Tiemann, P. A. J. Hilbers, and N. A. W. van Riel. An integrated strategy for prediction uncertainty analysis. *Bioinformatics (Oxford, England)*, 28(8):1130--5, Apr. 2012.

[113] J. Vanlier, C. A. Tiemann, P. A. J. Hilbers, and N. A. W. van Riel. Parameter uncertainty in biochemical models described by ordinary differential equations. *Mathematical biosciences*, 246(2):305--14, Dec. 2013.

[114] H. Y. Wang, S. Ducommun, C. Quan, B. Xie, M. Li, D. H. Wasserman, K. Sakamoto, C. Mackintosh, and S. Chen. AS160 deficiency causes whole-body insulin resistance via composite effects in multiple tissues. *The Biochemical journal*, 449(2):479--89, Jan. 2013.

[115] Q. Wang, R. Somwar, P. J. Bilan, Z. Liu, J. Jin, J. R. Woodgett, and a. Klip. Protein kinase B/Akt participates in GLUT4 translocation by insulin in L6 myoblasts. *Molecular and cellular biology*, 19(6):4008--18, June 1999.

[116] R. T. Watson and J. E. Pessin. Bridging the GAP between insulin signaling and GLUT4 translocation. *Trends in biochemical sciences*, 31(4):215--22, 2006.

[117] C. Weigert, A. M. Hennige, T. Brischmann, A. Beck, K. Moeschel, M. Schaüble, K. Brodbeck, H.-U. Häring, E. D. Schleicher, and R. Lehmann. The phosphorylation of Ser318 of insulin receptor substrate 1 is not per se inhibitory in skeletal muscle cells but is necessary to trigger the attenuation of the insulin-stimulated signal. *The Journal of biological chemistry*, 280(45):37393--9, Nov. 2005.

[118] C. Yu, Y. Chen, G. W. Cline, D. Zhang, H. Zong, Y. Wang, R. Bergeron, J. K. Kim, S. W. Cushman, G. J. Cooney, et al. Mechanism by which fatty acids inhibit insulin activation of insulin receptor substrate-1 (irs-1)-associated phosphatidylinositol 3-kinase activity in muscle. *Journal of Biological Chemistry*, 277(52):50230--50236, 2002.

[119] A. Zeigerer, M. K. McBrayer, and T. E. McGraw. Insulin stimulation of glut4 exocytosis, but not its inhibition of endocytosis, is dependent on rabgap as160. *Molecular biology of the cell*, 15(10):4406--4415, 2004.

[120] A. Zelezniak, T. H. Pers, S. Soares, M. E. Patti, and K. R. Patil. Metabolic network topology reveals transcriptional regulatory signatures of type 2 diabetes. *PLoS computational biology*, 6(4):e1000729, Apr. 2010.

[121] Z. Zi, K. H. Cho, M. H. Sung, X. Xia, J. Zheng, and Z. Sun. In silico identification of the key components and steps in IFN-gamma induced JAK-STAT signaling pathway. *FEBS letters*, 579(5):1101--8, Feb. 2005.

[122] Z. Zi, Y. Zheng, A. E. Rundell, and E. Klipp. SBML-SAT: a systems biology markup language (SBML) based sensitivity analysis tool. *BMC Bioinformatics*, 9(1):342, 2008.

[123] J. Zierath, D. Galuska, L. Nolte, A. Thörne, J. S. Kristensen, and H. Wallberg-Henriksson. Effects of glycaemia on glucose transport in isolated skeletal muscle from patients with niddm: in vitro reversal of muscular insulin resistance. *Diabetologia*, 37(3):270--277, 1994.

[124] J. Zierath, L. He, A. Guma, E. O. Wahlström, A. Klip, and H. Wallberg-Henriksson. Insulin action on glucose transport and plasma membrane glut4 content in skeletal muscle from patients with niddm. *Diabetologia*, 39(10):1180--1189, 1996.

[125] R. Zoncu, A. Efeyan, and D. M. Sabatini. mTOR: from growth signal integration to cancer, diabetes and ageing. *Nature reviews. Molecular cell biology*, 12(1):21--35, Jan. 2011.

Summary

The insulin signalling pathway that leads to GLUT4 translocation is a prerequisite of the insulin-stimulated glucose uptake and therefore is an important element of glucose homeostasis. An impairment in the insulin signalling leads to insulin resistance which is an early symptom of Type 2 diabetes. To develop strategies for re-establishing normal glucose homeostasis in people with type 2 diabetes, understanding of the functioning and the dynamics of the insulin signalling leading to GLUT4 translocation is essential. Skeletal muscle is considered one of the primary tissues among insulin-sensitive tissues, because it accounts for 75 - 80 % of whole body insulin-stimulated glucose uptake. In this thesis, to study the functioning and the dynamics of the insulin signalling pathway in skeletal muscle, we adopt a Systems Biology framework in which we combine our in silico and in vitro studies. The main goal of this thesis is to construct the eINDHOVEN model (Insulin sigNalling Dynamics for Hypotheses, Observations and Virtual ExperimeNts) that can represent the dynamical behaviour of insulin signalling from insulin receptor to GLUT4 translocation in rat skeletal muscle cells.

Chapter 2 provides an introduction to the systems biology approach to analysis of the insulin signalling pathway. Here we employ a hypothesis driven modeling approach to construct the first version of our predictive computational model for the insulin signalling pathway. The model consists of a set of ordinary differential equations and kinetic parameters. The parameterization of the model is based on data collected from literature. However, limited time course data on the signalling intermediates leads to the uncertainty of the model parameters, which in turn leads to the uncertainty in our model predictions. This addresses the need for generating a high resolution time course data set for the development of a predictive model. To obtain high resolution experimental data, accurate quantification of raw data is as important as generating raw data. It is challenging especially for intracellular proteomics data due to the wide range of protein concentrations. Chapter 3 reports a discussion on the accuracy of the methods that are used to quantify the fluorophore-tagged proteins. In this

chapter, we show that a pixel based method that is often used may result in misinterpretation of the dynamics of the proteins. To overcome the issue, we propose an intensity based method by which an automatic quantification of fluorophore-tagged proteins is provided. This method is used to quantify our new data in Chapter 4.

In Chapter 4, we present the results of our study on the dynamics of the insulin signalling pathway in vitro. We perturb rat skeletal muscle cells with various insulin inputs and quantify the frequently sampled response of several intermediates in the pathway. Immunocytochemistry assays for phosphorylation of (p-) IRS-1, Akt-S473, Akt-T308, AS160, and GLUT4 proteins in the plasma membrane (PM) are combined with high-throughput fluorescence microscopy in order to trace and quantify the temporal profile of the proteins in the pathway. We show that the measured intermediates of the insulin signalling pathway have consistent dynamic behaviour among each other regardless of the inter-experimental heterogeneity. Correlation analysis shows that the temporal profile of p-Akt-S473 has high correlation with all the intermediates, particularly with GLUT4 protein in the plasma membrane. Based on these findings we conclude that p-Akt-S473 is the candidate to be the representative protein for insulin mediated GLUT4 translocation for further dynamics studies of the pathway.

Chapter 5 represents the integration of the generated data into the model developed in Chapter 2. The model is refined through a process that consists of several iterations of model development, testing of the hypotheses and virtual experiments. The overshoot behaviour of the signalling intermediates that is observed in the insulin signalling assays presented in Chapter 4 indicates that a negative feedback mechanism is required for the model. Based on residual analysis and correlation analysis, we propose that the phosphorylation of IRS is regulated by a delayed negative feedback from Akt-S473. The delay on the feedback may be due to the localisation of the downstream signalling intermediates or due to the involvement of a scaffold protein(s) that regulate(s) signal transduction and facillitates the localisation of the intermediates. Profile Likelihood and Multi Parameter Sensitivity Analysis (MPSA) show that the model parameters are identifiable and sensitive. Furthermore, MPSA based on the system output, which is the GLUT4 translocation, reveals that the intermediates of the insulin signalling pathway and their interactions are essential for GLUT4 translocation. Subsequently, we use our developed model of the insulin signalling pathway to test the hypotheses formulated in Chapter 4. Our model also depicts that, as well as the observed intermediates, non observed intermediates are highly correlated with each other despite the variability among the independent experiments and models. Therefore, our hypothesis on dynamics of the pathway cannot be rejected with model analyses: The insulin signalling pathway that leads to GLUT4 translocation can be proposed to be an isodynamic system.

Chapter 6 concludes the thesis with the main contributions and discusses future perspectives. In this thesis, we show that by applying a systems biology

approach, new hypotheses can be generated about the missing regulations in signalling pathways. Our predictive computational model can be used as a virtual skeletal muscle to assist in the identification of biomarkers, evaluate and validate drug targets, predict human response and design clinical trials.

Acknowledgements

This is the end of a long, tough journey in which I have learned a lot and grown in many aspects. I owe a debt of gratitude to many people who helped and supported me throughout this journey. It wouldn't have come to an end without their support.

First, I would like to express my gratitude to my promoter Peter Hilbers for giving me the opportunity to do a PhD study in Computational Biology (CBio) group. Peter, I have always been impressed by your endless enthusiasm in science and positivism. I am grateful for your trust in me even in the most difficult times and valuable comments throughout this research.

Next, I would like to extend my gratitude to my co-promoter Natal van Riel who has always fed hope with his scientific suggestions and insightful discussions on my research. Natal, thanks for your guidance and your availability when I needed. I am grateful to you for showing me how to always look on the bright side of research and also of life although I sometimes can still not manage to apply it thoroughly.

Furthermore, I would like thank my PhD committee members, Anton Wagenmakers, Jan Oscarsson, Gunnar Cedersund, and Christian Ottmann for taking part in my PhD committee and their evaluation of this thesis and kind comments. Additional thanks go to Jan Oscarsson for proposing and carrying out the exciting collaborative project. My sincere thanks go to our collaborator Anton Wagenmakers for welcoming me at the School of Sport and Exercise Sciences, University of Birmingham for a tranining in immunohistochemistry.

Besides, I would like to especially thank to my former supervisor Mehmet Çamurdan at Boğaziçi University for guiding me during my Masters study and encouraging me to conduct a PhD research.

I would like to acknowledge AstraZeneca for financially supporting this work and allowing me to conduct the fascinating experiments in AstraZeneca R&D facilities. I would like to give my special thanks to Samantha Peel for introducing me to the world of immunocytochemistry and helping me to carry out

the experiments. I am also grateful to James for his guidance and instructions in fluorescence imaging and analysis. Thanks to both of you for not only always being patient to my crazy schedules for the experiments and reviewing Chapter 4 thoroughly, but also all the good memories in Loughborough and Macclesfield.

My former office mate Christian, many thanks for helping me in applying your ADAPT method. Christian, it was always nice to have you as an office mate. Thanks for all the (non-)technical discussions we had and the tasty coffee you provied. I am also thankful to Joep V. for his help in image analysis and supplying mex file generators that provide an enormous decrease in the computational time of the analyses. Joep, also thanks for sharing your smiley post-its and your different perspective in our discussions. I would also like to acknowledge the former master student Haili for her valuable contribution to this work. Koen, thanks for your sincere willingness to always help and your detailed comments on the cover design to aesthetically improve it. Huili, many thanks for your caring like a sister and for being the cheer and the big smile of CBio. I would like to extend my thanks to my former and present colleagues in CBio for the nice working environment. Thanks to Fianne, Rik, Huili, Yvonne, Zandra and the former members of the group, Willemijn, Joep S., Joep V., Christian, and Sander for the PhD gatherings.

I would like to greatly acknowledge my friends who have contributed to the fun and joyful part of this journey. I feel so lucky to have such great old and new friends scattered around the Netherlands and Turkey, each of who has contributed and supported in a different manner to make this journey more enjoyable. I and actually also some of them well know that this acknowledgement never finishes if I would try to express my feelings to each of them in words. Many thanks for making me feel never alone and being there either physically or via phone and video calls whenever I needed. Dicilem (my little sister), Gözde (my unlimited comfort zone), Bahar (my source of tolerance), Müge E. (my empathetical twin), Döndü (atom karıncam), Buket (my fortune teller), Ayşegül (çop çopum civanım), Irmak (the absolute curiosity), Berna (yaşasın hemen şimdilerimiz!), Tuba (the artist), Roza (o u'ları o yapacağım!), Camille (the most colourful energy), Chiara (the expert for small surprises), Giulia (the holidays that could not become real), Michele (my honorary Turkish friend), Martin (en sevdiğim yabancı damat), Başar ('hayır, yanlış söylüyorsun'), Ali Can ('bak ben unutmadım aklımda!'), Tom (echoes and laughter), Bahadır (my anarchy advisor), Yunus (the source of an unexpected laughter), Akın (the serious laughter), Ezgi (the passionate scientist), Erman (babamdan sonra mangalcıların kralı), Seda (my constant cheer up leader), Sevince (my mirror of reality), Müge R. (acı bu!), Gizem (my memory card), Mustafa (nam-ı diğer Mustim), and Nehir (my sanity keeper). Each of you has a special and different place in my heart. I love you all! Cheers to all the nice memorable moments that I shared and will share with you.

I also feel so lucky to have such a great big family. Firstly, I would like to

give my warmest gratitude to my second mother and father, Sultan and Orhan Öncü, who have always been understanding, supportive, and caring. Eylem Öncü, thanks for becoming my older sister that I have always wanted to have. My mother Özgül, my father Tuğrul, I have been extremely fortunate to have you as my parents. Eternal thanks for your unconditional love and endless support that are my biggest treasure in life. You made me into who I am. My brother Özden İnan, thanks for being my dearest unique brother. No matter how far we are, I always take you, your songs, and our innocent childhood with me. Special thanks to the newest member of the family, my little niece Arya Kar who has been the source of life energy in the last and most difficult months. Finally, my long suffering other half Sinan, my life companion, *Dublem*. The past years have not been an easy ride for us as we together experienced the challenging PhD life in addition to many other steps that we took together in our life. Words are insufficient to describe your place in my heart. Thanks for your love and every value that you have added to me. Now it is time for our new ride!

Ceylan

Eindhoven, April, 2015

Curriculum Vitae

Ceylan Çölmekçi Öncü was born on 04.01.1983 in Karaman, Turkey. After finishing Izmir Bornova Anatolian High School in 2001, she entered Boğaziçi University to study Chemical Engineering. She received her Bachelor degree with honour and 3rd ranking in BSc Chemical Engineering graduates (2006), Boğaziçi University, Istanbul, Turkey. She continued her Master studies in the same department under supervision of prof.dr. Mehmet Çamurdan, focusing on the application of Control Theory for regulating the blood glucose levels of the patients with Type I diabetes. During her masters, she visited Control Laboratory of prof.dr. Ali Çnar, at Illinois Institute of Technology, in Chicago, USA. During her visit, she worked on the development of an adaptive blood glucose regulator to be implemented in automated insulin pumps for diabetic patients. She received her Masters degree with high honour in 2008. In December 2009, she started her PhD research in Computational Biology group of prof.dr. Peter Hilbers, under supervision of dr. Natal van Riel, at the department of Biomedical Engineering in Eindhoven University of Technology in the Netherlands. She worked on the mathematical modelling of the insulin signaling pathway in skeletal muscle. To carry out the experimental studies of the pathway, she visited AstraZeneca R&D in Manchester, UK several times. The results of her PhD research are presented in this dissertation.